Pore-water methane dynamics as an indicator of ecosystem functioning following Ecological Mangrove Rehabilitation (EMR) in South Sulawesi, Indonesia

by

Yaya Ihya Ulumuddin

Submitted in fulfilment of the requirements for the degree of
Doctor of Philosophy
of the Australian National University
November 2019

THE AUSTRALIAN NATIONAL UNIVERSITY

Candidate's Declaration

This thesis contains no material which has been accepted for the award of any other degree or diploma in any university. To the best of the author's knowledge, it contains no material previously published or written by another person, except where due reference is made in the text.

Yaya Ihya Ulumuddin　　　　　　　　　　　　　　　　　Date: 7 Nov 2019

Acknowledgements

This thesis is not the end of my journey but is only a single step of 1,000 milestones in my life. Admittedly, this step has not been achieved by me alone—many great and generous people have been involved in this lifelong journey. Many are people who shaped me in early life, teaching me to be aware of myself and my surroundings, to learn new skills and knowledge, and opening windows to the world. Those people brought me the opportunity to complete this research, culminating in the writing of this thesis. Many people have helped in this struggle from the beginning until finishing this thesis. Therefore, I would like to express my gratitude and show my sincere appreciation to those people.

To my supervisors, Dr Sara Beavis, Professor Michael Roderick and Professor Stephen Eggins (Australian National University), it has been a great experience to know you and work with you all in research. Your insight, patience, commitment and generosity have been extremely helpful. Sara helped me from the beginning, when I was applying for an Australian Awards Scholarship—particularly in shaping the research proposal and looking for a funding opportunity. I also really appreciate Sara visiting me when doing fieldwork and helping me maintain my spirit. Through Mike, I had a great supervisor team, so that I could impress the interviewer during selection of the scholarship. This team has different but complementary expertise and insight, which was invaluable for building my research experience, skills and confidence. Mike always asked me questions that pushed me to think beyond what I believed my capabilities were. I was always happy with the long hours of discussion with him, even though it was sometimes tiring. My sincere gratitude also goes to Steve for his generosity for providing the pore-water samplers (through Carlyle Were, RSES, ANU) and sending them to the field sites, and providing financial support. Steve's lecture of Marine Biogeochemistry, with Dr Michael Ellwood, and the textbook he gave me were valuable when I was still ignorant in this subject but wanted to undertake research about biogeochemistry. Steve also helped me in focusing my research proposal, which was extremely helpful. This was reflected in the research execution, which did not change much from the research plan in the proposal.

To my advisers, Professor Sukristijono Sukardjo (Research Center for Oceanography, RCO-LIPI, Indonesia) and Dr Irawan Sugoro (National Nuclear Energy Agency of Indonesia), it has been a pleasure to work with you when I was completing field study and intensive discussion with my supervisors was a bit difficult. Pak Kris gave me a confidence boost to execute the research plan in the field. His suggestions and encouragement helped me to face uncertainty when undertaking fieldwork. My gratitude goes to Pak Irawan and his wife, Teh Devi, for their generosity and for sharing his knowledge and laboratory for the microbial study of methane production. Also, many thanks to his student, M Rizky Mu'arif, who helped me in the laboratory.

This research was generously funded by the Department of Foreign Affairs and Trade (DFAT), the Government of Australia, through an Australian Awards Scholarship (AAS). My gratitude especially goes to Gina Abarquez—your welcome in the first day in Canberra has stayed in my mind—and Rozanna Muir, Elaine Ee and Imelda Manalac, who were always helpful for my study and life in Canberra. It includes the facility for using a service from Elite Editing to make a final touch for the thesis manuscript. In addition, this research was supported by Fenner School of Environment and Society, ANU. Thank you so much to the director and all staff—particularly Amy Chen, Dr Jack Pezzey and Julie Watson.

Thank you to my colleagues, who shared their knowledge of methane and mangroves, including Dr Guangcheng Chen (Third Institute of Oceanography, SOA, China), Professor Pramudji, I Wayan Eka Dharmawan (RCO-LIPI), Clint Cameron (Charles Darwin University) and Hanif Budiprayitno (RCO-LIPI). Their sharing of knowledge and insight influenced the shape of my research. I am grateful to Guangcheng for introducing me to 'methane emissions', giving me experience completing research on such a topic, and providing gas-tight sample bags. Pak Pramudji and Wayan are great colleagues and friends in the office and mangrove forests. Thank you to Wayan for telling me about the Greenhouse Gas Laboratory. Clint introduced me to the ecological mangrove rehabilitation site and shared his insight about mangroves and greenhouse gas emissions. Hanif has become a best friend throughout my study at ANU, who likes to share his insight and skills, so that we have mutual respect.

I would also like to thank the Blue Forest Foundation in Makassar, Benjamin Brown, Yusran Nurdin Massa, Akhzan Nur Iman, Musriadi, Yusuf, Muhammad Sadik and Muhammad Ikhsan Ismail, who provided support for field study at Tanakeke Island—and especially to Akhzan, who organised the team. Thank you to Daeng Tutu (Lantangpeo) and his family for their hospitality when Akhzan's team and I were staying at his house for the field study.

Special acknowledgement goes to Dr Endah Sulistyawati (Bandung Institute of Technology), who has opened windows into new worlds. Her lectures impressed and introduced me to 'climate change'—a topic that I found difficult to explain to my father. More importantly, she encouraged me to pursue higher studies, at a time when I was unsure if I could do that. Thus, she introduced me to Professor Mike Roderick.

Lastly, thank you so much to my wife, Windy Rahayu, and kids, Adhvaan Gaurava, Fidela Cerelia Farzana and Kandelia Dilshad Khumaira. Special thanks to my wife, who has sacrificed her life to look after my little family, particularly when I was away from home, in Canberra or Tanakeke. Thank you to my kids for being patient at home without me. My deepest gratitude to my big family, especially *Mimih* and *Bapa* and *Mama* and *Papa*, brothers and sisters. All of you are sources of energy to fuel my life, including finishing this thesis.

Canberra, 15 February 2019 (revised 6 November 2019).

Abstract

Increasing carbon sequestration in mangrove ecosystems has several benefits, including a potential role in climate change mitigation. However, mangroves are also known to emit methane (CH_4)—a potent greenhouse gas—and the net climate change benefit of planting mangroves is not yet fully understood. In this research, I investigated pore-water CH_4—a proxy for CH_4 production and export—in a mangrove rehabilitation area on an Indonesian tropical island. Initially, I established a new pore-water extraction method that is simple, cheap and reliable. This sampler was used to measure pore-water CH_4 in several mangrove rehabilitation sites on a tropical island in Indonesia. The pore-water CH_4 concentrations were very high (20 to 30,000 times the saturated value). However, my estimates of the CH_4 fluxes at the soil surface were very low, which agreed with previous studies. Therefore, I surmised that the exceptionally high levels of CH_4 in the pore-water would be exported not only through the sediment–air interface, but also by lateral tidal flow and especially via mangrove stem (sediment-root-stem-lenticel pathways). Temperature and pore-water chemistry were found to be ideal for CH_4 production, thereby implying that the major constraint was substrate supply. This was confirmed by the finding that the pore-water CH_4 concentration was associated with the stage of the mangrove regrowth, and roughly followed mangrove forest productivity, with the highest pore-water CH_4 concentration at intermediate stand ages. This was also confirmed by the dominant pathway of CH_4 production that was through the degradation of methylated compounds (supplied by mangrove vegetation), rather than via acetate or CO_2/H_2. Thus, this study indicates that mangrove vegetation plays a critical role in CH_4 production.

Contents

List of Figures

List of Tables

List of Equations

List of Acronyms and Abbreviations

Ah	Ampere Hour
BA	Basal Area
CB-EMR	Community-based Ecological Mangrove Rehabilitation
CFU mL^{-1}	Colony Form Unit per Millilitre
cm	Centimetre
DNA	Deoxyribonucleic Acid
dpm m^{-3}	Dissociation per Minute per Metre Cubic
dsrB	Dissimilatory Sulfite Reductase Beta Subunit Genes
EMR	Ecological Mangrove Rehabilitation
FID	Flame Ionisation Detector
GC	Gas Chromatography
GHG	Greenhouse Gas
GWP	Global Warming Potential
HDPE	High Density Polypropylene
ID	Inner Diameter
IPCC	Intergovernmental Panel on Climate Change
km	Kilometre
L	Litre
MAP	Mangrove Action Project
mcrA	Methyl Coenzyme M Reductase
Mg C ha^{-1}	Mega Gram Carbon (C) per Hectare
mg m^{-2} $hour^{-1}$	Milligram per Metre Square per Hour
mL	Millilitre
mL $hour^{-1}$	Millilitre per Hour
mm	Millimetre
MSL	Mean Sea Level
mV	Millivolt
NGO	Non-governmental Organisation
NPP	Net Primary Productivity
NSW	New South Wales
ORP	Oxidation Reduction Potential

pmoA	Particulate Methane Monooxygenase
ppb $year^{-1}$	Parts per Billion per Year
ppmv	Parts per Million by Volume
PVC	Polyvinyl Chloride
qPCR	Quantitative Polymerase Chain Reaction
RSES-ANU	Research School of Earth Science—Australian National University
SOC	Soil Organic Carbon
SRB	Sulfate-reducing Bacteria
UAE	United Arab Emirates
UHP	Ultra-high Purity
μm^2	Micrometre Squared
US	United States
V	Volt
W m^{-2} ppm^{-1}	Watt per Metre Square per Part per Million

Glossary and Terms

Acetotrophic	Relating to methane production that uses acetic acid as a precursor.
Artificial saliva	A solution that mimics saliva. In this research, this solution was used to grow methanogen microorganisms in the laboratory.
Biogenic (methane)	Methane gases that are produced by living organisms.
Blue carbon	Carbon storage and sequestration by oceans and coastal ecosystems, including saltmarshes, seagrasses and mangroves.
Cytoplasm	A semi-fluid substance that fills cells.
Ecological mangrove rehabilitation	A technique or approach for mangrove rehabilitation by restoring hydrological regimes to facilitate natural recruitment of mangrove seedlings.
Eddy flux covariance	A technique to measure and calculate vertical turbulent fluxes of gases within boundary layers.
Fermentative	Relating to or produced by fermentation—the process in which a substance breaks down into smaller and simpler substances, involving microorganisms.
Global warming potential	A quantitative measure of how heat can be trapped by greenhouse gases in the atmosphere, within a horizon time, compared with the heat because of CO_2.
Homoacetogenic	Relating to homoacetogenesis fermentation—that is, substrate degradation producing acetate.
Hydrogenotrophic	Relating to methane production that uses CO_2 and H_2 as precursors.
Hydrolytic	Producing or produced by hydrolysis.
Methanogen	Microorganisms that are involved with methane production.
Methanogenesis	Methane production.
Methanogenic	Relating to methane production.
Methanotroph	A group of bacteria that uses methane as a substrate.
Methylated compound	Chemical species containing methyl groups (CH_3).
Methylotrophic	Relating to methane production that uses methylated compounds (e.g., methanol, methylamines) as precursors.
Micron	Micrometre (µm).
Obligate	Restricted to a particular function or mode of life.
Osmolyte	Compounds that affect osmolysis.

Pyrogenic (methane)	Methane gases that are produced by combustion.
Relative radiative forcing	The relative impact of GHGs to absorb infrared radiance, re-radiate and heat back to the Earth's surface because of changes in greenhouse gas concentrations.
Residence time	The period that greenhouse gases live in the atmosphere.
Rumah panggung	Stage house.
Syntrophic	Relating to syntrophy, (micro) organisms that live together and are mutually dependent for food supply.
Thermogenic (methane)	Methane gases that are produced by geological activity in the deep subsurface of the Earth, with high temperatures and pressures.

Chapter 1: Introduction

1.1 Background

During the last two decades, the ability of coastal vegetation to sequester carbon dioxide (CO_2) has been increasingly recognised. Previously, this ability was overlooked in discussions of terrestrial and marine carbon cycles; however, a report produced in 2009 through an inter-agency collaboration between the United Nations Environment Programme; Food and Agriculture Organization; and Intergovernmental Oceanographic Commission/United Nations Educational, Scientific and Cultural Organization drew attention to this function (Nellemann *et al.*, 2009). This report also highlighted the risk of increased CO_2 emissions from degrading vegetated coastal ecosystems. Nellemann *et al.* (2009) coined the term 'blue carbon' to refer to carbon sequestration by these ecosystems (i.e., mangroves, saltmarshes and seagrass).

Mangrove forests accumulate a considerable amount of carbon in biomass and sediment, yet also emit greenhouse gases (GHGs). For example, Donato *et al.* (2011) reported that the above- and below-ground carbon stock of tropical mangroves in the Indo-West Pacific region accounted for 10^3 Mg C ha^{-1} on average, while global CO_2 emissions from mangrove deforestation constituted around 2 to 12 × 10^7 Mg C year^{-1}. Another important function of mangroves is the burial of large quantities of organic carbon in the sediment. Mangroves contribute 8 to 15% of all organic carbon burial in the marine environment, or 2.6 × 10^7 Mg year^{-1} (Breithaupt *et al*., 2012). However, few studies have been undertaken on CH_4 emissions from mangroves, although this gas is part of the carbon cycle and contributes to raising the Earth's surface air temperature (Saarnio *et al*., 2009).

Consequently, CH_4 emissions are increasingly in focus as we attempt to mitigate climate change. This is due to CH_4 being the second-largest of the long-lived GHGs. Further, this gas has a relative warming potential higher than CO_2. In other words, an additional one kilogram of CH_4 in the atmosphere causes an increase of the Earth's surface temperature that will be higher than that generated by an additional one kilogram of CO_2. For this comparison, the Intergovernmental Panel on Climate Change (IPCC) adopted an index called *global warming potential* (GWP), which contains parameters of *residence time*[1] and *relative radiative forcing*[2] (Forster *et al*., 2007). For example, with a 500-year horizon time, the GWP of methane is 3.7 times that of CO_2 (Lashof and Ahuja, 1990). This is due to CH_4 having a direct effect on *radiative forcing*. CH_4 oxidation also has this effect, as it generates CO_2 and H_2O (Wuebbles and Hayhoe, 2002). In addition, a shorter horizon time generates a larger GWP. For example,

---

[1] The period that GHGs live in the atmosphere.
[2] The relative impact of GHGs to absorb infrared radiance, re-radiate and heat back into the Earth's surface because of changes in GHG concentrations—W m^{-2} ppm^{-1} (Lashof and Ahuja, 1990).

with a time horizon of 100 years, the GWP of CH_4 is 25 times that of CO_2; however, when the horizon time reduces to 20 years, the GWP of CH_4 is 72 times that of CO_2 (Forster *et al*., 2007). Therefore, research into CH_4 emissions is as important as CO_2 sequestration.

1.2 Description of issues to be addressed

Indonesia represents a major part of the Indo-West Pacific mangrove region, with carbon storage potential in mangrove forests being extensively studied. The estimated carbon stocks of Indonesian mangroves are around 1,000 (± 378) Mg C ha^{-1} (Alongi *et al*., 2015; Murdiyarso *et al*., 2015). However, during the last three decades, 40% of the total mangrove area has been lost, and this has resulted in annual emissions of 7 to 21 × 10^7 Mg CO_2 equivalent.

The capacity of mangroves to store carbon enhances the importance of Indonesian mangrove rehabilitation projects, which were originally conceived for conservation benefits and to protect/enhance livelihoods. Mangroves' capacity to store carbon has encouraged mangrove planting not only by governments and non-governmental organisations (NGOs), but also by local communities. Areas have been rehabilitated by planting seedlings of a single species, which are mostly unsuccessful (Bosire *et al.*, 2008, Primavera and Esteban, 2008). In addition to this approach, one specific rehabilitation project uses a method called *ecological mangrove rehabilitation* (EMR). This approach prioritises the restoration of hydrological regimes to facilitate natural recruitment of mangrove seedlings (for further information, see Lewis, 2005). This is believed to be as successful and ecologically meaningful, since the method can potentially restore the mangrove communities to their former, natural condition.

To date, most studies have focused on CO_2 sequestration potential, with relatively few studies investigating the CH_4 emission potential from Indonesian mangroves. Chen *et al.* (2014) investigated CH_4 emissions from undisturbed mangroves in North Sulawesi. To the best of my knowledge, only Cameron *et al.* (2019a) have examined CH_4 emissions from sediments in mangrove rehabilitation area in Indonesia, contrasting between rehabilitation sites and undisturbed forests. Our study aimed to assess the dynamics of CH_4 following mangrove regrowth during the implementation of EMR project. We addressed this study by measuring dissolved CH_4 in the pore-water at sites with different stage of mangrove regrowth. In particular, the study focused on mangroves of Tanakeke Island, South Sulawesi, Indonesia. It was anticipated that the results of this study would provide quantifiable evidence regarding the effectiveness of EMR projects.

1.3 Thesis structure

The structure of this thesis is outlined in Fig. 1.1. Chapter 2 discusses the ways this thesis addresses the overall study aim by measuring pore-water CH_4, rather than CH_4 production and emission. This study is presented in three discrete yet interrelated sections, based on three specific aims and associated research questions, which are presented at the end of the literature review (Chapter 2). Chapter 3 describes the interrelationships among the study components and identifies the targeted outcomes of the research questions. The study location is also described in this chapter, with a general overview of the methods. Chapters 4, 5 and 6 are the three substantive components of this study. Chapter 7 comprises the conclusion and recommendations of this thesis.

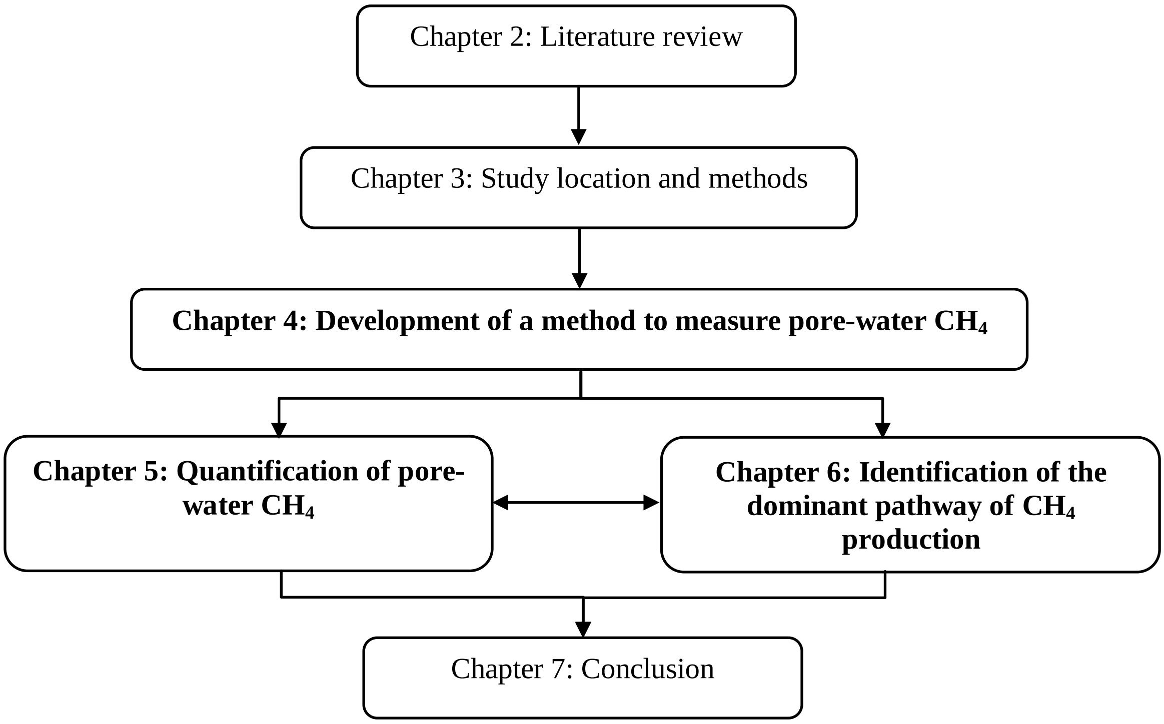

Figure 1.1. Thesis structure.

Chapter 2: Biogeochemistry of methane in mangrove ecosystems—A review

2.1 Introduction

An increase in atmospheric methane first became prominent in the 1980s (Whalen, 2005), with the atmospheric concentration now increasing at around 5 to 10 ppb year^{-1} (Reay *et al*., 2018). Attributing this increase is complex because global CH_4 sources and sinks are diverse and include wetlands, oceans, termites, rice farming, livestock farming, landfills, biomass burning, fossil-fuel burning and fossil-fuel mining (e.g., oil/gas/coal) (Milich, 1999). According to the processes involved in CH_4 production, the sources of CH_4 can be classified as either biogenic, thermogenic or pyrogenic CH_4 (Kirschke *et al*., 2013). Biogenic CH_4 is produced by a biological process (e.g., those typically occurring in wetlands and farming), while thermogenic and pyrogenic CH_4 are produced by physicochemical processes. Fugitive emissions resulting from fossil-fuel mining are the dominant source of thermogenic CH_4 (Kirschke *et al*., 2013). Recently, Schaefer *et al*. (2016) reported that the source of the increase in atmospheric CH_4 increase has shifted from thermogenic to biogenic origins. They identified the most likely biogenic source as agriculture (i.e., rice and livestock farming), rather than natural wetlands. However, wetlands might still contribute to an increase of biogenic CH_4 sources in the future, with projected warming expected to enhance the emission of CH_4 from wetlands (Milich, 1999; Chambers *et al*., 2014; Martins *et al*., 2016; Dean *et al*., 2018).

Studies of wetland CH_4 production estimate its contribution at around 23% of global emissions (Reeburgh, 2003). The first review paper on wetland CH_4 production ranked wetlands in order of CH_4 emissions as bogs, lakes, fens, swamps and marshes (Aselmann and Crutzen, 1989). The emissions ranged from 0.6 to 11 mg m^{-2} hour^{-1} and were generally lower than that reported from rice fields (13 mg m^{-2} hour^{-1}) (Aselmann and Crutzen, 1989). Later, studies of CH_4 in wetlands became prolific, producing multiple and detailed studies on, for example, the physics, microbiology and biogeochemistry of wetland CH_4 production. In the studies noted above, very few involved coastal wetlands. Further, Aselmann and Crutzen's (1989) review did not present CH_4 fluxes from coastal wetlands due to low values of CH_4 fluxes based on an earlier investigation in a saltmarsh by Bartlett *et al*. (1987). Moreover, a search using the online database Web of Science, using the keyword combinations of 'mangrove' and 'methane' and 'saltmarshes' and 'methane', displayed fewer than 200 and 300 papers, respectively (Fig. 2.1). According to the Web of Science (accessed 6 November 2019), the number of studies on CH_4 in coastal wetlands increased rapidly during the candidature of this PhD (2015 to 2019) (Fig. 2.1). This is coincident with both increasing concern and interest in coastal wetlands for climate change mitigation.

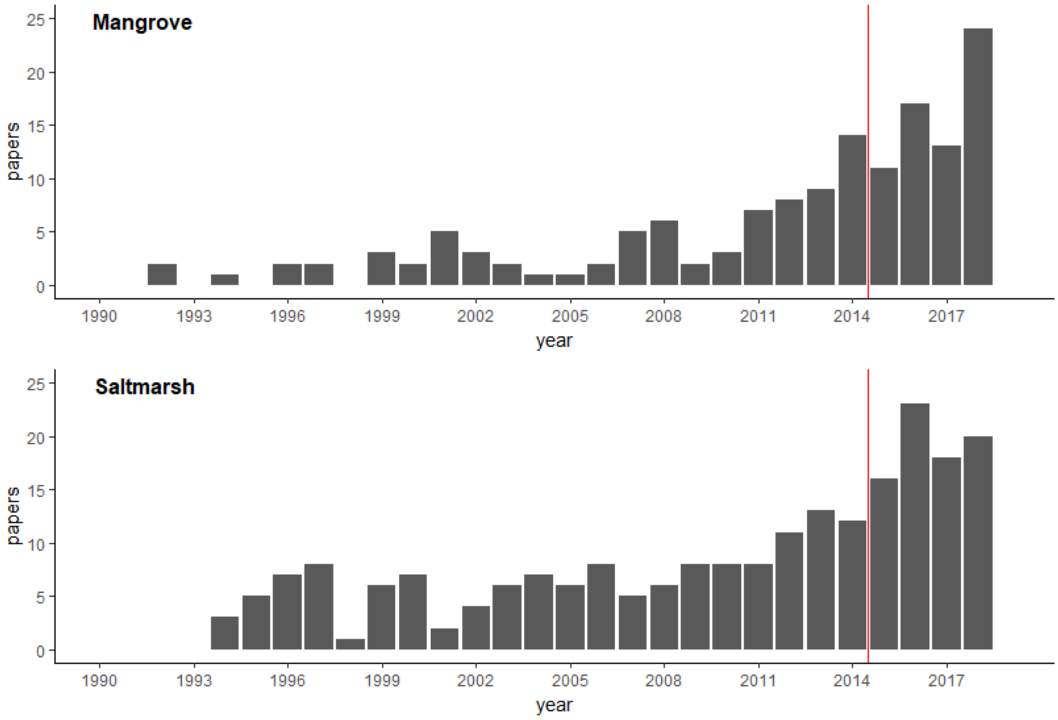

Figure 2.1. Number of scientific papers about CH_4 in Web of Science, accessed 6 November 2019. The red line denotes the year when this PhD thesis began (2015).

Many of the previous studies (Fig. 2.1) investigated CH_4 fluxes at the sediment–air interface. For example, in 2015, I identified 18 papers on CH_4 emissions from mangrove sediments, and since then a further 23 papers have become available. This may be due to CH_4 fluxes at the sediment-air interface is the central parameter in CH_4 emissions from mangrove ecosystems and its measurement is relatively simple and straightforward. On the contrary, pore-water CH_4 do not directly relate to CH_4 emissions, besides its measurement is a bit complicated, involving gas and liquid phase. Thus, investigations on pore-water CH_4 were only reported in a total of nine papers, with many of the early studies reporting no detectable pore-water CH_4. Identification of soil microbiomes, including the presence/absence of methanogenic and methanotrophic communities or even the balance between both groups, is also a sub-topic of major recent interest (19 papers). Another identifiable sub-topic of recent interest is CH_4 transport by tidal pumping (five papers since 2015). Several papers have also included a discussion of sulfate reduction, decomposition and geochemistry; however, to my knowledge, few have specifically focused on CH_4 biogeochemistry in mangrove ecosystems. Given the absence of mangrove–CH_4 specific studies, many authors have been forced to extrapolate using knowledge acquired from studies in freshwater wetlands or rice fields.

With that in mind, this chapter reviews current studies of CH_4 in mangrove ecosystems. This review is based on 154 papers identified using the Web of Science database that specifically investigated CH_4 in mangrove ecosystems, along with several related papers in other freshwater wetlands. The review includes CH_4 fluxes, CH_4 production pathways and biogeochemical aspects.

2.2 Geographical coverage

Studies of CH_4 fluxes at the sediment–air interface have mostly been undertaken in the old mangrove region (the Indo-West Pacific), across tropical latitudes (Fig. 2.2, top panel). The data on CH_4 fluxes in the 35 papers reported during the last two decades were generally collected by using static-chamber methods. There were 27 papers reported from studies in the Indo-West Pacific, including Australia (five), China (10), India (seven), Indonesia (one), the Philippines (one), Tanzania (one) and Thailand (one). The remaining studies were undertaken in the Atlantic-East Pacific (nine), including Brazil (one), the United States (four), Columbia (one), Mexico (two) and Puerto Rico (one).

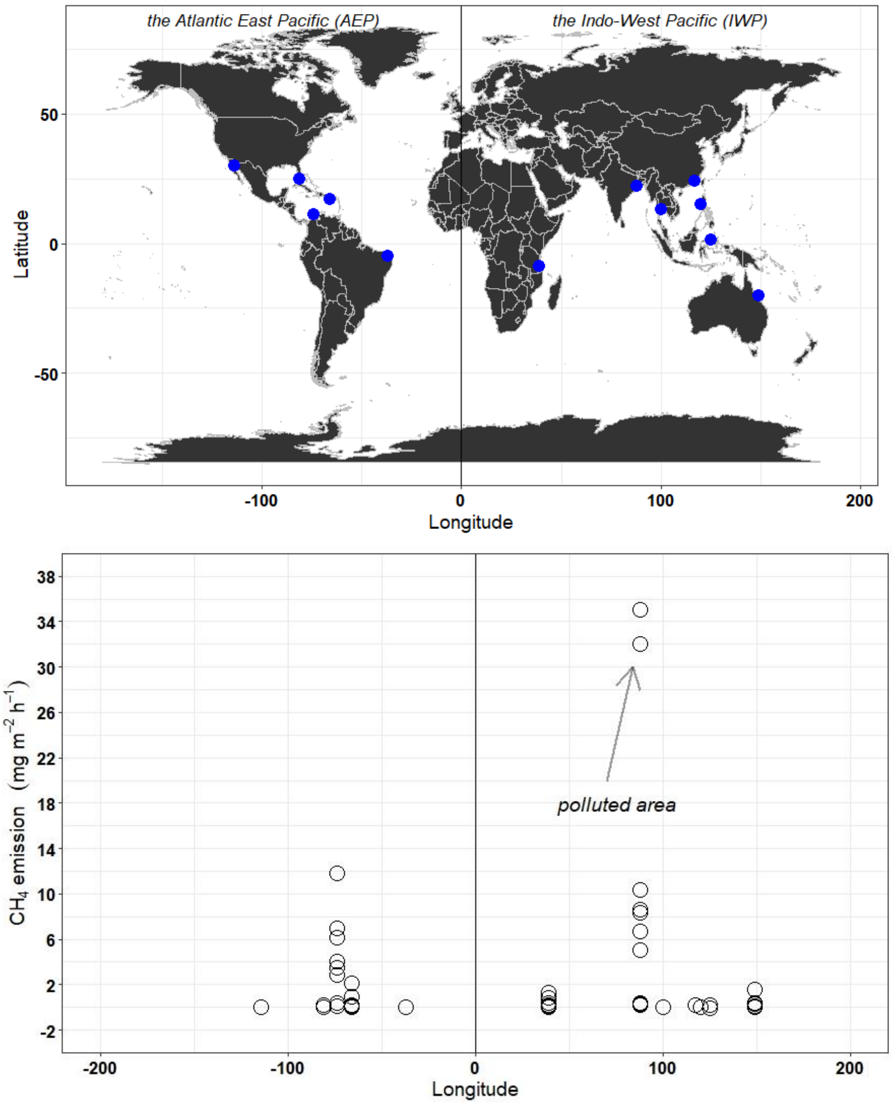

Figure 2.2. Summary of field studies reporting CH_4 fluxes from mangrove sediments. Top panel shows spatial distribution and lower panel shows average flux in sites reported in the 36 separate papers.

2.3 CH_4 fluxes from mangrove ecosystems

2.3.1 Sediment–air interface

Previous studies indicated wide variation in CH_4 fluxes from mangrove sediment-air interface and ranged from 'undetected' fluxes (Giani *et al*., 1996; Alongi *et al*., 2004) to a maximum of 82.69 mg m^{-2} $hour^{-1}$ (Chen *et al*., 2010) (see Fig. 2.2, lower panel). In general, reported CH_4 fluxes were very low or even negative. Only Chen *et al.* (2010) reported that CH_4 fluxes from mangrove sediment were relatively high (82.69 mg m^{-2} $hour^{-1}$) and they noted the reason was a high pollution in their study site. These studies have apparently highlighted again that CH_4 emissions in mangrove ecosystems is generally lower than in freshwater wetlands and even rice fields (see Aselmann and Crutzen, 1989). Thus, CH_4 emission from mangrove ecosystem was not yet fully characterized in scientific discourse of global CH_4 emission.

2.3.2 Water–air interface

Considering the total CH_4 flux from mangrove ecosystem may enrich the scientific discourse of CH_4 emissions in that ecosystem, but there are only a few investigations of CH_4 fluxes from water-air interface of the mangrove surrounding waters, i.e., river, creek, lagoon and coastal waters. CH_4 fluxes of up to 33.29 mg m^{-2} $hour^{-1}$ had been reported, and the fluxes were highly variable in both space and time (Ramesh *et al*., 1997; Purvaja and Ramesh, 2001; Rajkumar *et al*., 2008). Later studies reported how dissolved CH_4 in mangrove pore-water sediments amends CH_4 in coastal waters. Bouillon *et al*. (2007) indicated a gradual increase in CH_4 concentration in creek waters during ebb tide. Call *et al.* (2015) found evidence of a positive strong correlation between ^{222}Rn and CH_4 concentration at the creek mouth of subtropical mangrove measured for two weeks (Fig. 2.3). Given that the increasing concentration of ^{222}Rn represents a pore-water amendment to creek waters, they concluded that CH_4 came from the pore-waters. This demonstrates that the CH_4 flux from mangrove sediments not only occurs through the sediment–air interface, but is also laterally exported to surrounding waters. The export of CH_4 will be facilitated by tidal cycles, which are a characteristic of mangrove habitats. Hence, mangrove ecosystems may contribute higher CH_4 fluxes through water-air interface of the mangrove surrounding waters.

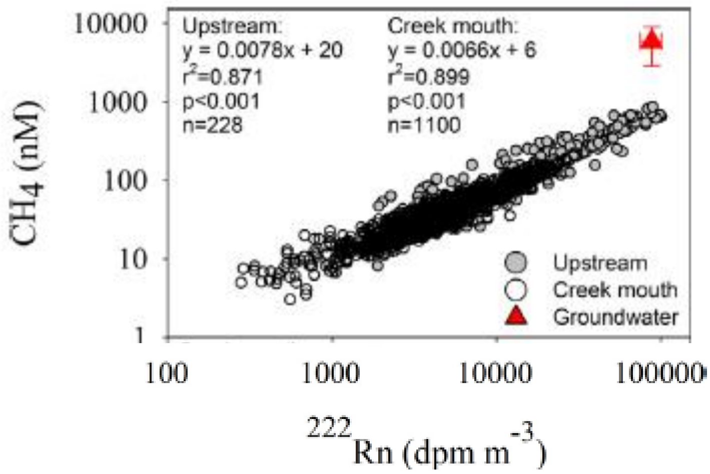

Figure 2.3. **Correlation CH_4 with ^{222}Rn in creek mouth and upstream (Call *et al*., 2015).**

2.4 Methane production

Methane production or methanogenesis is the final step in organic carbon mineralisation in anoxic sediments (Sarmiento and Gruber, 2006; Zhuang, 2014) (see Fig. 2.4). In oxic layers, aerobic bacteria break down carbohydrate using oxygen as electron acceptors. In the same layer, protein is decomposed and produces ammonia, and, eventually, nitrifying bacteria oxidise the ammonia to nitrate (NO_3^-). In between the oxic and anoxic layers, NO_3^- and MnO_2 replace O_2 as electron acceptors to decompose carbohydrate. After these acceptors are depleted, iron reduction continues mineralisation. When oxygen is totally absent, sulfate-reducing bacteria and methanogenic archaea compete for energy from organic carbon decomposition. The first microbe group generally out-competes the other, which is reflected in the standard energy yields ($\Delta G°$) (Fig. 2.4). However, this ideal sequence probably changes if there are aquatic plants supplying O_2 from the atmosphere to deep soil layers (as shown by Fritz *et al*., 2011) or if methanogens are not out-competed by sulfate reducers.

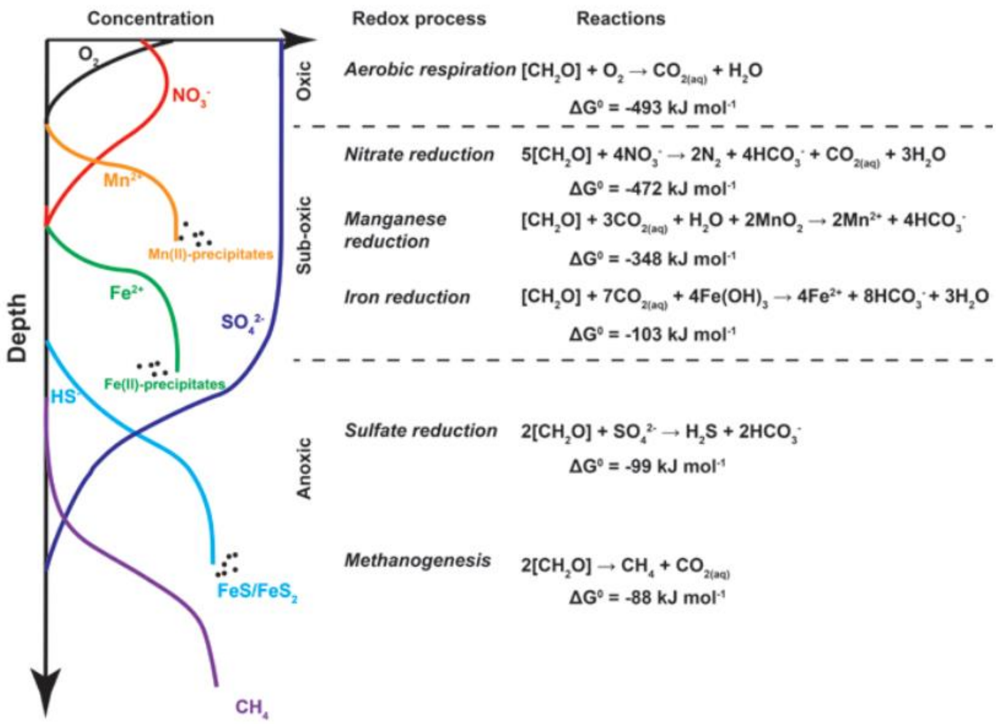

Figure 2.4. Sequence of organic carbon degradation in marine sediment and its chemical reaction with associated standard free energy yields (∆G°) (reproduced from Fig. 1.2 in Zhuang, 2014).

Some methanogens are out-competed by sulfate-reducing bacteria because they use the same substrates (i.e., H_2/CO_2 and acetate). Methanogens use specific substrates and, based on this, methanogens are usually divided into three groups: hydrogenotrophic, acetotrophic and methylotrophic methanogens. Hydrogenotrophs use CO_2 for an energy substrate and H_2 as electron donors, while acetotrophic methanogens specifically need acetate. These substrates are also used by sulfate-reducing bacteria. In contrast, methylotrophic methanogens produce CH_4 through reduction of methylated compounds, which are known as non-competitive substrates (Oremland and Polcin, 1982).

Hydrogenotrophic and acetotrophic pathways are considered major contributors of CH_4 production in wetland habitats. This is due to the abundance of carbohydrates or polysaccharides, with their decomposition producing CO_2/H_2 and acetate. Polysaccharides are degraded gradually by three consortia (hydrolytic, fermentative and homoacetogenic/syntrophic bacteria) with the production of CO_2/H_2 and acetate occurring in the last step (Garcia *et al.*, 2000). It has been noted that, stoichiometrically, hydrogenotrophs change CO_2/H_2 to CH_4 and contribute one-third of total CH_4 production, while acetotrophic methanogens use acetate to produce two-thirds of the production (Conrad, 2007). However, the exact proportions are dependent on H_2 production by homoacetogenic bacteria (Conrad, 1999). Given that these pathways are common in most wetlands, many authors conceptualise the stage of anaerobic degradation as shown in Fig. 2.5. (Garcia *et al*., 2000; Conrad, 2007; Liu and Whitman, 2008), disregarding the methylotrophic pathway.

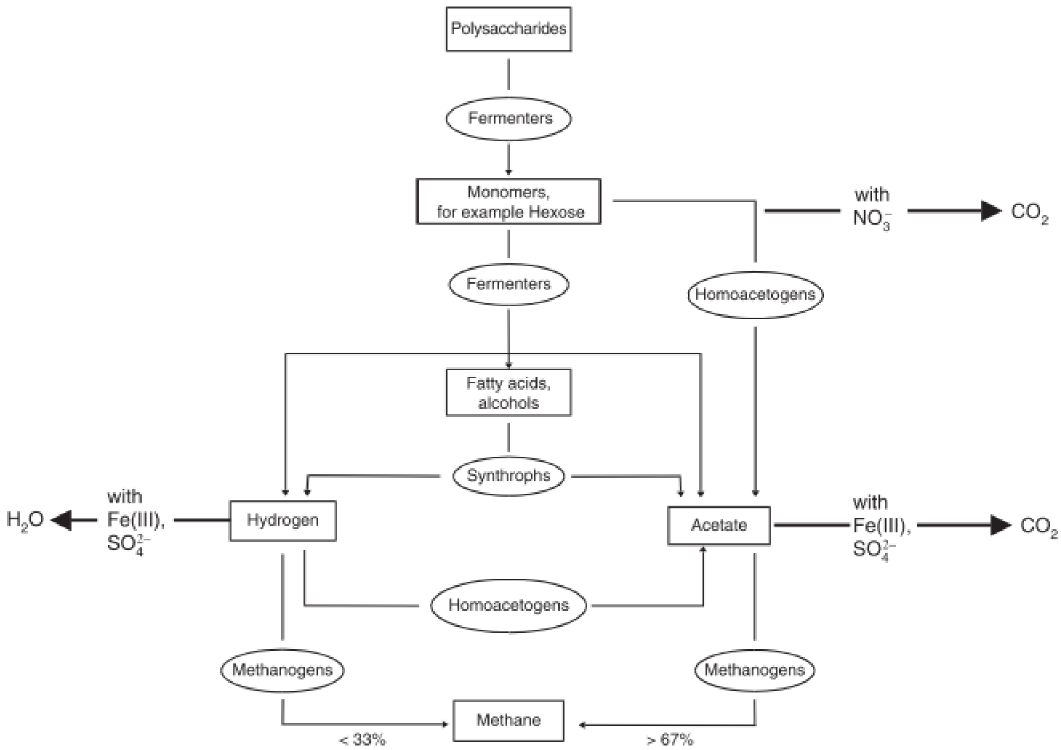

Figure 2.5. Anaerobic degradation of organic carbon-producing CH_4 in the terminal process (reproduced from Fig. 1 in Conrad, 2007).

Although methylotrophic methanogens were identified at the end of the 1970s (Weimer and Zeikus, 1978; Patterson and Hespell, 1979), methylotrophic pathways were at that stage considered minor contributors to CH_4 production. However, a later study found that these methanogens can coexist with sulfate-reducing bacteria generating CH_4 from methanol and trimethylamine (Oremland *et al*., 1982). Oremland *et al*. (1982) proposed the concept of non-competitive substrates in biochemistry pathways of methanogenesis, and used methanol, trimethylamine and methionine to test substrate competitions of methanogens and sulfate-reducing bacteria from salt marshes.

Later, the theory of non-competitive substrate of methanogens became a much-debated topic in the pathways of CH_4 production. For instance, Lyimo *et al*. (2009) found that sulfate-reducing bacteria from their mangrove sites reduced methanol and trimethylamine in laboratory conditions, yet at slower reduction rates than those by methanogens. For another non-competitive substrate, Lyimo *et al*. (2002) provided evidence that sulfate-reducing bacteria are involved in dimethyl sulfide degradation at low concentrations (10 µM), since sulfate-reducing bacteria have a higher affinity to the substrate. However, recent field studies reported that non-competitive substrates might exist to explain the high rate of CH_4 production in the sulfate-reducing zone of marine sediments (Young, 2005; Zhuang, 2014).

Prior to the study by Zhuang (2014), little was known about how much each methanogenic pathway contributed to CH_4 production in marine sediments in terms of substrate concentration and composition. Zhuang found that methylotrophic methanogenesis in the sulfate-reduction zone contributed 13 to 74% of the total CH_4 production, while, in the sulfate-depleted sediment, hydrogenotrophic methanogenesis was dominant, accounting for 67 to 97% of the total CH_4 production. Acetotrophic methanogenesis was shown to contribute up to 31% in organic-rich sediment. Zhuang (2014) also proposed a new concept of anaerobic degradation that involves marine algae and terrestrial input as carbon sources (Fig. 2.6).

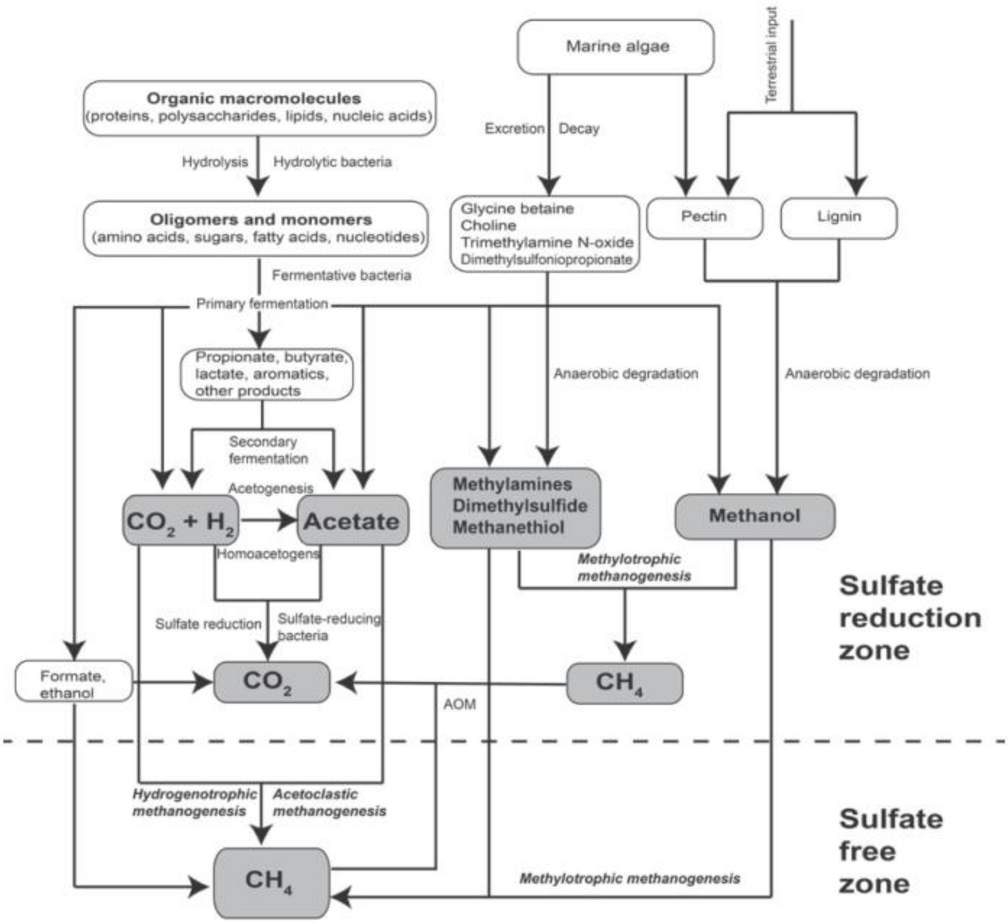

Figure 2.6. Revision concept of anaerobic degradation (reproduced from Fig. 1.3 in Zhuang, 2014).

Given that mangrove ecosystems occur at the interface between marine and terrestrial systems, the domination of the methanogenesis pathway is probably different from site to site. In fact, it is reflected in the extreme (space–time) variability in CH_4 fluxes, as discussed previously. The intertidal cycle and freshwater discharge largely determine the salinity gradient and sulfate content in mangrove sediment. In addition, these hydrological regimes control organic matter supply from mangrove primary productivity, marine algae and terrestrial inputs. Hence, changing substrate composition and environmental conditions will ultimately alter the microbial process of methanogenesis. To my knowledge, Reshmi *et al*. (2015) may be the first authors who attempted to study methane production *in situ* at a microbial level in mangroves. They found that acetotrophic methanogens were more abundant during the wet than dry season, while methylotrophic methanogens were relatively stable in both wet and dry seasons. Despite this recent work, the quantification of, and shifts in, methanogenic pathways in mangrove systems with respect to seasonal and spatial variation remain poorly documented.

2.5 Source of CH_4 variability

The magnitude of CH_4 emissions from mangrove soils and mangrove-influenced waters varies substantially across sites and seasons. Variability of measurement techniques may be one of the reasons for this, but a study by Yavitt *et al*. (1997) concluded that the variation of emissions across sites and time is the result of a complex interplay of CH_4 production, microbial CH_4 consumption and gas transport through the sediment and aquatic vegetation. This finding was supported by Borges and Abril (2011), who suggested that those processes are highly dependent on the supply of methane precursors to the soil; the presence of oxygen and other electron acceptors; and local conditions of hydrodynamics, temperature and salinity.

2.5.1 Organic matter

Of all the factors that control CH_4 production and emission, organic matter availability is likely the most important. In general, many studies have reported that soil organic carbon (SOC) content and its decomposition is positively correlated with increased atmospheric CH_4 and production (Verma *et al*., 2002; Cui *et al*., 2005; Belger *et al*., 2011; Dutta *et al*., 2013; Koebsch *et al*., 2013). Yu *et al*. (2013) and Konnerup *et al*. (2014) specifically found a positive relationship between CH_4 production and SOC (R^2 = 0.940, p = 0.006; R^2 = 0.563, p < 0.005, respectively—see Fig. 2.7).

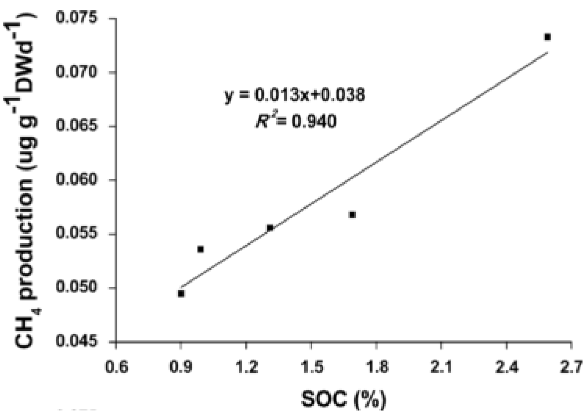

Figure 2.7. Correlation of CH_4 production (μg/g dry weight/day) with SOC (% of dry weight) (reproduced from Fig. 6 in Yu *et al*., 2013).

Given that the organic matter mainly comes from vegetation and phytoplankton, many authors have used productivity or plant biomass as a predictor of CH_4 production (C.B. Zhang *et* *al*., 2012; Koebsch *et al*., 2013). Earlier studies using *in vitro* measurements indicated organic matter as the major factor controlling CH_4 production (Boon and Mitchell, 1995). More recently, it was demonstrated that the larger biomass of invasive saltmarsh cordgrass (*Spartina alternifolia*) generates higher CH_4 emission rates than those in experimental mesocosms of native common reed (*Phragmites australis*) (Cheng *et al*., 2007). Chen *et al*. (2009) found a weak positive correlation between plant community height (used as a proxy for biomass) and methane emission rates (R^2 = 0.59, p < 0.01, n = 30). Further, data from Megonigal and Schlesinger (1997) revealed that CH_4 emission rates increase as a result of the higher activity of photosynthesis and organic carbon released into soils. Similarly, Joabsson *et al*. (1999) found in their experiment that the concentration of dissolved CH_4 in the rhizosphere was higher in vegetated plots than in plots where vegetation had been removed. Under dynamic conditions, Van Der Nat and Middelburg (2000) hypothesised that the rate of methane production was closely related to the growth cycle of plants.

The rate of CH_4 production and emissions in water systems (e.g., canals, rivers and estuaries) also depends on organic matter supply (Jayakumar *et al*., 2001; Datta *et al*., 2013; Dutta *et al*., 2013; Reshmi *et al*., 2015). Smith *et al*. (2000) demonstrated this phenomenon when they sampled soils four metres from the shoreline at Lake Merecure, Venezuela. The soils in this study were covered by decomposed plant material and emitted four to six times more CH_4 than did soils in the same position at Lake Mamo, where no plant material had accumulated. Aquaculture ponds also produced the most CH_4 when they were affected by sewage (Strangmann *et al*., 2008). In a tropical mangrove-dominated estuary off the northeast coast of Bay of Bengal, India, mangrove litter provides nutrients for phytoplankton, resulting in algal blooms and ultimately increasing CH_4 production (Biswas *et al*., 2007). The availability of high organic carbon contributes to enhanced decomposition rates, along with high temperatures, which lead to the production of substrates for methanogenic microorganisms (Boon and Mitchell, 1995; Cui *et al*., 2005; Krupadam *et al*., 2007).

In contrast, Sutton-Grier and Megonigal (2011) found a negative relationship between below-ground biomass and the production of CH_4 in their experimental mesocosms. In this case, plant-mediated oxygen supply to the root zone regulated the competition between methanogenic and non-methanogenic microorganisms. Given that more Fe^{2+} was oxidised, leading to increased Fe^{3+}, methanogens were out-competed by Fe^{3+}-reducing bacteria for organic matter (Sutton-Grier and Megonigal 2011; Megonigal *et al*., 2013). This condition may also occur in the case of sulfate-reducing bacteria in marine systems. High sulfate content in saline waters causes more favourable conditions for sulfate-reducing bacteria than for methanogens, which use competitive substrates—acetate and H_2/CO_2 (Boon and Mitchell, 1995; Giani *et al*., 1996; Van Der Nat *et al*., 1998). For example, Shalini *et al*. (2006) found a negative correlation between dissolved CH_4 and dissolved sulfate in the estuary of Pulicat Lake, India (R^2 = 0.49,

n = 52). In laboratory incubations, the sulfide production rate can reach up to 200 times greater than the CH_4 production rate. In addition, the suppression of methanogenesis also occurs when nitrate or manganese-reducing bacteria out-compete methanogens (Biswas *et al*., 2007; Krupadam *et al*., 2007). For these substrate competitions, Verma *et al*. (2002) demonstrated a negative relationship between CH_4 emissions and electron acceptors, including dissolved iron and manganese (R^2 = 0.77; R^2 = 0.98) and sediment iron and manganese (R^2 = 0.61; R^2 = 0.57).

2.5.2 Salinity

The competition for substrates between methanogens and non-methanogens in saline waters has been generally accepted, since the majority of methanogenesis uses acetate, H_2/CO_2 or other competitive substrates. As a result, CH_4 emissions in marine environments are expected to be negligible. However, the direction of that competition is likely to change if there is an abundance of organic matter or the presence of methylated compounds, as reported by Aulakh *et al*. (2001) and Reshmi *et al*. (2015) from mangrove sites in Tanzania and India, and by Zhuang (2014) from sea bottom sediment in Aarhus Bay, Denmark, and the Mediterranean Sea. In the first case, methanogens may be active after sulfate depletion, while, in the second case, methanogenesis and sulfate reduction can coexist.

Although organic matter and electron acceptors are the major factors in methanogenesis, salinity is considered an additional factor controlling CH_4 production. When scholars identify salinity as a predictor for biogenic production of CH_4 in marine environments (Ramesh *et al*., 1997; Verma *et al*., 2002; Koebsch *et al*., 2013), sulfate content is actually the salient factor. As long as non-competitive substrates do not exist, quantitative data have revealed strong relationships between salinity and CH_4 production and emissions or dissolved CH_4, as reported by Scranton and McShane (1991), Ramesh *et al*. (1997), Jayakumar *et al*. (2001), Verma *et al*. (2002), Shalini *et al*. (2006), Poffenbarger *et al*. (2011) and Dutta *et al*. (2013). In contrast, Reshmi *et al*. (2015) did not find that salinity influenced methanogenesis in estuarine soils (Ashtamudi, India) as a result of methylotrophic methanogen abundance (non-competitive substrate users).

2.5.3 Temperature

Higher temperatures generally increase the level of bacterial activity. However, methanogens can remain active under low temperatures if there is sufficient available organic matter. Many authors have identified soil or air temperature as limiting factors of CH_4 production and emission, such as Verma *et al*. (2002), Cui *et al*. (2005), Inamori *et al*. (2007), Poffenbarger *et al*. (2011), Zhang and Ding (2011), Datta *et al*. (2013) and Lofton *et al*. (2014). Specifically, Boon and Mitchell (1995) found in their *in vitro* experiments that methanogenesis is highest at 30°C and least at 5°C, with the exception in sediment enriched with methanol (maximum at 20°C). Meanwhile, in a coastal brackish fen, in Rostock, Northeast Germany, CH_4

emissions were almost undetectable in air temperatures < 10°C and water temperatures < 8°C (Koebsch *et al*., 2013). Dutta *et al.* (2013) noted that CH_4 emission from sediment is positively correlated with the sediment temperature (n = 8, R^2 = 0.35). However, another correlation analysis revealed that the relationship was not statistically significant (R^2 = 0.078, n = 40, p = 0.10) (Purvaja *et al*., 2004). The correlation analysis indicated that CH_4 production is not only dependent on temperature, but also on other factors.

Sun *et al*. (2013) and Reshmi *et al*. (2015) explained that organic matter input, salinity and plant community are interrelated with temperature to control the production of CH_4. Using a step-wise linear regression approach, Chen *et al*. (2009) found that plant community and inundation depth were more likely to be key factors explaining the spatial variability of CH_4 emissions, rather than temperature. Similarly, when temperature was excluded from the list of independent variables of a step-wise linear regression, the height of the water table was the best explanatory variable for daily variation of CH_4 emissions (Yang *et al*., 2013).

2.5.4 Acidity, dissolved oxygen and redox potential

Although acidity (pH) is likely to be a secondary factor, dissolved oxygen and redox potential are strong limiting factors, since most methanogens are obligate anaerobic. Methanogenic communities are generally dominated by neutrophilic species (Koebsch *et al*., 2013; Megonigal *et al*., 2013). As a result, some studies have revealed that no significant relationships exist between pH and annual CH_4 flux (Koebsch *et al*., 2013) or CH_4 production (Yu *et al*., 2013), even though CH_4 emissions have increased in acidic soils along with a negative redox potential (Krupadam *et al*., 2007; Megonigal *et al*., 2013). In another study, the pH value did not vary greatly (Reshmi *et al*., 2015); hence, this cannot explain CH_4 variability. Conversely, oxygen availability inhibits methanogen activity (Ramesh *et al*., 1997; Konnerup *et al*., 2014), with soil redox potential as an indicator of this aerobic–anaerobic condition. In a review, Aulakh *et al*. (2001) found that soil anaerobiosis occurs at redox potentials (Eh) below -100 or -200 mV. There may be a gradation between aerobic and anaerobic conditions with soil depth; hence, dissolved CH_4 concentration may change gradually with the change of redox potential. This can be inferred from a strong correlation between dissolved CH_4 and Eh obtained from diurnal and seasonal measurements (Zhang and Ding, 2011; Marín-Muñiz *et al*., 2015).

The presence of an aerobic zone for CH_4 oxidisers or methanotrophs is also important in controlling CH_4 loss to the atmosphere. This is because they consume 14 to 36% of gross CH_4 emissions (Vann and Megonigal, 2003), ~43% of the annual potential flux of CH_4 in the oxic zone (Roslev and King, 1996) or up to 90% of dissolved CH_4 in the unsaturated zone (Fechner and Hemond, 1992). In general, extensive aerobic zones occur when the surface sediment is exposed to the atmosphere (Roslev and King, 1996). These conditions can also be found within submerged leaf sheaths and as a thin layer in a sediment–water interface when the sediment is inundated (Inamori *et al*., 2007). In addition, inside roots and the rhizosphere of aquatic plants are aerobic, since they have aerenchyma structures that can transport oxygen from the atmosphere to the root zone (Chowdhury and Dick, 2013). In some studies, different oxygen concentrations from the soil surface to the depth of aerobic–anaerobic zones result in stratification of CH_4 oxidation rates (Sundh *et al*., 1995; Bodelier *et al*., 2000; Siljanen *et al*., 2011). This oxidation also possibly occurs in the water column, since some methanotrophs have been detected living as plankton (Ross *et al*., 2001).

CH_4 concentration in pore or column water seems to control CH_4 oxidation. Sundh *et al*. (1995) included water table position (as the extension of the aerobic zone for the methanotrophs) and pore-water CH_4 concentration as independent variables in the regression equation when calculating CH_4 oxidation rates. Meanwhile, Lofton *et al*. (2014) found that the rate of CH_4 oxidation increased linearly with increased CH_4 concentration in the water column. Similarly, Megonigal (2002) suggested that CH_4 oxidation rates respond positively to gross CH_4 emission rates (R^2 = 0.96). His data also revealed that methanotrophs were very dependent on CH_4 concentration, rather than O_2, since the change of gross CH_4 emissions and oxidation in response to large differences in incubation temperature was similarly consistent.

From the discussion of CH_4 oxidation, we can conclude that the combination of aerobic conditions, high CH_4 concentration and temperature provide ideal ambient factors to support methanotrophs in reducing CH_4. However, to some extent, this environmental setting can be less favourable when other groups of bacteria out-compete methanotrophs for oxygen or nitrate (Van Bodegom *et al*., 2001). For nitrate-reducing bacteria, this competition only occurs when nitrate concentration is high, which is only found in laboratory conditions (Boon and Lee, 1997).

Although aquatic plants are essential in CH_4 production by supplying organic matter to methanogens, these plants have two contradictory roles in reducing CH_4. The roots of some aquatic plant species provide micro-habitats for methanotrophs (Inubushi *et al*., 2001; Inamori *et al*., 2007). The plants supply oxygen to the root zone, taking it from the atmosphere and transporting it through the stem and root tissues. However, some authors have reported that aquatic plants act as ventilation (e.g., Shannon and White, 1994). CH_4 in the anaerobic zone egresses through plant tissue, without passing through the CH_4 oxidation zone within the sediments. For example, water hyacinth is expected to facilitate CH_4 transport via the aerenchyma tissues from sediment to the atmosphere (Verma *et al*., 2002). Plant structures in mangrove species, known as pneumatophores, can also help this transportation (Purvaja *et al*., 2004).

In the discussions about CH_4 emissions from mangroves and other wetlands, net CH_4 emissions are the result of complex interacting processes involving interrelated or counteracting factors. However, methanogenic substrates and microbial metabolism can both act as proxies to explain the variability of CH_4 emissions in mangrove ecosystems. Therefore, further investigation and experimentation into methanogens and energy sources for these bacteria are strongly recommended.

2.6 Formulation of research questions

Global CH_4 fluxes from mangrove sediments are generally negligible (< 5 mg m^{-2} $hour^{-1}$) relative to the typical range in freshwater wetlands (0.6 to 13 mg m^{-2} $hour^{-1}$). However, CH_4 fluxes from mangrove sediment could as high as 83 mg m^{-2} $hour^{-1}$ (Chen *et al*., 2010), because the site has nutrient polluted sediments. Furthermore, to characterised CH_4 emissions from mangrove ecosystem in the global CH_4 emissions, the investigations of CH_4 fluxes should not only on the sediment–air interface, but also on other sources (e.g., water–air interface). CH_4 fluxes from water-air interface may have a great contribution to the total CH_4 fluxes of mangrove ecosystem (see 2.3.2). The source of CH_4 in the mangrove surrounding waters is not only produced in the water column but also supplied from mangrove pore-water. Thus, pore-water CH_4 could act as a proxy for CH_4 fluxes/transport, as well as production and consumption. To address the aim of this study, I chose to investigate dynamics of dissolved pore-water CH_4.

This study focused on the role of mangrove regrowth following rehabilitation on dissolved CH_4 pore-water. It also investigated physicochemical factors that may be controlling CH_4 production and consumption, as well as the microbial metabolism involved in such processes. The specific study aims and research questions are presented as follows:

A. The development of a method to measure pore-water CH_4

1. How can filter and chamber modification affect the performance of a multilevel pore-water sampler designed by Martin *et al*. (2003) in various mangrove soils?
2. How to transport gas samples extracted from pore-water?

B. The quantification of dissolved CH_4 concentrations and identification of mangrove regrowth effects

1. What is the relationship between stand basal area (a surrogate of stand age) and pore-water dissolved CH_4?
2. How do the physicochemical characteristics of pore-water relate to dissolved CH_4?
3. How do pore-water CH_4 concentrations change seasonally?

C. The identification of the dominant methanogenic pathway

1. Can the dominant methanogenic pathways be determined using concentrations of SO_4^{2-}, S^{2+}, Fe^{2+}, Fe^{3+} and Cl^-?
2. How can the dominant pathway be identified through substrate (i.e., methanol, acetate, hydrogen) enrichment of mangrove sediment samples?
3. What is the relative abundance of methanogenic groups? What is the abundance of sulfate-reducing bacteria?

Chapter 3: Research approach, site descriptions and general methods

3.1 Research approach

As formulated in Chapter 2, the research consisted of three major components: (i) development of a method to measure pore-water CH_4, (ii) quantification of pore-water CH_4 and (iii) identification of the dominant pathway of CH_4 production (see Fig. 3.1). First, the development of a method to accurately measure pore-water CH_4 is urgently needed to overcome current methodological limitations in remote locations (Chapter 4). This includes the repeated non-destructive sampling of pore-water and the subsequent extraction of dissolved CH_4 using the headspace equilibration technique. To determine variability in pore-water CH_4 concentrations and the factors controlling such variability, this study measured dissolved CH_4 concentrations in mangrove sediments at contrasting sites and identified the effects of mangrove regrowth on dissolved CH_4 (Chapter 5). This study also identified the dominant methanogenic pathway to understand the microbial processes underpinning CH_4 productions (Chapter 6). Chapter 6 consisted of: (i) a geochemical study using the pore-water CH_4 measurement method described in Chapter 4 and (ii) a microbial study including abundance estimation of methanogens and sulfate-reducing bacteria, along with associated laboratory experiments that used methanogenic substrate enrichments of the soil slurry samples (i.e., methanol, acetate and hydrogen).

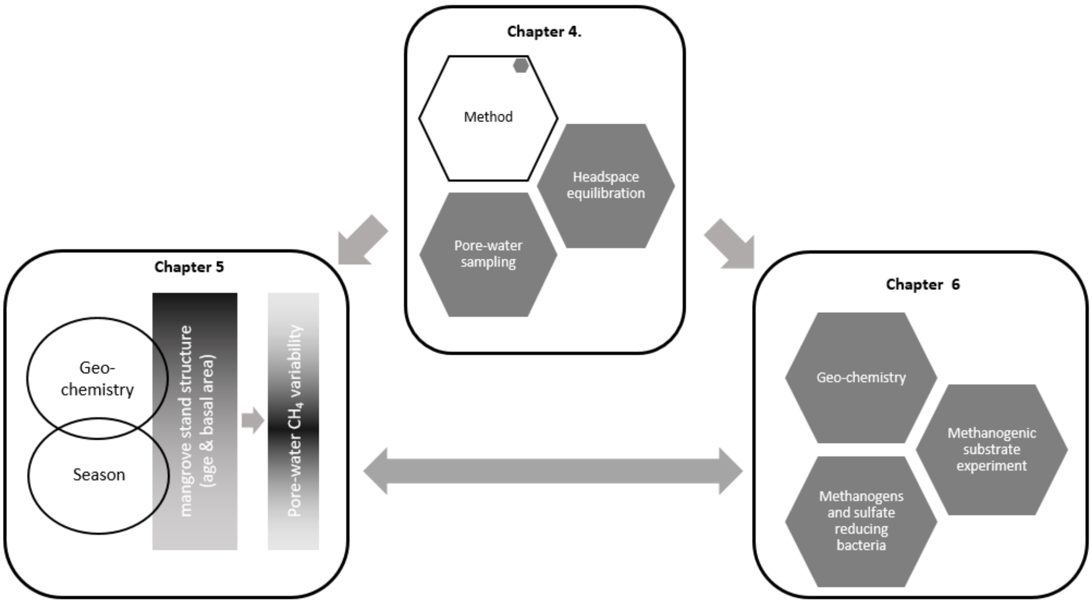

Figure 3.1. Study components, data chapters and the interrelationships.

Table 3.1 outlines the structure by which each research component was linked to key research questions and targeted datasets or outcomes. Chapter 4 will provide qualitative and quantitative data to indicate the performance of a modified pore-water sampler designed by Martin *et al*. (2003) in various mangrove soils. In addition, it will describe measurements of CH_4 gas standards with various concentrations that were stored in aluminium gas-tight bags and transported from the field site to the laboratory via a commercial aircraft. Chapter 5 will focus mainly on investigating the effect of mangrove regrowth on dissolved CH_4, complemented by analysing potential confounding factors. Chapter 6 will provide depth profiles of key ion parameters involved in methanogenesis and sulfate reduction. In addition, it will present the results of laboratory experiments investigating the effect of substrate enrichments (i.e., methanol, acetate and hydrogen) on the flux of CH_4 released from the sediment samples. Together with these results, the relative abundance of methanogen and sulfate-reducing bacteria will elucidate the dominant methanogenic pathways in the study site.

Table 3.1. Summary of research questions and outcomes of each study component.

Study component	Research question(s)	Outcomes
Chapter 4 Development of a method to measure pore-water CH_4	How can filter and chamber modification affect the performance of a multilevel pore-water sampler designed by Martin *et al*. (2003) in various mangrove soils?	Qualitative data taken from laboratory experiments using freshwater with different colours Quantitative data of depth profiles of physicochemical parameters and dissolved CH_4
	How to transport gas samples extracted from pore-water?	CH_4 measurements of gas standard kept in aluminium gas bags, transported by plane
Chapter 5 Quantification of pore-water CH_4 concentrations and identification of mangrove regrowth effects	What is the relationship between stand basal area (a surrogate of stand ages) and pore-water dissolved CH_4?	Relationship of pore-water dissolved CH_4 concentration and stand basal area
	How do the physicochemical characteristics of pore-water relate to dissolved CH_4?	Relationships of pore-water dissolved CH_4 concentrations and physicochemical factors
	How do pore-water CH_4 concentrations change seasonally?	Seasonal variation of pore-water dissolved CH_4 concentrations
Chapter 6 Identification of the dominant pathway of CH_4 production	Can the dominant methanogenic pathways be determined by concentrations of SO_4^{2-}, S^{2+}, Fe^{2+}, Fe^{3+} and Cl^-?	Depth profiles of SO_4^{2-}, S^{2+}, Fe^{2+}, Fe^{3+}, Cl^- and CH_4 concentrations
	How can the dominant pathway be identified through substrate (i.e., methanol, acetate, hydrogen) enrichments of mangrove sediment samples?	CH_4 concentrations released from mangrove sediment slurry after substrate enrichments
	What is the relative abundance of methanogenic groups? What is the abundance of sulfate-reducing bacteria?	Relative abundance of methanogens and sulfate-reducing bacteria

3.2 Site descriptions

The empirical data of this research were primarily based on a field study in Dusun Lantangpeo, Tanakeke Island, South Sulawesi, Indonesia (5° 27’ S and 119° 17’E) (Fig. 3.2). This is one of a series of mangrove rehabilitation sites implementing the EMR approach in Indonesia. This rehabilitation site was selected for this thesis because there was an active EMR project that had been successful in terms of mangrove recruitment (Brown *et al.*, 2014). A physical description of the site is given below and a more detailed description of the EMR program follows in a later section.

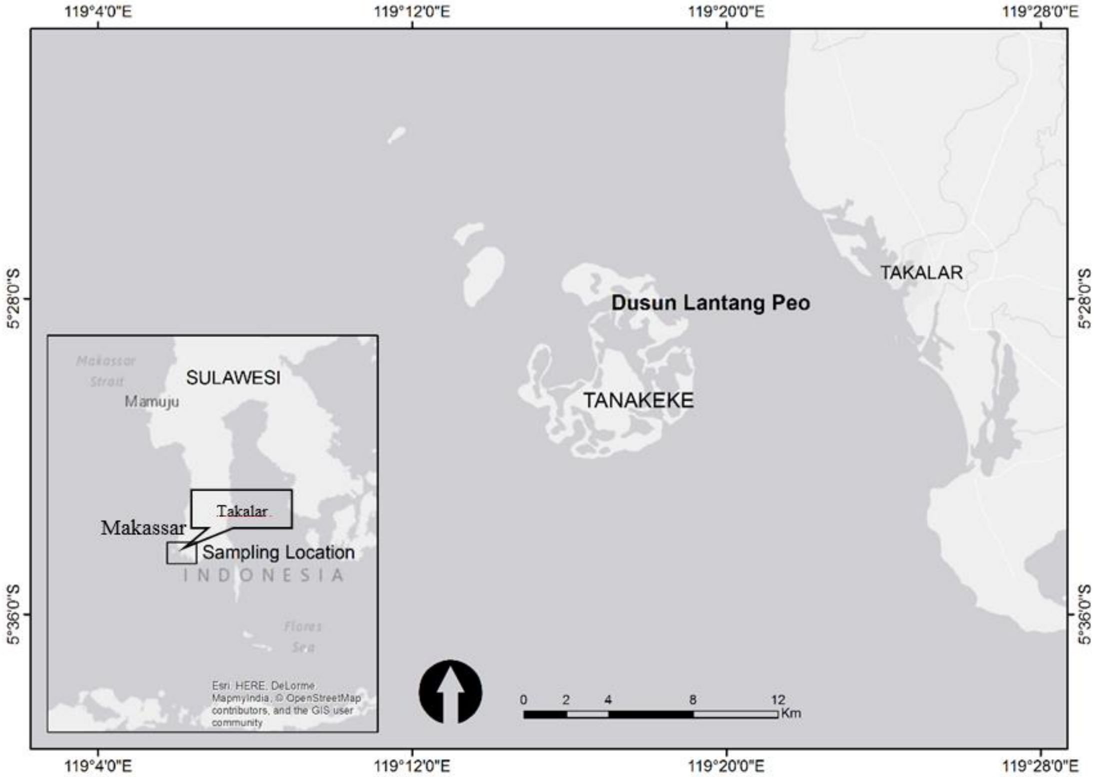

Figure 3.2. Regional map showing location of the field site at Lantangpeo, Tanakeke Island.

Tanakeke is a coralline island located around 10 km from the mainland of Sulawesi and falling within the Takalar (administrative) District, Province of South Sulawesi (Fig. 3.2). It is about 40 km southwest of Makassar, the capital city of the province. The island has a tropical climate, with two distinct seasons. It experiences a wet season from November to April, although occasional dry season rainfalls do occur (Fig. 3.3). The annual average precipitation is around 3,000 mm, and around 80% of that typically falls in the wet season. Air temperature is reasonably stable with respect to small diurnal or seasonal fluctuations (Fig. 3.3). The annual mean minimum and maximum air temperature is around 25°C and 32°C, respectively, with an overall annual mean air temperature close to 28°C.

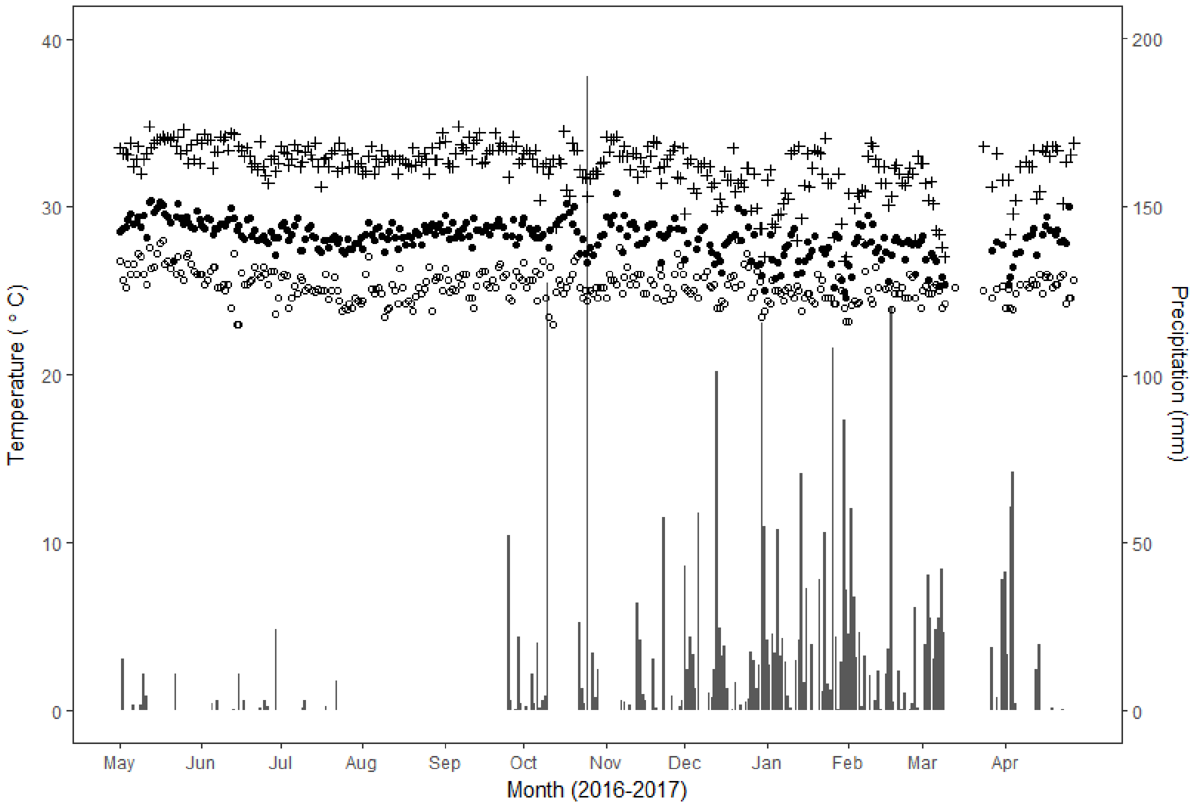

Figure 3.3. Climate data from May 2016 to April 2017 showing daily precipitation (bars, right axis) and daily air temperature (left axis). Open circles, closed circles and plus symbols indicate minimum, mean and maximum temperature, respectively (Meteorological, Climatological, and Geophysical Agency—Stasiun Meteorologi Maritim Paotere, Makassar).

In Tanakeke, mangrove vegetation grows in sandy sediments, adjacent to seagrass beds and coral reefs, which are a dominant feature of the island. The mangrove vegetation is inundated by tides on a (near) daily basis. There is approximately one low and one high tide per day, with a maximum range of 1 m difference between low and high tide. At the highest high tide, there is around 0.5 m depth of sea water covering the soil surface. The mangrove vegetation is characterised as an overwash mangrove, dominated by *Rhizophora stylosa* (Setiawan and Mursidin, 2018). A further 10 species compose commonly occurring mangrove communities on the island, including *Avicennia alba*, *Bruguiera gymnorrhiza*, *Excoecaria agallocha*, *Gymnanthera paludosa*, *Heritiera littoralis*, *Lumnitzera racemosa*, *Pemphis acidula*, *Rhizophora apiculata*, *Rhizophora mucronata* and *Sonneratia alba*.

In Lantangpeo, nine study sites were selected systematically, based on the variation in canopy density of the mangrove stands as a result of natural regeneration and EMR (Fig. 3.4). The site selection was to accommodate the research objective of Chapter 5, where long-term measurements of pore-water dissolved CH_4 were undertaken. First, two different groups of sites were selected. Sites 1 to 3 were chosen to represent new (< 5 years) regeneration sites, while Sites 4 to 6 represented old (> 10 years) regeneration sites. I also selected three sites (Sites 7 to

9) that contained natural mangroves to act as control sites. These sites were selected after consultation with local inhabitants. The field evaluation for the pore-water samplers (Chapter 4) and microbial analysis (Chapter 6) were conducted only on Sites 3, 5 and 8, which associated with the rehabilitation/regeneration status.

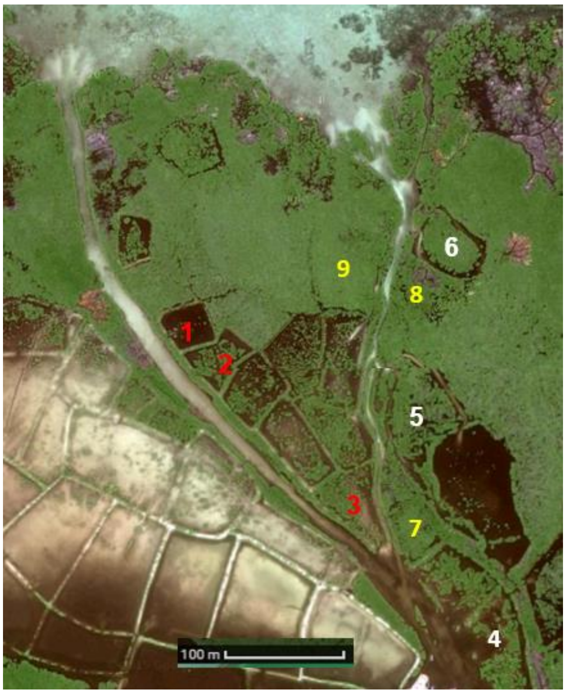

Figure 3.4. **Site locations in the study area. Distribution of sampling sites (1 to 9) plotted on Google Earth imagery, depicting the landscape of aquaculture ponds and mangroves with two creeks splitting the landscapes. White and brown colour spotted by green (lower section of figure) depicts recently abandoned ponds; patches of green colour surrounded by a brown line depict long abandoned ponds; green colour blocks show undisturbed mangrove vegetation.**

3.3 History of mangrove rehabilitation in Tanakeke Island

According to 2016 Census, Department of Statistics, Takalar District, Tanakeke was inhabited by around 7,700 people in 2016, residing in settlements on the terrestrial part of the island. Some of the inhabitants had built a kampong or hamlet in shallow water adjacent to mangroves and fishponds. They reclaimed the shallow waters by using coral stones, sands and stranded coarse woody debris (e.g., logs and branches) and then built a *rumah panggung* or 'stage house' on top of this reclaimed land. The study area at Lantangpeo was one of the kampongs in the north of Tanakeke and had around 400 inhabitants. Unlike other kampongs, this kampong had not yet been connected to the electricity grid, and the local inhabitants relied on a fossil-fuel generator that operated for four hours each night to supply electricity. In addition, Lantangpeo had no access to freshwater and the local inhabitants had to purchase freshwater from adjoining kampongs or harvest rainwater.

Overall, the islanders gained their livelihood from fishing and farming (Brown *et al*., 2014). Capturing fish in mangrove lagoons and coral reefs was generally undertaken for subsistence needs, although villagers could also sell surplus captures. A few residents who lived on the terrestrial part of the island also cultivated rice and vegetables, but this agriculture activity had previously ceased when shrimp farming in ponds became more profitable. After shrimp farming collapsed because of disease, the islanders abandoned this activity and only a few continued using the ponds for milkfish culture. For those who owned rice fields, these were revitalised to support their livelihoods. At the time of the research, most of the islanders relied on seaweed farming in the adjacent lagoons for their livelihoods.

The shifting of livelihoods in Tanakeke Island, particularly to shrimp farming, has changed the environment and landscape of the island significantly over the last three decades. In 1979, unlike most mangrove forests in the Takalar district, mangrove forests in Tanakeke were intact ecosystems (Malik *et al*., 2017; see Fig. 3.5). However, a success story in aquaculture business within the broader region triggered farmers on Tanakeke Island to clear the available mangrove stands for aquaculture ponds. Hence, by 1996, almost 70% of the former mangrove stands on Tanakeke were occupied by aquaculture developments (Fig. 3.5). In 2003, aquaculture activities collapsed because of white spot disease outbreaks attacking shrimp cultures (Tangko and Pantjara, 2007). Thus, aquaculture was no longer profitable, and the farmers abandoned the aquaculture ponds (Brown *et al*., 2014). At that time (2003), there was no rehabilitation of the abandoned aquaculture ponds, but mangrove stands could naturally regenerate in some abandoned ponds.

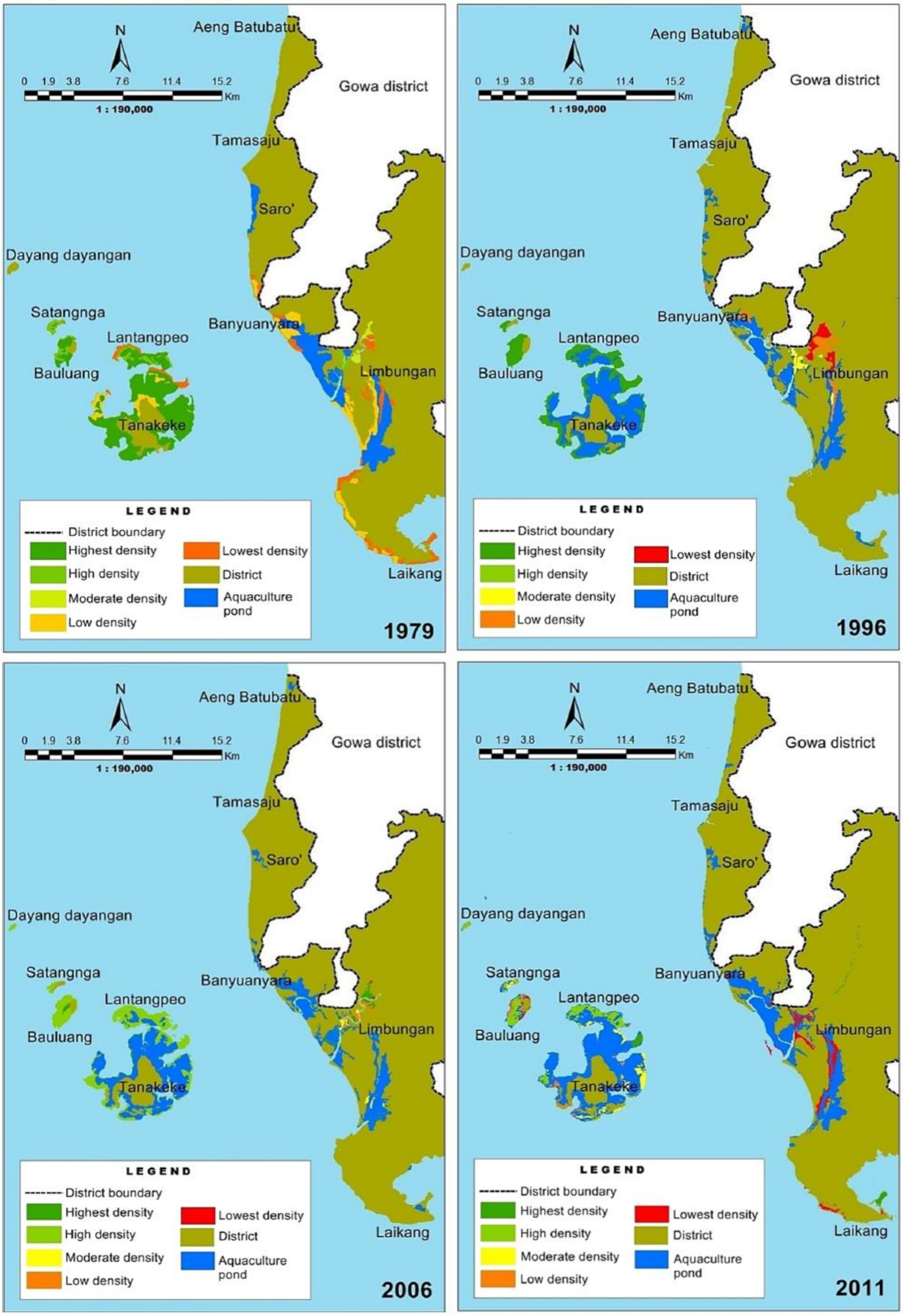

Figure 3.5. **Historical development of aquaculture and effect on mangrove stands in the Takalar District (1979–2011). Mangroves are classified into five classes (highest to lowest) based on canopy density (reproduced from Fig. 2. in Malik *et al*., 2017).**

To restore the local economy and the environment in the abandoned aquaculture ponds that could not or were less occupied by mangrove seedlings, Mangrove Action Project—Indonesia (MAP–Indonesia) combined with a variety of NGO partners to undertake social and physical works through *Community-based Ecological Mangrove Rehabilitation* (CB-EMR) in 2012. This is an adaption of EMR to involve socioeconomic aspects, particularly in the issue of land tenure. Of the 400 ha of ponds in the broader Tanakeke EMR project, 64 ha were located in Lantangpeo (Brown *et al*., 2014).

EMR is a rehabilitation or restoration method that attempts to create conditions that facilitate natural recruitment and regeneration of mangrove vegetation (Lewis and Brown, 2014). This is a general approach that can be readily adapted to a variety of local situations and circumstances. There are at least six steps to be followed, including: (i) preliminary assessment, (ii) biophysical assessment, (iii) socioeconomic assessment, (iv) site selection, (v) project design and (vi) project implementation and monitoring. Further information on EMR can be found in *Ecological Mangrove Rehabilitation: A Field Manual for Practitioners* (Lewis and Brown, 2014).

In the EMR case study of Tanakeke, MAP–Indonesia led a number of institutions and communities to implement the project (Brown *et al*., 2014), including the Canadian International Development Agency and Oxfam Great Britain as sources of project funding. Yayasan Konservasi Laut, a local NGO, was the main collaborator at the community level. In addition, numerous Indonesian government agencies, from provincial to village levels, acted to assist in terms of coordination, training and policy development, while universities were involved in the project by providing technical support, background studies and guidance.

Brown *et al*. (2014) claimed that the Tanakeke EMR project, covering six locations, was successful, at least based on the criteria of plant recruitment and early growth. They selected a relatively pristine site on the island of Panikiang, 150 km north of Tanakeke, as a reference site to determine the benchmark criteria of plant recruitment, which was 1,250 plants per ha. They reported that the EMR project in Lantangpeo exceeded that benchmark after 32 months.

3.4 General methods

The rehabilitation site in Lantangpeo was considered suitable to meet the principal aim of this research. The main requirement was that pore-water dissolved CH_4 should be mainly affected by mangrove regrowth. In this research, mangrove regrowth was defined as an increase of mangrove stand basal area over time in a rehabilitation site (see Chapter 5). Therefore, all potential confounding factors should be minimised. Fortunately, the rehabilitation site in Lantangpeo was relatively homogenous in terms of species composition, which was predominantly *Rhizophora stylosa*. All the rehabilitation sites were in the same hydrological regimes (i.e. tidal cycle and relative position to mean sea level), with more or less the same sediment types—coralline sands. Located on a small island, these sites were unlikely to have influences from terrestrial inputs, which could affect methanogenesis because of changes in geochemistry or the supply of organic carbon.

Nevertheless, because of Lantangpeo being relatively remote in terms of access to freshwater and electricity, fieldwork that required electric power or freshwater would not be suitable. Transportation was also another issue for fieldwork in this study location. Therefore, only two possible approaches applied in this situation: using portable equipment with long-lasting batteries and minimising the transport of samples back to the laboratory. Although I worked with sediment samples, data collection in the current study heavily relied on pore-water samples. I needed a large volume of pore-water samples to undertake repeated measurements of several parameters, including dissolved CH_4 and various physicochemical factors. Consequently, I developed a pore-water sampler that could overcome the limitations of working in Lantangpeo (see Chapter 4 for further explanation). In addition, I expelled dissolved gas from the pore-water samples and stored the gas samples in gas-tight aluminium bags for ease of transportation. I used field portable instruments to measure physicochemical factors at the time of sampling (see Chapters 4 and 5). Hence, only small amounts of pore-water and sediment samples were transported to a laboratory for parameters that could not be analysed *in situ*, such as Cl^- content and abundance of methanogen and sulfate-reducing bacteria.

Chapter 4: Measuring dissolved methane in mangrove pore-water

4.1 Introduction

Increases in atmospheric methane (CH_4) concentration are an important anthropogenic forcing of the global climate. Although the current atmospheric concentration of CH_4 (~1.8 ppm) is substantially smaller than carbon dioxide (CO_2, ~400 ppm), on a mass basis, CH_4 has 25 times the Global Warming Potential (GWP) of CO_2 (Forster *et al*., 2007). In addition, current understanding suggests that atmospheric CH_4 has experienced a 150% increase since the 1700s (IPCC, 2013; Reay *et al.*, 2018), while CO_2 has increased by around 40% over the same period (IPCC, 2013). An increase in the atmospheric concentration of these two greenhouse gases increases the Earth's surface temperature, which then, in a classic positive feedback, has the potential to further increase CH_4 emissions either from natural or anthropogenic sources (Dean *et al.*, 2018; Reay *et al.*, 2018).

CH_4 production by methanogenic microorganisms in the anoxic sediments of coastal wetlands is mainly controlled by carbon source availability, temperature and the frequency of inundation (Dean *et al.*, 2018). Methanogens derive their carbon source from photosynthetic organisms (i.e., vegetation and phytoplankton). The productivity of vegetation and phytoplankton usually (Gamage *et al.*, 2018; Lahijani *et al.*, 2018; Xie *et al.*, 2018), but not always (e.g., Keys *et al*., 2018; Obermeier *et al*., 2018), increases with CO_2, implying the future possibility of greater substrate availability for CH_4 production. In addition, phytoplankton productivity in coastal wetlands can also increase for other reasons including, most commonly, nutrient enrichment from polluted rivers (Purvaja and Ramesh, 2000; Chuang *et al*., 2017). However, methanogens can only use the carbon substrate in anoxic environments (Wang *et al*., 1993; Le Mer and Roger, 2001). Sea level rise could promote new anoxic zones through an expansion of coastal wetlands (Geselbracht *et al*., 2015; Tabak *et al*., 2016) and alteration in the extent and frequency of inundation (Grenfell *et al*., 2016) leading to increased potential CH_4 emissions (Lu *et al*., 2018). Hence, there is widespread interest in CH_4 production and emission from coastal environments.

The role of mangrove vegetation in the global CH_4 budget is still under debate, and this situation is at least partly due to the lack of empirical studies. The available empirical data report CH_4 emissions from the sediment surface, varying from near zero (Giani *et al*., 1996; Alongi *et al*., 2004) to around 80 mg m^{-2} h^{-1} (Chen *et al*., 2010). Based on several previous studies that reported low CH_4 emissions from the sediment of mangrove ecosystems with low CH_4 emissions, Twilley *et al*. (2017) disregarded CH_4 emissions in their calculations of the global mangrove carbon budget. However, some recent studies have suggested that CH_4 emissions in mangrove ecosystems also occur at the interface of surrounding water bodies and the atmosphere (Linto *et al*., 2014; Call *et al*., 2015; Rosentreter *et al*., 2018). Furthermore, the dissolved CH_4 in the water bodies (i.e. mangrove creeks and estuarine waters) is mainly derived from mangrove pore-water, exported through tidal pumping (Call *et al.*, 2015). In addition, a number of recent studies in vegetated wetlands have demonstrated substantial CH_4 emissions through the stems of woody plants (Terazawa *et al*., 2015; Pangala *et al.*, 2017; Pitz *et al.*, 2018), which apparently also apply in mangrove wetlands (Jeffrey *et al*. 2019). Therefore, the CH_4 contribution to the carbon budget of mangrove ecosystems remains uncertain.

To address current gaps in the mangrove CH_4 budget, I proposed studying CH_4 dissolved in the pore-water within the sediments. The concentration of CH_4 in the pore-water at a given time is the result of a balance between the various processes involved in CH_4 production, consumption and transport. These processes occur at both short (diurnal) and longer (seasonal) timeframes. In addition, CH_4 production and consumption both vary with depth in sediment, which is apparently mainly due to the variability of carbon content and aerobic/anaerobic conditions with depth (Wassmann *et al*., 2000; Gonsalves *et al*., 2011; Xu *et al*., 2015; Islam *et al*., 2018). Further, vertical transport of (either gas phase or dissolved) CH_4 through the sediment would affect the pore-water CH_4 variability with depth, and eventually determine CH_4 emission variability (Bazhin, 2003).

The most advanced method of dissolved CH_4 measurement in pore-water is *in-situ* Raman measurement (X. Zhang *et al*., 2012), but this remains expensive and not widely used. To date, most studies of CH_4 pore-water have been based on pore-water extracted from sediments (Dutta *et al*., 2015; Chuang *et al*., 2016; Schile *et al*., 2017) either *ex-situ* or *in-situ* (Bufflap and Allen 1995; Prayitno, 2016). The ex-situ approach extracts pore-water in a laboratory from sediment cores using mechanical force (i.e., squeezing, centrifugation). This approach is simple, inexpensive and rapid, yet has the potential for oxidation, redox potential and temperature artefacts (Bufflap and Allen, 1995). In addition, it cannot be used for repeated sampling at the same location.

The *in-situ* approach withdraws pore-water from the sediment using either dialysis or suction-filtration. A dialysis pore-water sampler relies on the diffusive equilibration between a solute in the dialysis chambers and pore-water, separated by a semi-permeable membrane. Although the dialysis approach is unlikely to have potential artefacts, it can take up to 24 hours for equilibrium to be achieved (Xu *et al.*, 2012). The 24 hour time frame precludes the use of this method for diurnal sampling. The suction-filtration approach is undertaken by pumping out the pore-water in the field. This approach is both artefact-free and the sample volumes allow the possibility of, for example, diurnal sampling (Martin *et al*., 2003; Nayar *et al*., 2006; Beck *et al*., 2007). Current designs of suction-filtration samplers have been specific to particular applications and there is no generic design as yet. For example, Nayar *et al*. (2006) and Gao *et al*. (2012) developed a pore-water sampler for a single depth sample, while Martin *et al*. (2003)

and Beck *et al*. (2007) constructed a multilevel pore-water sampler for application in estuarine and intertidal flat sediments. Liu *et al*. (2018) further improved the multilevel pore-water sampler for use in deep-sea sediments.

Here, I describe the development of a complete CH_4 measurement system suitable for use in remote field locations. The pore-water sampler was constructed based on modifications to a design originally described by Martin *et al*. (2003) for collecting a minimum sample of 200 mL of pore-water. This volume of pore-water is necessary for measuring dissolved CH_4 using Magen *et al.* (2014) approach and some physicochemical parameters. Instead of transporting the pore-water samples to a laboratory, like in Magen *et al.* (2014), I evacuated gas dissolved in the pore-water samples in the field and stored that gas in aluminium gas-tight bags for transport to the laboratory. The gas samples are easy to be transported through various modes of transportation because it is obviously lighter than pore-water samples. The overall aim was to develop a new method for use in mangrove forests located in remote areas where transportation of samples can include traditional wooden boats, cars, and various types of aircraft. The method developed here would be suitable for use in other similarly located mangrove forests. In this paper, I (i) describe the design and performance of the new pore-water sampler in various mangrove soils, and (ii) report a series of tests to evaluate the reliability of the aluminium gas-tight bags to store and transport the extracted gas. Finally, I show typical CH_4 and related physicochemical data to demonstrate the utility of the new system.

4.2 Design and construction

I modified the pore-water sampler designed by Martin *et al*. (2003) and combined that with an adapted headspace equilibration method developed by Magen *et al*. (2014). The aim was to develop a new method for use in mangrove forests located in remote areas where transportation of samples can include traditional wooden boats, cars and airplanes. The method developed here would be suitable in other similarly located mangrove forests.

I initially developed several prototype pore-water samplers at the Engineering Workshop, Research School of Earth Science, Australian National University (RSES-ANU). The assessment of the sampler prototype was conducted at the Marine Biogeochemistry Laboratory, RSES-ANU, and in mangrove forests in Batemans Bay, New South Wales (NSW), Australia. I assessed each prototype in terms of the extraction rate of pore-water at multiple depths. The assessments described below include initial data, as well as data collected during a subsequent one-year field study in the mangrove forests of Lantangpeo, Tanakeke Island, South Sulawesi, Indonesia.

Here I will only shows the last two designs of pore-water samplers. This is because I perform a complete assessment for these samplers, including in the laboratory and fields (described in Section 4.4).

The near-final prototype consisted of three chambers located at 10, 40 and 70 cm from the cone-shaped end (Fig. 4.1A). Chambers are one of improvements in our design of pore-water sampler which previously designed by Martin *et al*. (2003).The chambers were made of solid PVC that was machined to make suitable grooves and holes (Fig. 4.1B and C). At each chamber position, the pipe wall was drilled to make six holes, with a curve-edged rectangular shape (1 cm × 2.5 cm). The holes were made along the circumference of the pipe, with a gap between holes of 1.5 cm (Fig. 4.1B). For the fabrication of the chamber ports, mesh screens were set between the chambers and pipe walls covering the holes. While, Martin *et al*. (2003) used a polypropylene mesh screen with mesh size of 210 µm, I constructed three prototypes of the pore-water samplers, using different sizes and materials for the mesh screens. The first was a polypropylene mesh with a mesh size of 20 µm, while the other two were made of stainless steel, with mesh sizes of 90 µm and 160 µm.

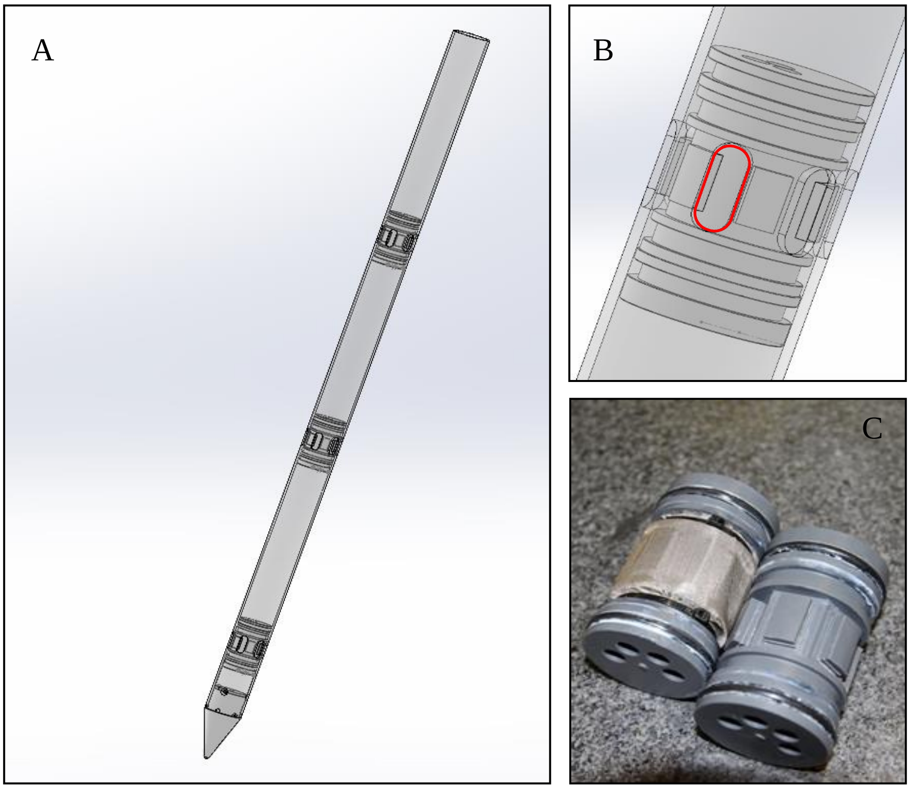

Figure 4.1. Prototype design of pore-water sampler with three chambers. (A) Whole body, (B) transparent inset of a chamber showing a hole of a port with curve-edged rectangular shape, (C) chambers with (left) and without (right) the mesh screen.

The final design of the pore-water samplers consisted of 10 chambers located at 10 cm intervals along the pipe length (Fig. 4.2AB). As previously mentioned, these pore-water samplers were made from 4.5 cm ID PVC pipe. In the final design, the chambers were simpler than those in the prototypes. They were made of 4.5 cm length and 2 cm ID PVC pipes and assembled inside the 4.5 cm ID pipe horizontally. The two ends of the 2 cm ID pipe were attached to the walls of the 4.5 cm ID pipe, where the wall had been drilled to make a round hole with 2 cm diameter (Fig. 4.2C). Stainless steel mesh (size 90 µm) covered the holes sandwiched between the outer walls of the pipe and patches. The patches were made of half round PVC pipe, with ID size of 5.5 cm.

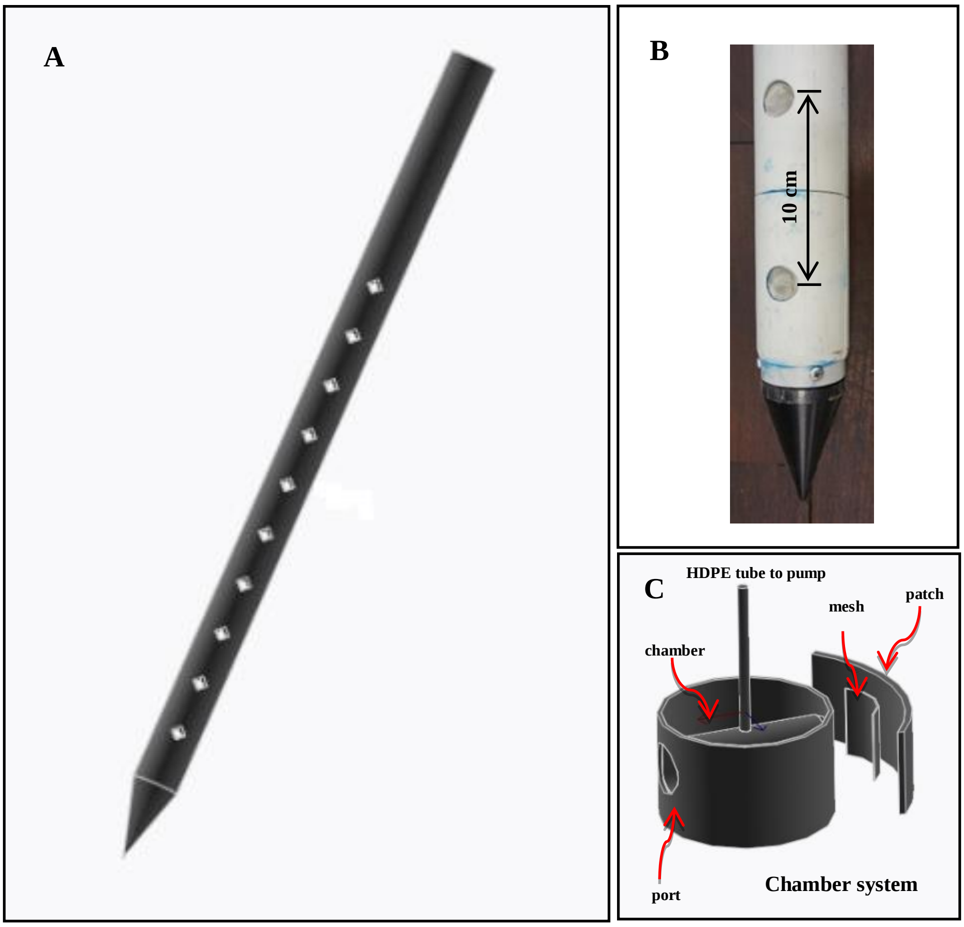

Figure 4.2. Final design of pore-water sampler. (A) Sampler body showing the 10 chambers, (B) inset of two chambers and circular holes of the ports, (C) port with installed stainless steel mesh (size 90 µm) screen.

4.3 Deployment and sampling

The deployment of the samplers in soft sediments was undertaken by pushing the samplers into the sediment. However, in some circumstances, I needed to make a hole using a hand corer or an additional PVC pipe that had the same diameter as the pore-water samplers. Making a hole was usually easy during low tide. Once the pore-water samplers were installed, the pore-water could be extracted at sequential sampling intervals. I used a small 12-volt peristaltic pump for each chamber. The pump had a maximum capacity of 100 ml water per minute. The power supply for the pump came from a 12 V, 100 Ah, sealed lead-acid rechargeable battery. The pore-water samples were collected into 120 ml glass bottles and sealed with a rubber stopper.

4.4 Initial evaluation of performance

During the prototyping, I tested the effectiveness of the mesh screen, including its opening size and material, to collect pore-water samples in different sediment types. The evaluation was based on both laboratory and field experiments.

4.4.1 Laboratory experiment

I undertook an initial laboratory experiment using a 20 µm square mesh screen. I used three sediment types, which included sand, silt and a composite sand-silt mixture in separate buckets to which tap water was added. The pore-water sampler was inserted into the sediment, so that the bottom chamber of the sampler was buried. Using a peristaltic pump, the pore-water was pumped out and the extraction rate (ml hour^{-1}) was measured. The extraction rate of pore-water from sandy sediment was the highest, accounting for 12,600 ml hour^{-1}. Extraction rates of 400 and 200 ml hour^{-1} were found in a finely textured sand-silt mixture and in silt sediments, respectively. The higher extraction rates from the coarse-grained (sand) sediment were expected (Masch and Denny, 1966).

4.4.2 Field experiment

I undertook field experiments using three identical pore-water samplers each fitted with a different mesh size (20 µm, 90 µm, 120 µm). The 20 µm mesh was made of polypropylene, while the other two mesh sizes were made from stainless steel. The samplers were sequentially installed into two different sediment types (inland mangrove, creek levee, see Table 1) within existing mangrove vegetation at Batemans Bay, NSW, Australia. Prior to installing the pore-water samplers, I used a PVC pipe with the same 4.5 cm ID to both create a suitable hole and to extract sediment for subsequent grain size analysis. I deployed the three samplers with a 1 m separation. Once the installation was completed, I extracted the pore-water using a peristaltic pump installed in each chamber. The extraction rate from all chambers was measured simultaneously.

The results were for extraction rates of 3000 to 4250 ml hour^{-1} in near pure sand that were independent of depth or mesh size (inland mangrove, Table 4.1). In contrast, at the other site with finer sediment texture (creek levee, Table 1), the extraction rates were again more or less independent of mesh size but they did vary with depth. The highest extraction rates were at the surface (~ 4000 ml hour^{-1}) with the extraction rate declining to 400 ml hour^{-1} at 75 cm depth. Because the sediment texture was more or less uniform with depth, I did not see the sediment texture is the salient factor controlling the extraction rates. At this stage, nevertheless, I did not further evaluate why the extraction rates varied with depth, because the minimum volume of all samples of pore-water was more than sufficient for CH_4 analysis. In particular, the system was capable of collecting the necessary 200 ml pore-water sample in 3-30 minutes.

Table 4.1. Extraction rates of pore-water measured from experiments using the prototype pore-water sampler in the Batemans Bay region of NSW (Prayitno, 2016).

No.	Opening filter size	Locations	Depth (cm); sediment	Extraction rate (ml $hour^{-1}$)
1	$20 \times 20\ \mu m^2$	Inland mangrove	Top (15); 73% sand, 22% silt, 5% clay	4,160
			Middle (45); 72% sand, 24% silt; 4% clay	4,250
			Bottom (75); 67% sand, 29% silt; 4% clay	600
		Creek levee	Top (15); 96% sand, ~0% silt, 4% clay	4,250
			Middle (45); 98% sand, 1% silt, 1% clay	4,250
			Bottom (75); 98% sand, ~0% silt, 2% clay	3,000
2	$90 \times 90\ \mu m^2$	Inland mangrove	Top (15)	4,000
			Middle (45)	800
			Bottom (75)	600
		Creek levee	Top (15)	4,500
			Middle (45)	4,250
			Bottom (75)	4,250
3	$120 \times 120\ \mu m^2$	Inland mangrove	Top (15)	4,250
			Middle (45)	2,800
			Bottom (75)	400
		Creek levee	Top (15)	4,300
			Middle (45)	4,250
			Bottom (75)	4,250

Our study has made progress in the extraction of pore-water, particularly in terms of extracted sample volume within a practical time scale. The performance of this sampler is generally similar to that developed by Martin *et al.* (2003), although the size of mesh screens used here (i.e., 20, 90 and 120 µm) are smaller than the earlier design (210 µm). In addition, the volume of extracted pore-water sample is considerably higher than those previously reported (cf. Table 4.1 and Table 4.2). The previous studies generally extracted a small volume of pore-water, mostly because of technical limitations of the methods. For example, squeezing or centrifugation approaches depend on the volume of the samples and water-holding capacity of the sediment. In Table 4.2, the highest volume extracted using the squeezing approach is 75 ml, which required 15 minutes of extraction time (Sasseville *et al*., 1974). Similarly, the extraction volume of dialysis pore-water samplers is dependent on the chamber size. Moreover, dialysis approaches need a longer time for equilibration—at least 24 hours (Xu *et al*., 2012), and the longest equilibration time reported is six weeks (Steinmann and Shotyk, 1996).

Table 4.2. Comparative analysis of volume rates of pore-water using various approaches.

Approach	Sediment type	Extracted volume (mL)	Time required	Sources
Squeezing	Unspecified (lake)	75	15 minutes	Sasseville *et al*. (1974)
	Unspecified (lake)	20	10–20 minutes	Robbins and Gustinis (1976)
	Unspecified (acid mine)	49	18 minutes	Lopes and Ribeiro (2005)
	Sand	1–10	Not informed	Huerta-Diaz *et al*. (2007)
	Clay	2–12	8–32 days	Fernández *et al*. (2014)
	Clay	10	15–20 minutes	Mazurek *et al*. (2015)
Centrifugation	Unspecified (marine)	5–10	60 minutes	de Lange *et al*. (1992)
	Unspecified (grassland)	6–10	50 minutes	Ronday (1997)
	Unspecified (acid mine)	49	45 minutes	Lopes and Ribeiro (2005)
Dialysis	Unspecified (bog)	5	7 days	Thomas and Arthur (2010)
	Unspecified (salt marsh)	20	2 weeks	Ugo *et al*. (1999)
	Unspecified (lake)	0.014	24–72 hours	Xu *et al*. (2012)
	Unspecified (mud flat)	30	2 weeks	Bertolin *et al*. (1995)
	Sand	3	< 1 week	Huerta-Diaz *et al*. (2007)
	Peat	30	4–6 weeks	Steinmann and Shotyk (1996)
Suction-filtration	Unspecified (lake)	5–10	30 minutes	Shotbolt (2010)
	Unspecified	6	1–12 hours	Darrouzet-Nardi and Weintraub (2014)
	Unspecified (lake)	0.01–0.05	< 0.5 minutes	Torres *et al*. (2013)
	Sand	Unlimited	Not informed	Beck *et al*. (2007)
	Sand	> 60	> 5 minutes	Nayar *et al*. (2006)
	Sand	Unlimited	Not informed	Martin *et al*. (2003)
	Sand	4000	1 hour	Current study

4.5 Extraction of dissolved methane

In this section I describe the entire procedure used to measure pore-water dissolved CH_4. Briefly, gas was extracted from the pore-water samples and subsequently transferred to aluminium gas-tight bags (Shanghai Sunrise Instrument Co., Ltd., Shanghai, 10 x 10 cm^2, 20 mL) while in the field. The aluminium gas-tight bags were then transported (by boat and aircraft) from the field site to the Greenhouse Gases Laboratory, Research Institute for Agricultural Environment, Indonesian Agency for Agricultural Research and Development, Pati, Central Java. The CH_4 gas concentration was determined using Shimadzu type 14A gas chromatography (GC) equipped with a flame ionisation detector (FID) and a packed column of Porapak Q. The temperatures of the GC were set at 25°C (injector), 50°C (column) and 300°C (detector). This instrument has a limit of detection of 0.12 ppmv for CH_4. I used the result of the GC measurement to calculate the concentration of CH_4 dissolved in the pore-water samples. A detailed calculation is described in the Appendix.

In more detail, the field-based procedure followed that used by Magen *et al.* (2014) with modifications as described below. In the field, the pore-water samples for gas extractions were stored in suitably labelled 120 ml glass bottles. The sample bottles were then carefully sealed with grey butyl stoppers without gas space at the top and transported to the field base camp. At room temperature, 25 ml of the pore-water solution was removed from each bottle and replaced with 25 ml of ultra-high purity (UHP) nitrogen (N_2) gas to a final pressure of 1.8 atm in the bottle head-space. Unlike the procedure described by Magen *et al*. (2014), in which the pore-water bottles were then sent to the laboratory, I extracted 20 ml of gas from the bottle headspace using a plastic syringe after vigorously shaking the bottles (~30 seconds). The extracted gas was then injected into aluminium gas-tight bags that were subsequently transported to the laboratory for further analysis. While the reliability of dissolved CH_4 measurement had been previously described by Magen *et al.* (2014), I had introduced an additional step into the procedure, i.e., the extraction and storage in gas-tight aluminium bags in the field.

Previous studies have noted the possibility of gas leakages and contamination (Fisher and Reddy, 2013; Sturm *et al.*, 2015) that would compromise the results. Accordingly, I evaluated the additional procedural step to confirm that the aluminium bags could store the gas samples and reliably transport them to a laboratory without any contamination. For this evaluation, I put known concentrations of standard CH_4 into several aluminium gas-tight bags (Shanghai Sunrise Instrument Co., Ltd., Shanghai, 10 x 10 cm^2, 20 mL) that were subsequently transported to the laboratory (~ 6-day delivery) and analysed for CH_4 concentrations. In this case, I only had two concentrations of certified standard CH_4 available—10.3 and 2055 ppm. These standards are diluted in nitrogen (N_2), supplied by PT Linde Indonesia, The Linde Group. I made 10 replicates for each concentration with each gas-tight bag having a volume of 20 ml. The GC measurement for the standard CH_4 (10.3 ppm) ranged between 8.2 and 10 ppm with a median from the 10 measurements of 9.6 ppm (Fig. 4.3). For the second CH_4 standard (2055 ppm) the GC measurements ranged between 1867 and 2038 ppm with a median from the 10 measurements of 2013 ppm. In both cases the GC measurement was slightly less than the corresponding standard but the difference was small and I concluded that the aluminium gas-tight bags were a reliable way to store and transport gas samples for a week long period.

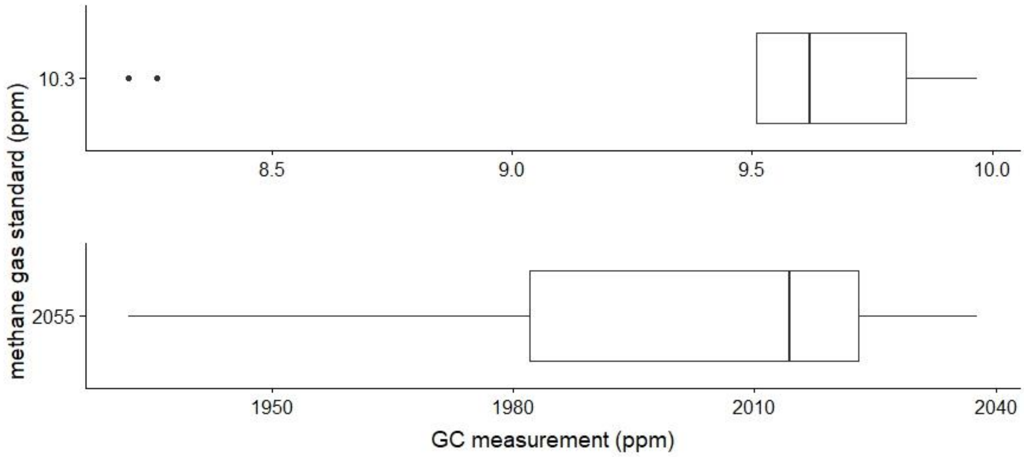

Figure 4.3. **Boxplot showing distribution of measured concentrations of CH_4 standards. Box shows inter-quartile range.**

4.6 Final design

After evaluating the performance of the various pore-water sampler prototypes, I finally adopted a 90 × 90 μm^2 mesh screen made of stainless steel for the final design. This was subsequently used in an extensive fieldwork program in mangrove forests of Lantangpeo, Tanakeke Island, South Sulawesi, Indonesia. I chose three sites for the evaluation reported here. Two sites represented a low- and a high-density mangrove regrowth stand (Fig. 4.4). The third site was a control site—a natural mangrove stand that was identified after consultation with local inhabitants.

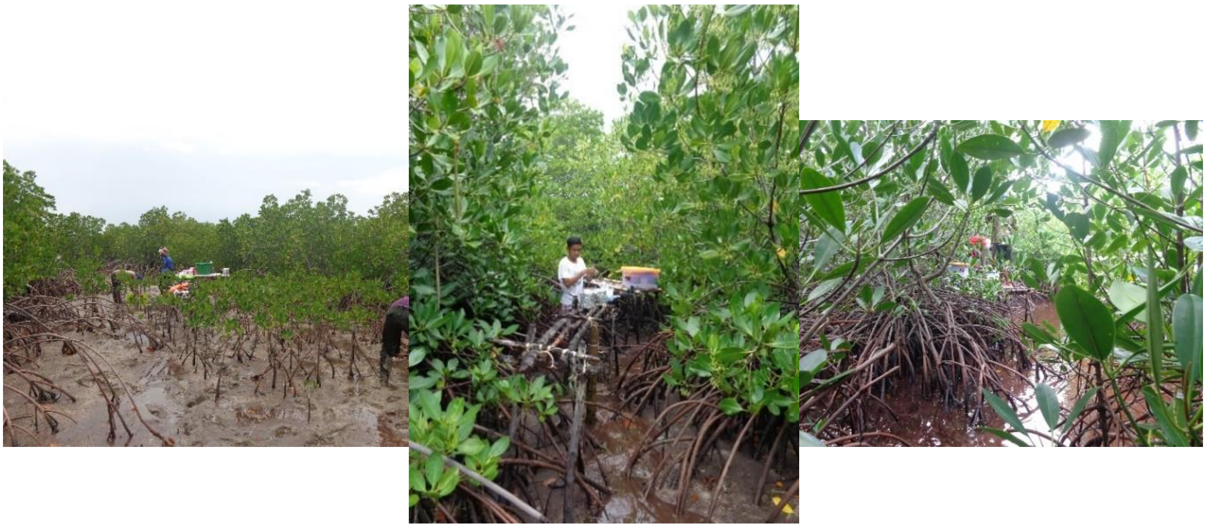

Figure 4.4. **The selected sites for evaluation of field performance for the final design pore-water samplers. (A) low- and (B) high-density mangrove regrowth sites, and the (C) natural mangrove site that was used as a control.**

4.7 Evaluation of field performance

When using the pore-water samplers during fieldwork, I had no major problems in acquiring the necessary volume (~200 mL) in a reasonable time frame (e.g. < 20 min). The sediment at the field sites was mostly coarse sand and the short time required to collect a sample was consistent with earlier tests using sandy sediments (Table 1). Occasionally, I experienced a blockage in some ports, but these blockages were always temporary. At this stage, I are confident with the broad applicability of the pore-water samplers, particularly for use in sandy sediments. I note that many mangrove systems occur in silt- (Gonthar et *et al*., 2014; Ha *et al*., 2018) or clay-dominated sediments (Ólafsson, 1995; Noronha-D'Mello and Nayak, 2015) and further evaluation of the sampler would be needed for those sediments.

The evaluation of field performance of the entire system was undertaken during an extensive fieldwork program measuring CH_4 using the method explained previously. In addition, I measured related physicochemical parameters. I present only two ancillary parameters for this evaluation, i.e. redox potential (ORP) and acidity (pH). Pore-water ORP is a useful parameter to define the presence of anaerobic conditions which is a requirement of CH_4 production. Pore-water pH is a factor indirectly controlling CH_4 production. The measurements were undertaken using Mi151 pH/ORP/Temperature Laboratory Bench Meter (Milwaukee, USA) in the field basecamp. The ORP value (Eh) was normalized with respect to a standard hydrogen electrode by adding +200 mV (Jardim, 2014; Bourgeois *et al*., 2019). Thus, based on the two ancillary parameters (pH and ORP), I demonstrated the performance of the pore-water sampler to provide reliable data of pore-water dissolved CH_4 and the underpinning biogeochemical mechanisms of CH_4 variability.

4.7.1 Depth profile from a single site

With each sampler having 10 chambers, I was able to derive depth profiles for dissolved CH_4 gas, as well as other relevant physicochemical variables. An example is shown in Fig. 4.5. For this sample, pore-water dissolved CH_4 was 11 µmol L^{-1} at 10 cm depth and increased gradually, with a peak of 40 µmol L^{-1} at 50 cm depth before gradually declining to very low values (~1 µmol L^{-1}) at 100 cm depth. By contrast, pore-water ORP and pH did not show significant variations with depth. The ORP and pH measured here fall within the optimum range for methanogenesis (Wang *et al.*, 1993; Le Mer and Roger, 2001; Inglett *et al.*, 2004). Accordingly, I concluded that in this environment, other variables (e.g., sulfate and sulfide concentrations [Chuang *et al*., 2016]) would likely be needed to fully interpret the concentration of dissolved methane in pore-water.

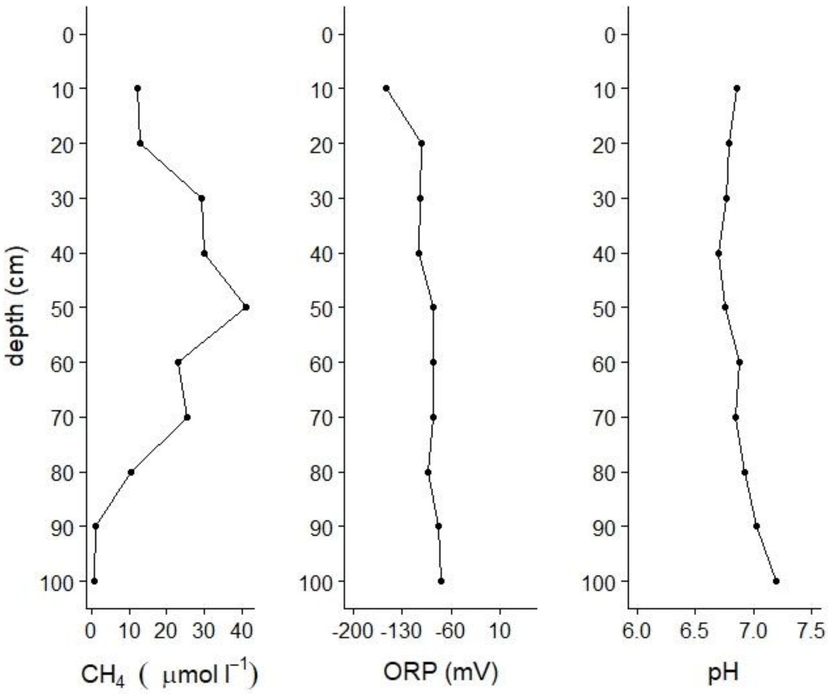

Figure 4.5. Example depth profile of pore-water CH_4 concentration, ORP and pH measured at one pore-water sampler located in a low-density mangrove regrowth site.

4.7.2 Diurnal sampling of depth profile from repeat sampling at a single site

With rapid extraction rates, the pore-water samplers can also provide measurement data over a day (i.e., a diurnal cycle) at multiple depths (Fig. 4.6. Top). Such data is needed to study interactions between pore-water CH_4 and the tidal cycle. Here I show a typical example of sampling every two hours during daylight at five different depths for CH_4, ORP and pH. In this example, again from the same low-density mangrove regrowth site (Fig. 4.4), the results indicate that CH_4 production was occurring at a depth of 20 cm in the morning between 8.00 and 10.00 am. There was no indication of CH_4 oxidation during low tide, as CH_4 concentration at this depth was stable (Fig. 4.6. Bottom). Changes in dissolved CH_4 at depths of 30 and 40 cm indicate vertical movement of CH_4 within the profile during the afternoon hours. pH was relatively stable over the daylight hours, while ORP showed a variability but still fell within the optimal range for CH_4 production (Fig. 4.6).

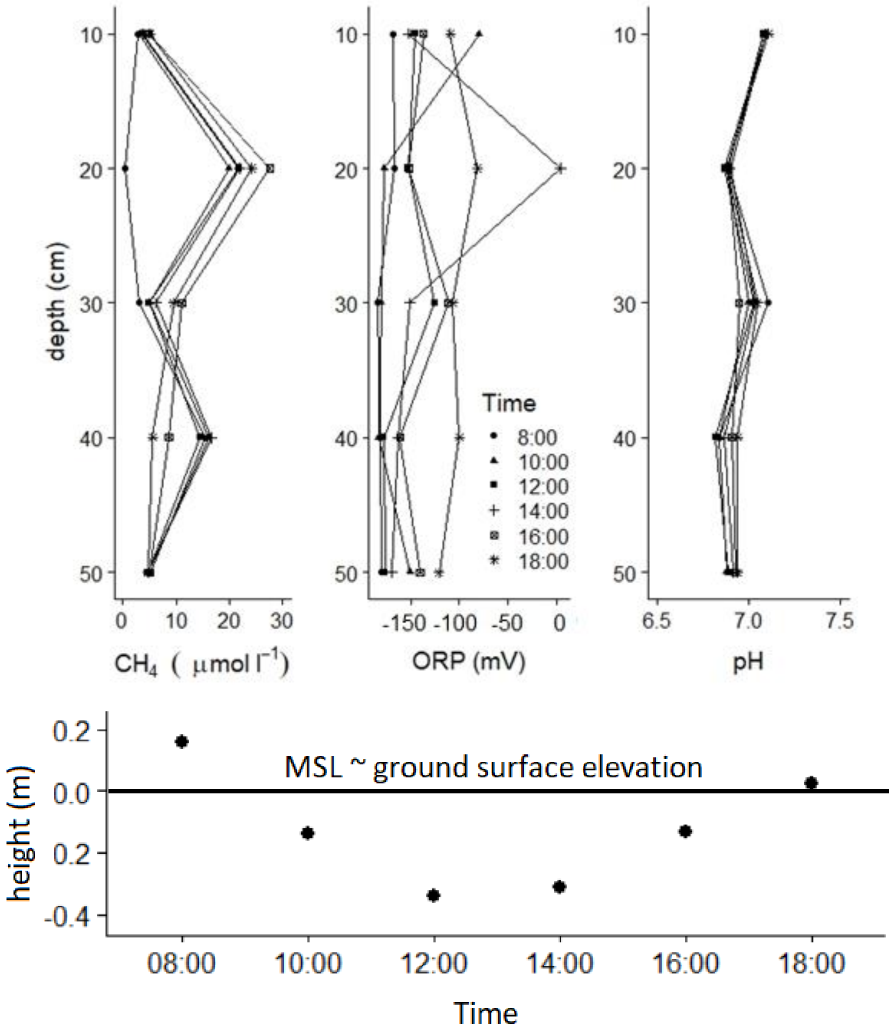

Figure 4.6. **(Top) Example depth profiles of pore-water CH_4 concentration, ORP and pH measured every two hours (from 8.00 to 18.00) in a low-density mangrove regrowth site. (Bottom) Tide height (m) relative to MSL**

4.7.3 Depth profile from three sites, three replicates

The pore-water samplers were also used to investigate local-scale spatial variation in the CH_4 concentration, ORP and pH. At each of the previously mentioned (three) sites, I examined differences in the variables sampled at three replicates located only 1 m apart to gain an appreciation of local scale variability (Fig. 4.7). These results showed that, even though the pore-water samplers were deployed in almost the same location (within 1 m), they generated variable data for all three variables. For instance, two depth profiles in the low-density site (Fig. 4.7) had a similar pattern, having a low concentration of CH_4 (1 - 4 µmol L^{-1}). In contrast, one depth profile had CH_4 concentrations of 5 and 8 µmol L^{-1} at depths of 20 and 30 cm, respectively. Moreover, the depth profiles of ORP showed a random pattern, although the values were within the range expected for anaerobic conditions (Wang *et al.*, 1993; Le Mer and Roger, 2001, Inglett *et al.*, 2004). Nonetheless, the high density and natural sites (Fig. 4.7) exhibited a low variability of pH values in replicates. Consequently, a research design of pore-water CH_4 in future studies should devote attention to this local-scale spatial variation.

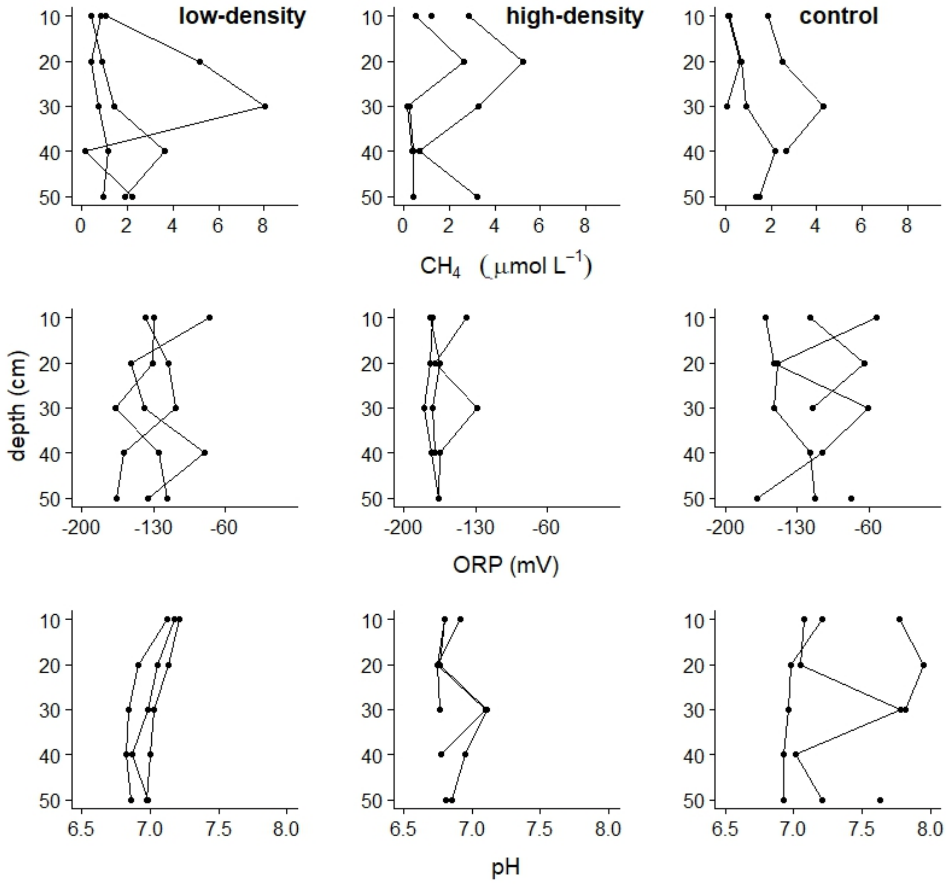

Figure 4.7. Depth profiles of (top) pore-water CH_4, (middle) ORP and (bottom) pH measured at the (left) low and (middle) high-density mangrove regrowth sites, and the (right) control site located in natural mangroves. Three replicates (separated by 1 m distance) were installed at each site to investigate local-site spatial variation.

4.8 Discussion

Field studies of pore-water dissolved CH_4 in mangrove ecosystems are scarce, probably because of methodological difficulties. The method described here has been successfully used to measure pore-water CH_4 and other relevant physicochemical variables in mangrove sediments in a remote field location. The main challenges were to design a system that could be used for repetitive non-destructive sampling of pore-water, with the CH_4 gas extracted from the pore-water in the field before transport to the laboratory for chemical analysis.

To address the aforementioned challenges, I modified the pore-water sampler originally developed by Marten *et al.* (2003) and adapted the method of dissolved gas extraction and CH_4

measurement described by Magen *et al.* (2014). In our final design of the pore-water sampler, I chose 90 µm mesh made from stainless steel, while Marten *et al.* (2003) used 210 µm screen made from polypropylene. This smaller selected mesh size (90 µm) is to minimize suspended sediment content in the pore-water samples. In the new design described here, chambers were installed between the ports and tubes (Fig. 4.2), while in Marten *et al.* (2003) the tubes were directly connected to the ports, which are covered by a polypropylene mesh screen. Chambers in the new design were added to prevent blockages. Under field conditions, primarily in sandy sediments, I found that blockages still did occur but were self-correcting as long as the pump kept working.

The CH_4 measurement method I developed can extract sufficient water samples in reasonable time frames. The pore-water sampler described here can extract a minimum volume of pore-water of around 4,000 ml per hour from mangrove forest with sandy sediments. This compares favourably with the 200 ml of pore-water that is needed to estimate dissolved CH_4 gas using the method described by Magen *et al.* (2014) and related physicochemical parameters. Hence, in a typical situation, I can collect sufficient pore-water for sampling in around three minutes (i.e., 200/4,000 hours ~3 minutes).

I am optimistic that our pore-water sampler can be used for repeat non-destructive sampling of pore-water. Moreover, I successfully measured pore-water CH_4 in mangrove sediments, as well as ancillary physicochemical variables. For instance, the depth profiles at 10 cm intervals down to a maximum depth of 100 cm demonstrated variations in pore-water CH_4 gas with depth (Fig. 4.5). With non-destructive repeat sampling capability, our method was also used to examine temporal (Fig. 4.6) and fine-scale spatial variations (Fig. 4.7) of pore-water CH_4.

The limitation in the CH_4 measurement method described here is the capacity of the gas sample storage containers to store and transport gas samples. The aluminium gas-tight bags used in this study were verified for storing the gas samples for a week (0.8-8% differences, see Fig. 4.3). This storage container has a relatively small mass/volume and was ideal for transport (e.g., boat, car, aircraft). However, the bags need to be handled with care, particularly during the injection of collected gas. Occasionally I found that the syringe needle can slip and puncture the bag wall. In addition, when transporting the gas-tight bags to a laboratory, they should be stored in a rigid box to prevent compression of the gas bags. In retrospect, placing the gas-tight aluminium bags in an ice box filled with frozen chill blocks would be a better approach to storage and transport.

The ultimate accuracy of any method to measure CH_4 gas concentrations will be limited by the sensitivity of the GC-FID. Fortunately, I used a GC with a detection limit of 0.12 ppmv, equivalent to 2.48 nmol L^{-1} for water with a salinity of 30 ppt at 30°C (see Appendix for the calculation). If I was to use a GC with a detection limit of 1 ppmv, then I would be able to measure pore-water CH_4 down to 0.3 µmol L^{-1}. For example, Giani *et al.* (1996) reported that their GC could not determine CH_4 concentrations in the pore-water samples less than 0.2 µmol L^{-1}. Meanwhile, Alongi *et al.* (1999) noted that they found no pore-water CH_4 in their samples by using a GC thermal conductivity detector. This is because it can only be used for a sample gas with CH_4 concentration greater than 100 ppmv or equivalent to 2 µmol L^{-1} (Magen *et al.*, 2014).

The method described here has the potential to expand the study of pore-water CH_4 in mangrove ecosystems. For example, pore-water CH_4 profiling can provide datasets to simulate CH_4 turnover (Chuang *et al.*, 2016). Diurnal measurements of pore-water CH_4 would be important for understanding the tidal effects on pore-water CH_4 dynamics and the diurnal role of photosynthesis in providing labile exudates to the soil (Girkin *et al*., 2018; Lu *et al*., 2018). This could potentially be integrated with tidal pumping studies using $_{222}Rn$ isotopes (Call *et al*., 2015) or pore-water CH_4 pumping based on observations of CH_4 enrichment in adjacent mangrove creeks, lagoons or estuaries (Jacotot *et al*., 2018; Rosentreter *et al*., 2018).

In summary, this study has established a method of measuring pore-water CH_4 in mangrove ecosystems. The pore-water extraction method is simple and inexpensive, being constructed using readily available PVC pipe and stainless steel mesh. In addition, this method offers artefact-free repeated extractions at a relatively high extraction rate (~4,000 ml $hour^{-1}$ in sandy sediments). When combined with sensitive GC or other gas measurement equipment, the CH_4 measurement system in this study can be operated at high temporal resolution, subject to labour constraints. Use of this method for CH_4 studies in mangrove ecosystems can help to resolve the importance of mangrove carbon budgets because of the lateral transport of dissolved inorganic and organic carbon in mangrove pore-water (Alongi, 2014; Twilley *et al*., 2017; Rosentreter *et al*., 2018).

Chapter 5: Mangrove regrowth may enhance dissolved methane in pore-water—A year-long study of an ecological mangrove rehabilitation site in Indonesia

5.1 Introduction

Methane (CH_4) emissions are becoming a global concern because of its positive feedback to climate change. CH_4, together with CO_2, causes an increase of Earth's surface temperature, and this could make a further increase in CH_4 emissions (Gedney *et al*., 2004). Also, CH_4, on a mass basis, is 25 times more potent in heating the Earth's surface than CO_2 (Forster *et al*., 2007). Its atmospheric concentration is steadily increasing, and is projected to be 2,200 ppb in 2030 (IPCC 2013). The contribution of wetland CH_4 emissions is about 23% of global CH_4 sources (Reeburgh, 2013) and represents around 60% of emissions from all natural sources (Kirschke *et al*., 2013).

Wetland contribution to CH_4 emissions may be increasing because of warmer temperatures as well as another climate change phenomenon (e.g., sea-level rise). Climate change modifies three main factors that control CH_4 emissions from wetlands: (1) soil temperature (controlling bacterial activity rates) (Inamori *et al*., 2007; Datta *et al*., 2013; Lofton *et al*., 2014), (2) water inundation (changing oxic–anoxic soil layers) (Zhang and Ding, 2011; Marín-Muñiz *et al*., 2015) and (3) soil carbon availability (providing favourable substrates for methanogens) (Yu *et al*., 2013; Konnerup *et al*., 2014).

Like other wetlands, mangrove ecosystems naturally produce and emit CH_4 because they accumulate soil organic matter and exist in primarily anaerobic and hydro-dynamically complex environments (Bouillon *et al*., 2008; Weston *et al*., 2014). However, the relative contributions of mangrove ecosystems to atmospheric CH_4 are still debatable (Chen *et al*., 2016; Cabezas *et al*., 2018). Studies measuring CH_4 emissions from mangrove ecosystems indicate a large range, from zero (Giani *et al*., 1996; Alongi *et al*., 2004) to around 80 mg m^{-2} h^{-1} (Chen *et al*., 2010).

To date, studies on CH_4 in mangrove ecosystems have focused primarily on soil surface CH_4 emissions (Giani *et al*., 1996; Chauhan *et al*., 2008; Krithika *et al*., 2008; Chen *et al*., 2016; Cabezas *et al*., 2018). Other studies have sought to explain the variability of methane emissions from mangrove ecosystems. For example, CH_4 produced in the soil can be transported to the atmosphere through the vascular tissue (i.e., stems) of herbaceous and woody plants (Van Der Nat *et al*., 1998; Bazhin, 2004; Pangala *et al*., 2013; Pangala *et al*., 2017; Maier *et al*., 2018). A recent study on the Amazon wetlands reported that CH_4 emissions from woody stems accounted for around 40% of total emissions and far exceeded soil surface emissions (~15% of the total). The remaining emissions (~45%) were from open water surfaces and the stems of herbaceous plants (Pangala *et al*., 2017). The results from this recent report provide evidence that previous estimates of mangrove contributions to ecosystem CH_4 emissions based only on soil surface CH_4 fluxes are likely to be underestimates.

In the present study, I observed dissolved CH_4 in mangrove pore-water as a source of the mangrove CH_4 emissions. This may be more representative of the contribution of mangrove ecosystems to global CH_4 emissions for two reasons. First, as aforementioned, mangrove tree-mediated CH_4 emissions may be mainly responsible for ecosystem CH_4 emissions. Indeed, recent literature reported this pathway of CH_4 emissions (Jeffrey *et al*. 2019). Second, although sulfate-reducing bacteria (SRB) may out-compete methanogens because of an extensive sulfate supply from seawater, methylotrophic methanogens—which use a different substrate (methylated compounds, rather than acetate or CO_2/H_2)—can keep producing CH_4 under conditions of high sulfate concentrations (Chuang *et al*., 2016; Jing *et al*., 2016). In that case, the CH_4 production will be reflected in the pore-water dissolved CH_4. In addition, empirical results have indicated a strong relationship between ecosystem CH_4 fluxes and pore-water CH_4 (Bartlett *et al*., 1987; Wassmann *et al*., 2000; Yoshikawa *et al*., 2014).

The objective of this study was to investigate dissolved CH_4 heterogeneity at two contrasting rehabilitation sites and its changes throughout seasons. Regarding this, Cameron *et al.* (2019) recently reported that CH_4 emissions, in the EMR site at Tanakeke Island, increased following the redeveloped mangrove forest from the abandoned ponds. My study may be complementary with Cameron's, and this will improve understandings of how the state of mangrove regrowth controls dissolved pore-water CH_4. I also measured several physicochemical parameters (e.g., pH, redox potential, temperature and salinity) that could help to explain the CH_4 heterogeneity, besides the mangrove regrowth. The results provided seasonal data on pore-water dissolved CH_4 in rehabilitated mangrove stands, identified possible factors controlling its variability, and highlighted the importance of including CH_4 emissions in the calculation of a carbon budget in mangrove rehabilitation projects.

5.2 Study area and sampling sites

This study was undertaken in a rehabilitation site applying EMR as well as natural regeneration. The site was located at Dusun Lantangpeo, Tanakeke Island, South Sulawesi, Indonesia (Fig. 3.2). Detailed information about this study area has been provided in Chapter 3, including the geography, ecology and regional socio-economy.

I used a contrasting approach to investigate the changes of dissolved CH_4 in the pore-water of mangrove sediment due to natural regeneration and EMR. Sampling was undertaken at contrasting sites. Sites 1 to 3 represented new (< 5 years) regeneration sites, while Sites 4 to 6 represented old (> 10 years) regeneration sites. Given that the EMR was designed to follow natural succession, the rehabilitation/regeneration status of Sites 1 to 6 could be distinguished by their canopy cover. Three more sites (Sites 7 to 9) were selected in the natural mangroves representing as control sites. These sites were selected after consultation with local inhabitants. I selected a further two control sites in unvegetated areas (Sites A and B)—mangrove creeks (Fig. 5.1). All sites can be seen in Google Earth imagery (Fig 5.1, left) with site 1 to 6 all located in abandoned fish ponds. In addition, all the sites were in a similar position in relation to mean sea level (MSL), ranging from -11.8 to 6.9 cm relative to MSL. At the study area, the maximum tidal range was 112 cm and the average flooding period was 13 hours per day. This implies that long inundation was observed, and thus soil at the sites contained a great volume of pore-water (Cameron *et al.*, 2019a).

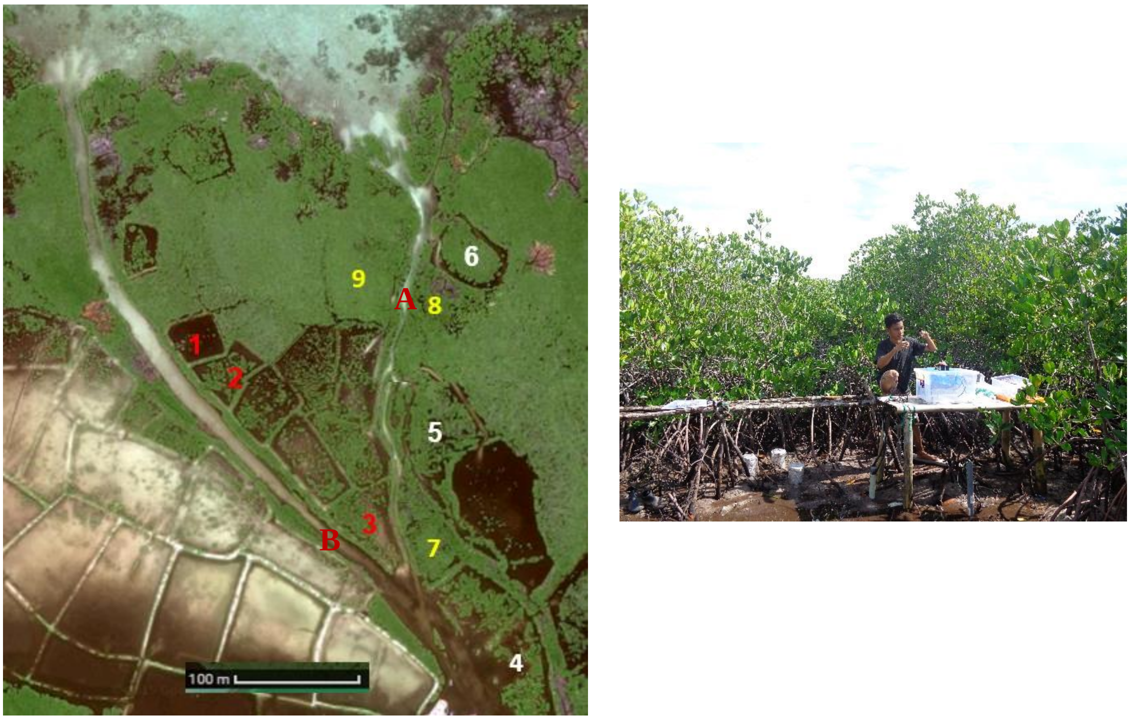

Figure 5.1. Site locations in the study area. (Left) Distribution of sampling sites plotted on Google Earth imagery, depicting the landscape of aquaculture ponds and mangroves with two creeks splitting the landscapes. White and brown colour spotted by green colour (lower left) depicts recently abandoned ponds; patches of green colour surrounded by a brown line depict long abandoned ponds; green colour blocks show undisturbed mangrove vegetation. (Right) Photograph at Site 4 showing the elevated work bench.

To confirm the sequence of sites based on their successional stages, I undertook a forest structure assessment using measurements following Kauffman and Donato (2012). I selected stand basal area (BA) as a measure of forest structure reflecting successional stages, rather than canopy cover or stand density. This is because BA increases logarithmically with successional stages (Lohbeck *et al.*, 2012; Cheng *et al.*, 2013; Gosper *et al.*, 2013; Pszwaro *et al.*, 2016), while tree density increases in the early successional stages, reaches a peak and then decreases because of self-thinning (Schulze *et al.*, 2005).

For CH_4 monitoring, at each site, I deployed one multilevel pore-water sampler and constructed an elevated work bench to avoid disturbing the mangrove soil while collecting samples (Fig. 5.1, right). At the nine sites, seasonal variations were observed by repeated sampling undertaken every month from May 2016 to March 2017 (Fig. 3.3). Heavy rain during January 2017 caused a cancellation of the fieldwork in that month.

5.3 Sample collections and analytical methods

5.3.1 Pore-water dissolved CH_4

The concentration of pore-water dissolved CH_4 was determined by using GC-FID. At the selected sites, pore-water samples were pumped out from mangrove sediments by using the recently developed pore-water sampler (see Chapter 4). The pore-water samples were initially collected in glass bottles. The dissolved CH_4 concentrations in the pore-water samples were determined indirectly by measuring CH_4 concentrations of gas samples extracted from the pore-water. Later, the concentrations of pore-water dissolved CH_4 were calculated based on the CH_4 concentration of the extracted gas samples. The detailed steps of extraction and calculation can be seen in Chapter 4 and Appendix 1. An example calculation is included in Appendix 2.

5.3.2 CH_4 fluxes

Based on the concentration of pore-water dissolved CH_4 in the top layer of soils or at 10 cm depth ($[CH_4]_{pw}$) in mol m^{-3}, methane fluxes ($Flux_{CH4}$) in mg m^{-2} h^{-1} were estimated by using the gas-transfer equation (Sarmiento and Gruber, 2006; Wanninkhof *et al*., 2009; Wania *et al*., 2010):

$$FluxCH4 = k\,([CH4]pw - \beta\,[CH4]a) \qquad \textbf{Equation 5.1}$$

where k is a transfer coefficient and $[CH_4]_a$ is the concentration in the near-surface air. The reasons for and assumptions of choosing this model are explained in Appendix 2.

Soil surface CH_4 fluxes to the overlying atmosphere depend on the difference concentration between pore-water dissolved CH_4 in the surface soil ($[CH_4]_{pw}$) and atmospheric CH_4 on the top of the surface soil ($[CH_4]_a$). Multiplication between the Bunsen coefficient (β) and $[CH_4]_a$ represents CH_4 concentration in the air in liquid phase, when it reaches equilibrium. Measurements of $[CH_4]_a$ were not available and it was subsequently assumed to be equal to the global atmospheric CH_4 concentration, and set to 1.8 ppmv or 7.2×10^{-5} mol m^{-3} at 30°C. To calculate the gas transfer coefficient (k in cm h^{-1}) in Eqn. 5.2, the following equation was applied, which is a result of reconciliation of the assumptions of several equations reported by Borges *et al*. (2004), Wania *et al*. (2010) and Rosentreter *et al*. (2017)—see Appendix 2 for further explanation:

$$k = 2.03\left(\frac{Sc}{600}\right)^{-0.5}$$ **Equation 5.2**

where S_c is the Schmidt number as a function of temperature (T) in °C (Wanninkhof, 1992):

$$Sc\ (CH_4) = 2101.2 - 131.54\ T + 4.4931\ T^2 - 0.08676\ T^3 + 0.000707\ T^4$$ **Equation 5.3**

As an illustration, an example of calculation for Eqn. 5.1 to 5.3 is provided in Appendix 2.

For comparison, CH_4 fluxes from the soil surface were also measured by using the static-chamber method; however, unfortunately, the results indicated that the CH_4 fluxes were much too small to be realistic. Then, I used estimations of CH_4 fluxes from soil surface in mangrove sites in Tanakeke, reported by Cameron *et al.* (2019), which were small, too. CH_4 fluxes at, including two rehabilitation sites and mature mangrove forests, accounted for 0.14 ± 0.0, 0.09 ± 0.0 and 0.45 ± 0.09 mg m^{-2} h^{-1}.

5.3.3 Physicochemistry of pore-water

From the beginning of the research design, site selection was established in similar biogeochemical and hydrological settings to avoid potential confounding factors. However, wetlands are inherently complex, meaning that multiple parameters control CH_4 production and fluxes. Therefore, several physicochemical parameters of pore-water were also observed to help understanding pore-water CH_4 variability across sites and seasons. These included physical parameters (e.g., pH, temperature and redox potential) and ion species that are closely related to methanogenesis (i.e., Fe^{2+}, Fe^{3+}, SO_4^{2-} and S^{2-}). All physicochemical parameters were determined by measuring the porewater samples stored in HDPE bottles, subsequently after sampling in the field. The redox potential (ORP), temperature and pH of pore-water samples were measured using a Mi180 pH/ORP/Conductivity/TDS/NaCl/Temperature Laboratory Bench Meter by Milwaukee Instruments, Inc., United States (US). This instrument has ±0.01 pH, ±0.4 °C and 0.2 mV accuracy and it can measure the range of -2.00-16.00 pH, -20-120 °C and -699.9-699.9 mV. The ORP value (Eh) was normalized with respect to a standard hydrogen electrode by adding +200 mV (Jardim, 2014; Bourgeois *et al*., 2019). Ion content including Fe^{2+}, Fe^{3+}, SO_4^{2-} and S^{2-} was measured using a DR 2700 Hach Portable Spectrophotometer. This instrument can detect the range of 0.02-3.00 (±0.01) mg L^{-1} of Fe^{2+}, 2-70 (±10) mg L^{-1} of SO_4^{2-} and 5-800 (±16) µg L^{-1} of S^{2-}.

5.4 Results

5.4.1 Stand basal area, pore-water dissolved CH_4 and CH_4 fluxes

Basal Area (BA), as a measure of forest structure confirmed that the sequence of sites based on their successional stages, with two exceptions. First, during the fieldwork program, local inhabitants collected firewood at Site 7 and this site was subsequently excluded from the analysis. Second, the BA at Site 6 indicated that this was apparently a much older rehabilitation site. Accordingly, I decided to display the results ordered by BA, and Fig. 5.2 displays the pore-water dissolved CH_4 concentrations for each month, at five depths across the (eight) sites based on the sequential BA. Unvegetated sites are not displayed in the figure, because it did not cover the same period of measurements as the other sites (i.e. only Dec 2016).

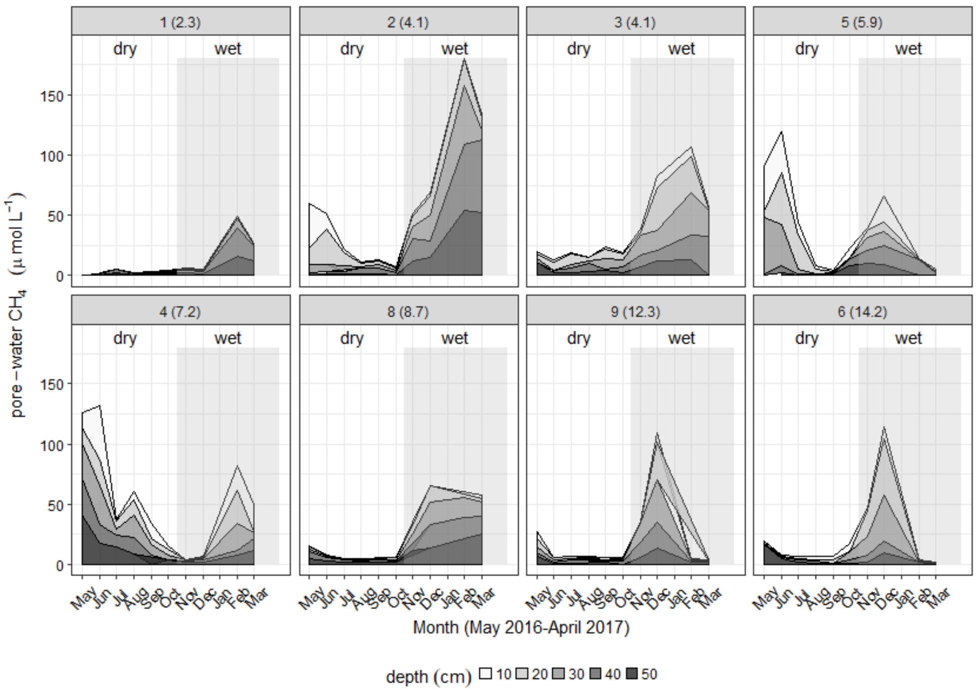

Figure 5.2. **Seasonal variability of pore-water CH_4 concentrations at the eight sites over a year (dry season = May–Oct and wet season = Nov–Apr [shaded]). Stacked area chart (grey gradations) indicate the pore-water CH_4 concentration at different depths from 10 to 50 cm. The top of each panel shows the site number (see Fig. 5.1) with the BA (m^2 ha^{-1}) in brackets. The panels are ordered by their BA, ranging from 2.3 to 14.2 m^2 ha^{-1}. Unvegetated sites are not displayed, while the control sites are panel 8 (8.7) and 9 (12.3).**

Pore-water CH_4 concentrations of ~400 samples (5 depths × 8 sites × 10 months) ranged from 0.04 to 59.87 µmol L^{-1}, with an average of 7.3 µmol L^{-1} (Fig. 5.3). Compared with methane concentration in equilibrium with the atmosphere (i.e., 1.75 × 10^{-3} µmol L^{-1}), CH_4 saturation levels ranged from 20 to 30,000 times the mean atmospheric values. Therefore, all pore-water samples were supersaturated with CH_4 with respect to the atmosphere. In addition, according to CH_4 concentrations of pore-water at 10 cm depth substituted to Eqn. 5.1, CH_4 fluxes from soil surface in the study area ranged from 0.02 to 17 mg m^{-2} h^{-1}, with an average of 2.1 mg m^{-2} h^{-1}.

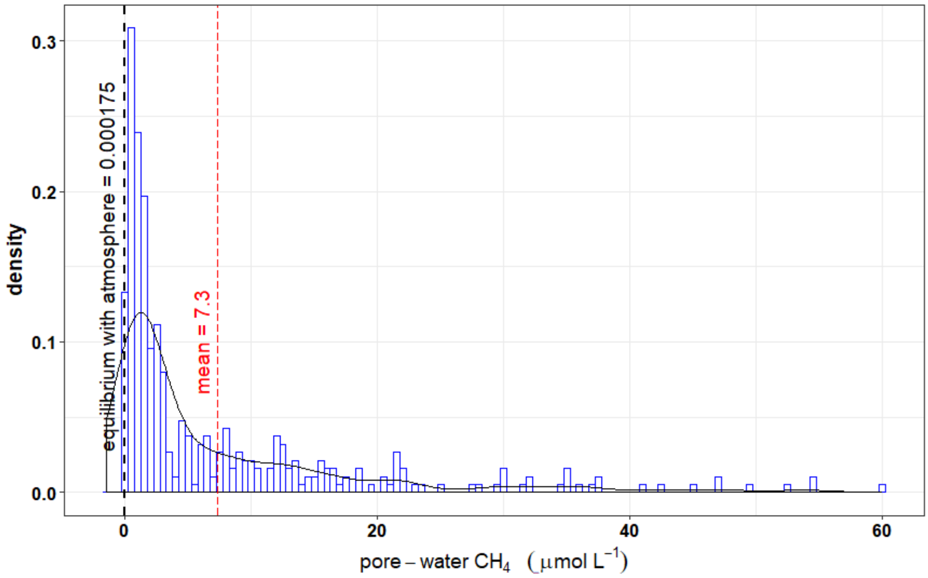

Figure 5.3. Data distribution of pore-water CH_4 concentrations, collected from ~400 pore-water samples.

Pore-water CH_4 concentrations varied considerably among sites and seasons. Generally, the sites with low (Sites 1, 2 & 3) and high (control sites 8/9 and Sites 6) BA exhibited higher pore-water CH_4 concentrations in the wet season (November to April) than those in the dry season (May to October). However, sites with intermediate BA (Sites 5 and 4, see Fig. 5.2) showed the highest pore-water CH_4 concentrations in the dry season (May to October). Seasonal differences led the CH_4 concentrations to be different by up to two orders of magnitude. For example, at Site 3 (BA = 4.1 m^2 ha^{-1}), the range of CH_4 concentrations was 0.6 to 11.3 and 0.05 to 35.9 µmol L^{-1} in the dry and wet season, respectively. As noted above, Sites 4 and 5 showed an opposite trend, with the dissolved CH_4 concentrations being greater in the dry season. In addition to this, those two sites also had extremely high seasonal variability in pore-water CH_4 concentrations.

5.4.2 Physicochemical parameters

Overall, temperature ranged from 27 to 35°C (Fig. 5.4A), while pH ranged from 6.2 to 7.7 (Fig. 5.4B). Within this range of soil pH and temperature, there was no indication that the pH or temperature significantly reduced CH_4 production. Moreover, at the same pH or temperature values, pore-water CH_4 was observed over the full range. Therefore, there was no reason to expect that these two parameters were salient factors that influenced CH_4 production and emission at the study sites.

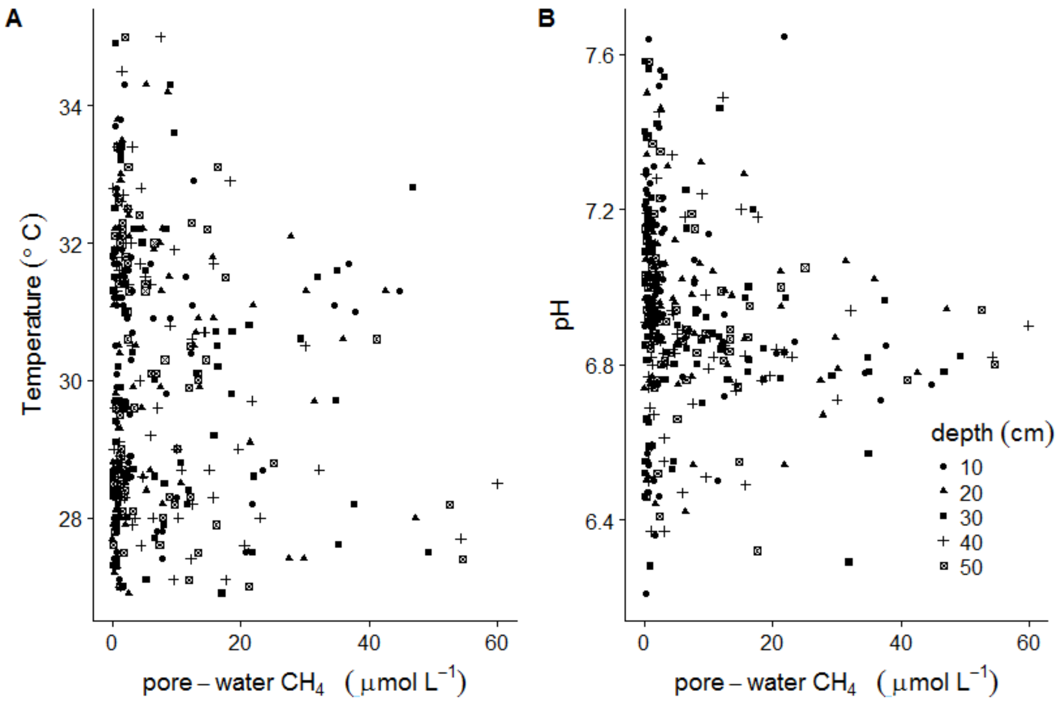

Figure 5.4. **Relationship between pore-water CH_4 concentrations and (A) temperature (*r* = -0.09, *p* = 0.08) and (B) pH (*r* = -0.17, *p* = 0.0009) at the eight sites. pH and temperature were measured in the field at the time of collection, and approximate the in-situ conditions. Legend denotes the depth.**

Similar to pH and temperature, ORP values were generally at the optimum range for methanogenesis. In my data, only 13 samples exhibited ORP > 100 mV and they were associated with the nearly zero pore-water CH_4 (Fig. 5.5). Most of the samples were found in the top layer, which was, to some extent, easily oxidised. Some were at a depth where O_2 might come from roots or animal burrows. However, the vast majority of data on pore-water ORP were in the range of -200 and 0 mV (Fig. 5.5). In this range, high CH_4 concentrations were consistently detected, although some low concentrations were also observed. This finding indicated that ambient ORP was perfect for methanogenesis.

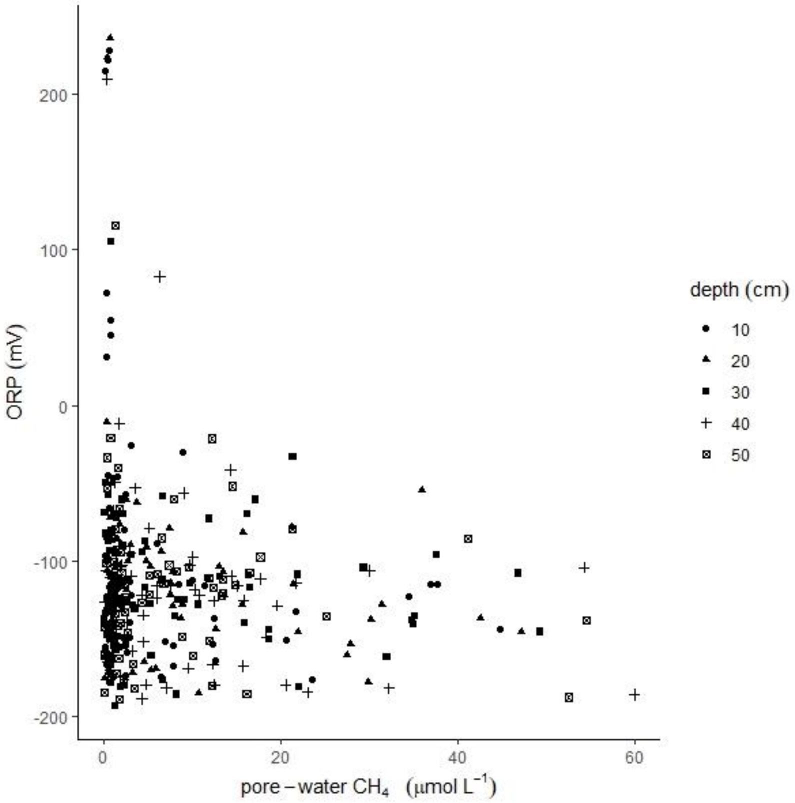

Figure 5.5. Relationship between pore-water CH_4 concentrations and pore-water redox potential (*r* = -0.15, *p* = 0.004). Redox potential was measured in the field at the time of data collection, and approximates the in-situ conditions. Legend denotes the depth.

Among measured ions, the data for Fe^{2+} and Fe total are not presented because the concentrations were low (< 1 ppm) and most were below the instrumental detection limits. Pore-water SO_4^{2-} ranged between 3.1 and 59.3 mmol L^{-1}, while S^{2-} ranged between 0.3 and 1,622 µmol L^{-1} (Fig. 5.6). In relation to dissolved CH_4 concentration, there was no clear pattern in SO_4^{-2} ($r = 0.25$, $p = 3.4 \times 10^{-4}$). While S^{2-} showed a positive relationship with CH_4, there was considerable noise in low concentrations ($r = 0.67$, $p < 0.001$). Therefore, the relationships between CH_4 and SO_4^{2-}/S^{2-} indicated that CH_4 productions were little affected by the abundance of SO_4^{2-}.

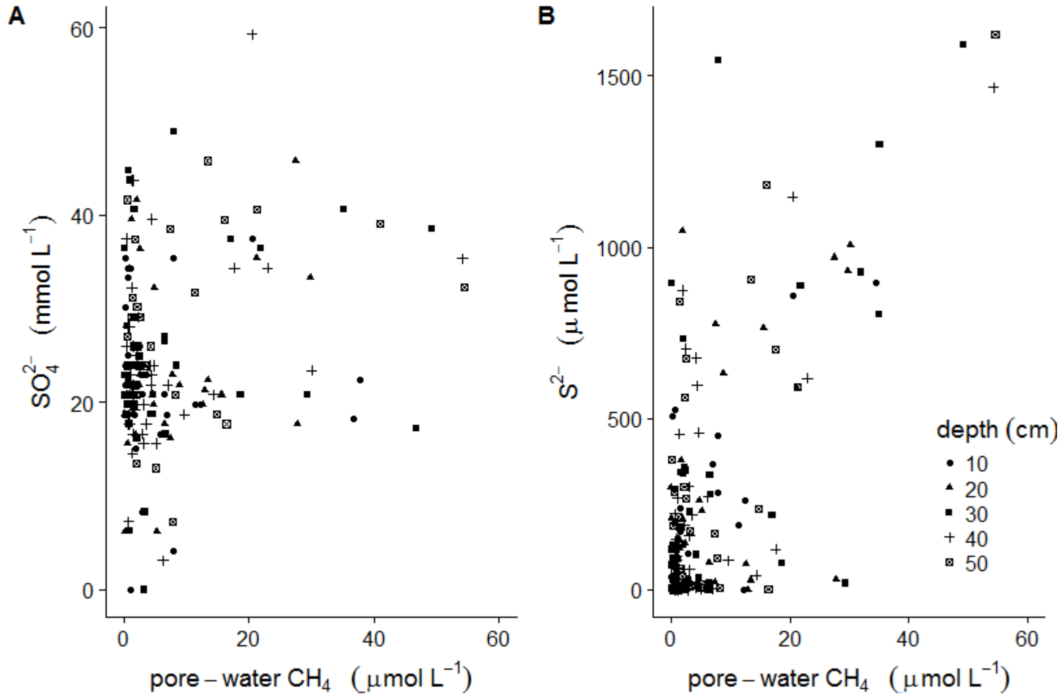

Figure 5.6. **Relationship between pore-water CH_4 concentrations and (A) SO_4^{2-} and (B) S^{2-} at the eight sites. SO_4^{2-} and S^{2-} were measured in the field at the time of data collection, and approximate the in-situ conditions. Legend denotes the depth.**

5.4.3 Relationships between pore-water CH_4 and stand basal area

The relationship between dissolved pore-water CH_4 and BA showed a hump shape, with a rise of CH_4 concentrations from sites with low mangrove cover—Site 1 (2.1 m^2 ha^{-1})—to a peak at intermediate BA (Sites 2 and 3), and then started to decrease at higher BA, which is control sites and Site 6 (Fig. 5.7). Although there was much scatter, I fitted a smooth curve to the data (Fig. 5.7), and the pore-water CH_4 at all depths showed a peak at an intermediate BA of around 6 m^2 ha^{-1}. By using linear model, the pore-water and BA relationship was fitted to a polynomial model, $y = 4.02x - 0.5x^2 + 0.02x^3 - 0.4$, $R^2 = 0.109$, $p < 0.05$.

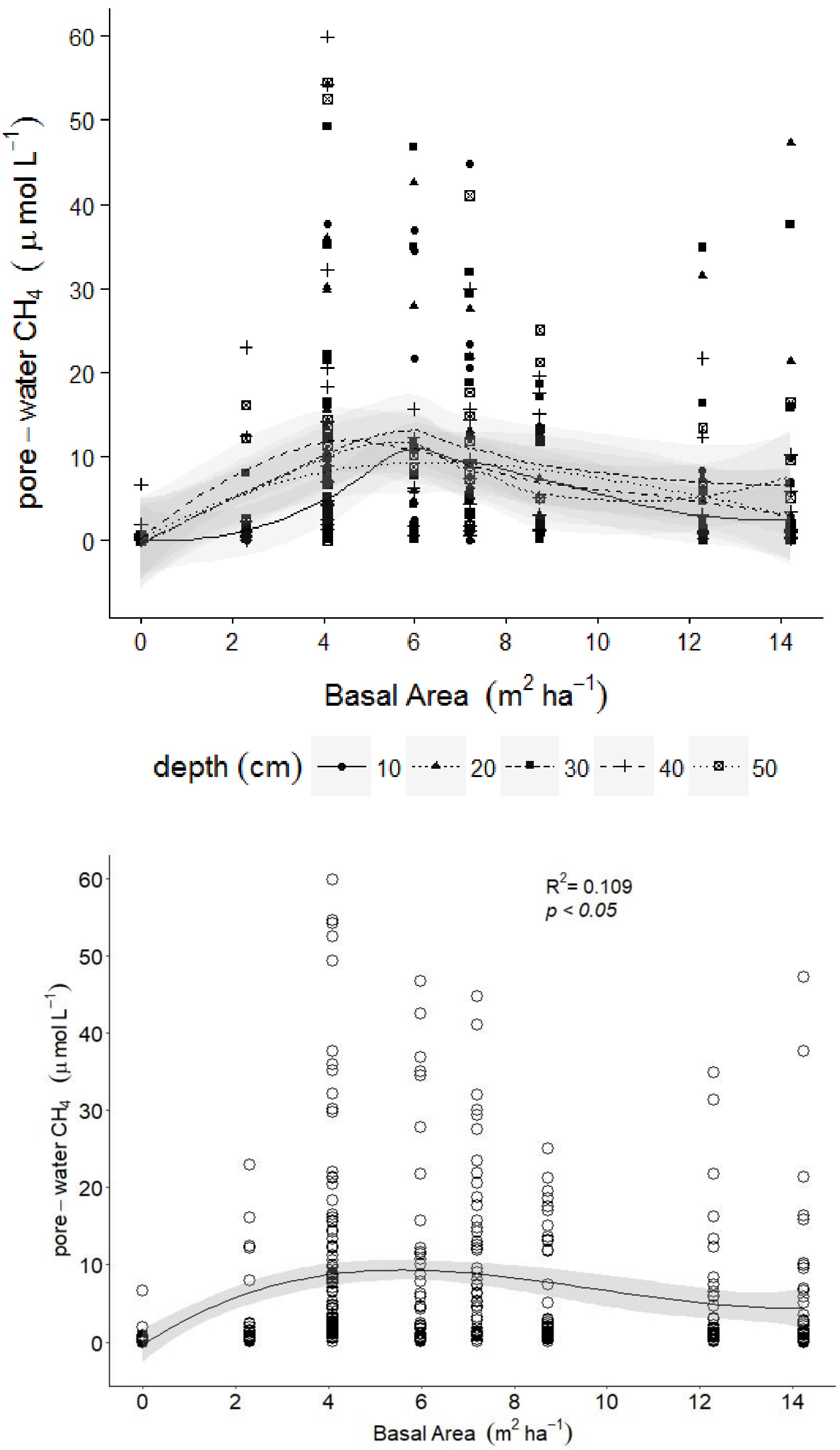

Figure 5.7. Relationship between pore-water CH_4 concentrations and mangrove stand BA. BA was measured in the sites where the pore-water samplers were located at the centre of the site. (top) CH_4 concentrations at five depths, across sites with different BA and general pattern of the relationship, with locally estimated scatterplot smoothing (span = 0.8). Legend denotes the depth. (bottom) Relationship model for the whole data set, $y = 4.02x - 0.5x^2 + 0.02x^3 - 0.4$.

5.5 Discussion

In the literature, there are only a handful of studies on pore-water dissolved CH_4 from mangrove ecosystems (Giani *et al*., 1996; Lee *et al*., 2008; Strangmann *et al*., 2008; Dutta *et al*., 2015; Schile *et al*., 2017). In addition, when researchers did examine CH_4 in pore-water, they measured it without investigating variation with depth, season or stand age/status. My study provides data on the pore-water CH_4 measured on a monthly basis at different depths (up to 50 cm) over a full year. Accordingly, the results offer a new clue to understand the effects of mangrove regrowth on the pore-water CH_4, which may be responsible for CH_4 emissions.

5.5.1 Effects of seasons and mangrove regrowth on dissolved CH_4

In general, the range of pore-water CH_4 concentration (0.04 to 59.9 µmol L^{-1}) in this study is comparable to previous works in mangrove ecosystems (Table 5.1). These values are in a similar range to those in oceanic mangrove islands in Belize (Lee *et al*., 2008) and the pristine mangroves at Balandra, Mexico (Strangmann *et al*., 2008). The CH_4 concentrations are lower than those reported from the coastal sabkha ecosystem, United Arab Emirates (UAE) (Schile *et al*., 2017), but are much higher than in a study of Balandra mangroves (Giani *et al*., 1996). Interestingly, pore-water CH_4 in the current study could be up to one order of magnitude higher concentration than that from an earlier study involving pristine mangroves in Sundarban, India (Biswas *et al*., 2007; Dutta *et al*., 2013; Dutta *et al*., 2017). However, it is lower than the values in most non-mangrove wetlands, such as peatland and brackish marsh (Gross *et al*., 1993; Pangala *et al*., 2013).

Table 5.1. Ranges of pore-water CH_4 (µmol L^{-1}) in this study compared with worldwide data from mangrove and other wetland ecosystems.

No.	References	Locations	Ecosystem	Pore-water CH_4 µmol L^{-1}
1	Current study	EMR site, Tanakeke, Indonesia	Mangrove	0.04–59.9
2	Schile *et al*. (2017)	Coastal sabkha ecosystem, UAE		125–875
3	Lee *et al*. (2008)	Oceanic mangrove islands, Belize		0–80
4	Strangmann *et al*. (2008)	Pristine mangrove soils, Balandra, Mexico		0–77.7
5	Dutta *et al*. (2017)	Mangrove, Sundarban, India		2.0–6.0
6	Dutta *et al*. (2015)	Mangrove, Sundarban, India		2.8–4.0
7	Giani *et al*. (1996)	Balandra and Ensenada La Paz mangrove, Mexico		0–2.1
8	Terazawa *et al*. (2007)	Forest floodplain, northern Japan	Forest floodplain	5.6–28.4
9	Pangala *et al*. (2013)	Sebangau river catchment, Sumatra, Indonesia	Peatland	113.0–1539.0
10	Pangala *et al*. (2015)	Forested peatland, Flitwick, Bedfordshire, United Kingdom		0–450.0

11 12	Gross *et al*. (1993) Tong *et al*. (2015b)	Delaware brackish marsh, US Oligohaline marsh, Min River estuary, southeastern China	Brackish marsh	0–700.0 17.1–94.5
13	Biswas *et al*. (2007)	Sundarban mangrove water, India	Estuarine	0.8–1.5
14	Chuang *et al*. (2016)	Mangrove-dominated coastal lagoon, Mexico	Lagoon	20–3,500
15	Ding *et al*. (2004)	Sanjiang Mire Wetland Experimental Station, northeast China	Freshwater marsh	8–232

Although many studies have found pore-water physicochemical factors to be responsible for controlling CH_4 turnover (Inamori *et al*., 2007; Poffenbarger *et al*., 2011; Zhang and Ding, 2011; Dutta *et al*., 2013; Marín-Muñiz *et al*., 2015), it may be less important here. The temperature and ORP found here (Fig. 5.4 and 5.5) are within the optimum range for methanogen bacteria to convert organic matter to CH_4 (Wang *et al*., 1993; Le Mer and Roger, 2001). Further, the ranges of pH (Fig. 5.4B) are favourable for methane production and reach a maximum at a range of 6.8 to 6.9, which agrees with Wang *et al*. (1993). In addition, abundance of SO_4^{2-} is unlikely to affect CH_4 production. A weak correlation between SO_4^{2-} and pore-water CH_4 is an indication of no competition for the organic matter between methanogens and SRB (Fig. 5.6). Thus, in general, these physicochemical factors indicate favourable conditions for CH_4 production.

The only measured parameter correspond well with pore-water CH_4 concentrations is stand basal area (BA, Fig. 5.7). Therefore, soil organic carbon (SOC) availability may be the most likely explanation for a regulatory factor of pore-water CH_4 concentration in my study. This can be inferred from findings in Cameron *et al.* (2019b) that SOC in the newly abandoned ponds is lower than the sites with mangrove regrowth post-EMR in Tanakeke, where I did my study. Sasmito *et al.* (2019) further provide evidences that soil carbon content linearly increases following the successional or regeneration age (R^2=0.441, p<0.05), while BA has a linear positive correlation with the regeneration age (R^2=0.667, p<0.001). Also, Sasmito *et al.* (2019) found that belowground carbon increases and reaches the plateau at some period of time.

The abundances of carbon sources are a conducive environment supporting methanogen bacteria to produce CH_4. This was reflected in the fact that the full range of CH_4 concentrations was observed at the same value of some physicochemical factors—temperature, pH, ORP and SO_4^{2-} (Fig. 5.4 to 5.6). This meant that high pore-water CH_4 concentration could be detected when substrates for methanogen bacteria were available. Conversely, it could be low if the sites had a lack of organic carbon, even if the physicochemical environments at the sites were optimal for methanogenesis. In addition, this idea was supported by Tong *et al*. (2015a) when studying CH_4 production variability at a small scale, who reported that the best predictor of CH_4 concentration was the availability of organic carbon. Further, Marinho *et al.* (2012) reported a similar idea, where they found that methane concentration in pore-water was a function of the amount of carbon, mainly associated with the occurrence of vegetation. In the sampling sites of this current study, mangrove vegetation was likely to be the major source of soil organic matter because the study area was located on a small island, separated from the mainland by about 10 km. In addition, the base rock was coralline rubble and sand, both of which lack organic matter (Cameron *et al.*, 2019b).

SOC supply from vegetation is highly dependent on photosynthesis and the allocation of photosynthates. Forests actively fix CO_2 by photosynthesis, whereby some amount of the fixed carbon is emitted back to the atmosphere by autotrophic respiration, and the rest is allocated to biomass and root exudates. Litterfall and root biomass are thought to be the sources of soil organic matter (Lallier-Vergès *et al.*, 2008; Marchand *et al.*, 2008; Marchand, 2017; Ha *et al.*, 2018). They accumulate in the soil because of slow decomposition rates, particularly in waterlogged soils. Meanwhile, root exudates exhibit a rapid turnover and are generally thought to account for a small proportion of soil organic matter (Allen *et al.*, 2010).

Regarding methane production, a further explanation of the soil organic matter might be related to its type or source. Some literature shows a straightforward relationship between total soil organic matter and methane flux (Xiang *et al.*, 2015; Yu *et al.*, 2013; Konnerup *et al.*, 2014) and several studies have specifically examined the response of CH_4 production to different carbon sources (Lu *et al.*, 2000; Lin *et al.*, 2015; Girkin *et al.*, 2018; Lu *et al.*, 2018). Those studies found that labile organic matter, which mainly comes from root exudates, is preferable for methanogen bacteria. In addition, the exudates can induce decomposition of large and complex organic compounds (van Nugteren *et al.*, 2009) through activating microbial metabolisms that can decompose insoluble and recalcitrant soil organic matter (Kuzyakov, 2010; Mason-Jones and Kuzyakov, 2017). This eventually leads to the production of labile organic matter from decomposition of recalcitrant organic matter.

The body of knowledge explained above provides a basis for interpreting the pattern of pore-water CH_4 reported here, where seasonal variability was dependent on the age of rehabilitation sites (see Fig. 5.2). In Fig. 5.2, sites are arranged based on the BA of the mangrove stand, which is a representation of successional stages. The figure indicates that sites in the early (Sites 1 to 3) and late (control sites 6, 8 and Sites 9) successional/regeneration age had similar patterns of pore-water CH_4. Those sites all exhibited low concentrations during the dry season, yet high concentrations during the wet season. However, the intermediate stage sites (Sites 4 and 5) showed a reverse pattern (Fig 5.2). Thus, I speculate that there is a shift in the relative abundance of labile to the total soil organic matter, which would then cause differences in the seasonal pattern of dissolved CH_4 among sites. Rocha *et al*. (2015) suggested that root exudates—a form of labile organic matter—are produced seasonally, and production is higher during the growing season. Similarly, as a major source of soil carbon in mangrove ecosystems, fine root production is also closely related to seasons (Poungparn *et al.*, 2016; Xiong *et al.*, 2017). While root exudates are readily digested by methanogen bacteria as soon as they are released to the soil (King *et al.*, 2002; Dorodnikov *et al.*, 2011; Tokida *et al.*, 2011), fine roots need several months of active decomposition before the residues can form labile organic matter (Robertson and Alongi, 2016; Liu and Xiong, 2017).

The slow decomposition rate of fine roots might affect a shift in the abundance and sources of labile organic matter for methane production. At the intermediate stage sites (4 and 5), methanogens might use labile organic matter from fine root decompositions as the main substrates (see Fig. 5.2). However, slow decomposition might cause a lag in methane production during the peak production periods of fine roots. Fine root necromass, which is abundantly produced during the wet season, decomposes more rapidly in the dry than the wet season (Poungparn *et al.*, 2016). Hence, in the dry season, methane production might increase, even though root exudate releases are in low concentrations. Meanwhile, in the mature forests (Sites 6, 8 and 9), much slower decomposition could cause methanogens to produce CH_4 mostly using root exudates. Therefore, at these sites, pore-water CH_4 concentrations in the wet season are greater than in the dry season. The slow decomposition causes a gradual carbon accumulation in soils over periods of time; hence, the more developed mangrove stands also have higher soil carbon reserves (Marchand, 2017; Sasmito *et al.* 2019). Zhang *et al.* (2013) found a much slower decomposition rate in late successional vegetation, which is consistent with an increase in soil carbon. Therefore, in the mature forests, root exudates might be more abundant than labile organic matter from decomposition, especially in the wet season. In contrast, having similar seasonal patterns in pore-water CH_4 with the mature forests, the early successional stages (Sites 1, 2 and 3) might rely on labile organic matter from both root exudates and decomposition. During production periods of fine roots and exudates, the decomposition rate in these sites would be faster than in the intermediate stages (Sites 4 and 5), as Zhang *et al.* (2013) indicated. Thus, together with root exudates, labile organic matter from decomposition amplified methane production during the wet season.

Further, since fine roots and root exudates are integral components of forest production, net primary productivity (NPP) could also be a proxy to explain pore-water CH_4 variability across sites in the current study. From freshwater wetland studies, a review paper concluded that a positive correlation between NPP and CH_4 emission is evident (Aselmann and Crutzen, 1989). Interestingly, in my study, pore-water CH_4 concentrations across chronosequence sites seemed to follow the successional pattern of NPP (Fig. 5.7). The general pattern of forest NPP across successional stages has long been known (Day Jr *et al.*, 1996; Chen *et al.*, 2002). In brief, NPP increases rapidly at the young ages, peaks in the middle ages and declines slowly as the vegetation stand matures (Chen *et al.*, 2002; Wang *et al.*, 2011; L. He *et al.*, 2012). Likewise, this very general pattern is followed in mangrove ecosystems (Okimoto *et al.*, 2008).

Specifically, Aksornkoae (1993) concluded that NPP of *R. apiculata* stands starts to decline at the age of five to six years after they exhibit an exponential increase in the initial growth. Meanwhile, Ong *et al*. (1985) noted that the decline starts at 10 years. Thus, these explanations support the inference that mangrove productivity at the Indonesian sites would peak at around six years, and subsequently lead to the highest dissolved CH_4 concentrations in the pore-water.

5.5.2 Potential mangrove contribution to CH_4 emissions

Based on values calculated using the gas-transfer model, soil surface CH_4 fluxes in the current study could be higher than in most mangrove ecosystems that have been reported, as well as comparable with those recorded at freshwater wetlands (Table 5.2). Mangroves in the current study area covered low and high emitters (0.02 to 17 mg m^2 h^{-1}), although the majority of CH_4 fluxes were less than 10 mg m^{-2} h^{-1}, with an average and median value of 2.1 and 0.6 mg m^{-2} h^{-1}. This is in agreement with most CH_4 studies in mangrove ecosystems (Table 5.2, No. 6 to 24), particularly Cameron *et al.* (2019a) who measured CH_4 flux at the same study location. Interestingly, the average CH_4 flux is similar to that observed in freshwater wetlands, which have been relatively well studied and hence included in the global carbon budget (Table 5.2, No. 25). As a comparison to the average CH_4 flux in the current study (2.1 ± 3.6 mg m^{-2} h^{-1}), the averages from lakes, fens, swamps and floodplains account for 1.8, 3.3, 3.5 and 4.2 mg m^{-2} h^{-1}, respectively.

Table 5.2. Ranges of CH_4 fluxes from soil surface in this study (gas-transfer model) compared with worldwide data from mangrove and freshwater wetland ecosystems (static-chamber method).

No.	References	Locations	Ecosystem	CH_4 flux ranges [average] mg m^{-2} (ground surface) h^{-1}
1	**Current study**	**Mangrove rehabilitation, Tanakeke, South Sulawesi, Indonesia**	**Mangrove**	**0.02–17 [2.1]**
2	Chen *et al*. (2010)	Shenzhen and Hong Kong mangroves, south China		0.2–82.7 […]
3	Konnerup *et al*. (2014)	Mangrove in Ciénaga Grande de Santa Marta, Colombia		0–31.6 […]
4	Wang *et al*. (2016)	Mangrove, Fujian, China		0.4–30.8 […]
5	Allen *et al*. (2007)	Southeast Queensland mangrove, Australia		0–17.4 […]
6	Arai *et al*. (2016)	Mangrove, Ca Mau, Vietnam		4.4–7.3 […]
7	Biswas *et al*. (2007)	Lothian Island mangrove, Bengal, India		0.9–3.5 […]
8	Sotomayor *et al*. (1994)	Southwest coast mangrove, Puerto Rico		0.01–3.4 […]
9	Chauhan *et al*. (2008)	Bhitarkanika mangrove, East India		0.1–3.2 […]
10	Purvaja *et al*. (2004)	Pichavaram mangrove, South India		0.03–2.7 […]
11	Chauhan *et al*. (2015)	Bhitarkanika mangrove, India		0.1–2.3 […]
12	Allen *et al*. (2011)	Subtropical mangrove, Southeast Queensland, Australia		0.05–1.6 […]
13	Krithika *et al*. (2008)	Muthupet mangrove, South India		0.8–1.6 […]
14	Lyimo *et al*. (2002)	Mtoni mangrove, Tanzania		0.02–1.3 […]
15	Chauhan *et al*. (2008)	Pichavaram mangrove, South India		0.6–0.9 […]
16	Dutta *et al*. (2013)	Sundarban mangrove biosphere, India		0.2–0.4 […]
17	Kreuzwieser *et al*. (2003)	Queensland mangrove, Australia		0.02–0.4 […]
18	Cameron *et al.* (2019a)	Mangrove rehabilitation, Tanakeke, South Sulawesi, Indonesia		0.09–0.45 […]
19	Lu *et al*. (1999)	Dongzhai Harbour mangrove, China		0–0.2 […]
20	Chang and Yang (2003)	Kang-nan wetland mangrove, northern Taiwan		0.04–0.1 […]
21	Cabezas *et al*. (2018)	Southwest Florida, US		0.01–0.1 […]
22	Chen *et al*. (2010)	Guangdong, China		0–0.1 […]
23	Lekphet *et al*. (2005)	Ranong, Thailand		0–0.01 […]
24	Chen *et al*. (2014)	North Sulawesi, Indonesia		0–0.01 […]
25	Alongi *et al*. (2005)	Fujian, China		0–0.01 […]

Table 5.2. (continued) Ranges of CH_4 fluxes from soil surface in this study (gas-transfer model) compared with worldwide data from mangrove and freshwater wetland ecosystems (static-chamber method).

No.	References	Locations	Ecosystem	CH_4 flux ranges (average) mg m^{-2} (ground surface) h^{-1}
26	Aselmann and Crutzen (1989), a review	Bogs	Freshwater wetlands	0.04–2.1 [0.6]
		Lakes		0.7–3.7 [1.8]
		Fens		1.2–9 [3.3]
		Swamps		2.4–4.6 [3.5]
		Floodplain		2.4–8.3 [4.2]
		Marsh		5.7–16.6 [10.5]
		Rice paddies		7.5–18.3 [12.3]

In the literature presented in Table 5.2, four articles (No. 2 to 5) reported relatively high CH_4 fluxes from mangrove environments, accounting for greater than 10 mg m^{-2} h^{-1}. All the articles explicitly agreed with the explanation that high CH_4 fluxes were due to high discharges of sewage to the study sites, except Wang *et al.* (2016). However, the study site of Wang *et al.* was located at the estuary of Jiulong River, China, and had been experiencing sewage discharges from agriculture, industry and settlements (Cao *et al.*, 2005; Wu *et al.*, 2017). The mechanism behind the discharge of sewage is nutrient enrichment in mangrove waters, which may lead to eutrophication, triggering algal blooms (Pacheco *et al.*, 2014). In general, eutrophication causes increased methane emissions for two main reasons. First, increasing algal biomass provides an abundance of carbon sources for methanogen bacteria, particularly labile organic carbon (West *et al.*, 2012; DelSontro *et al.*, 2018). Second, with organic matter accumulation because of eutrophication, dissolved oxygen decreases to decompose the organic matter, thereby generating anoxic environments that are conducive to methane production (Howarth *et al.*, 2011; Jenny *et al.*, 2016).

Finally, comparing CH_4 fluxes from the soil surface in the current study to the worldwide mangrove data indicated that mangrove ecosystems are generally low methane emitters; however, anthropogenic activities may amplify CH_4 emissions in these ecosystems through eutrophication. Moreover, the magnitude of CH_4 fluxes in the eutrophic mangroves could be as high as an anthropogenic wetland (i.e., rice paddies) or even greater. For example, in a world data synthesis, CH_4 fluxes from the soil surface of rice paddies ranged from 7.5 to 18.3, with an average of 12.3 mg m^{-2} h^{-1} (Aselmann and Crutzen, 1989), while mangroves could range from 0.2 to 82.7 mg m^{-2} h^{-1} (Chen *et al.*, 2010)—see Table 5.2.

5.5.3 Indication of CH_4 releases through mangrove trees

Methane dissolved in the pore-water can be removed from sediments by either consumption or transport. In my study area, pore-water geochemistry indicated that CH_4 consumption might be apparent only at the top 10 cm depth. This could be the reason why CH_4

flux measurements and estimations gave too small result, which agreed with Cameron *et al.* (2019a) who measured CH_4 fluxes in the same location. Unfortunately, I was not measured pore-water CH_4 at the top 10 cm depth. Thus, methane transports could be an alternative explanation for pore-water CH_4 removals as there are emerging insights in tidal pumping transporting pore-water CH_4 horizontally (e.g. Call *et al.*, 2015) and CH_4 releases to the atmosphere through lenticels of mangrove stems (e.g. Jeffrey *et al.*, 2019).

According to tidal cycles, pore-water geochemistry and depth profiles of pore-water CH_4, CH_4 is more likely to be released through the woody tissue of mangrove trees (i.e. lenticels of the stems and pneumatophore), rather than through tidal pumping. Anoxic environments were mostly detected in all pore-water samples that is obviously not favourable for methane oxidation at the depth < 10 cm (Fig. 5.5). In addition, anaerobic methanotrophy coupled with sulfate reduction was unlikely because I did not observe a strong relationship between CH_4 and SO_4^{2-} (Fig. 5.6). In the mechanism of anaerobic methanotrophy, SRB uses H_2 as an electron donor to reduce sulfate, and this creates a more favourable environment for CH_4 oxidation (Hanson and Hanson, 1996; Chowdhury and Dick, 2013). Then, if CH_4 oxidation exists, SO_4^{2-} and CH_4 would disappear simultaneously, which was not detected in my experiments. Although another anaerobic methanotrophy pathway could be occurring, which is driven by nitrate, but I did not undertake observation of this parameter. Horizontal (tidal pumping) CH_4 transports would be unlikely in my study sites because: (i) all the sites were located in a similar position at low-lying elevations, susceptible to flooding and inundated for around 13 hours per day. If this is the case, pore-water could not be drained during low tide—see Susilo *et al*. (2005) and Xia and Li (2012) for the relationship between pore-water, tidal cycles and tidal pumping; and (ii) ORP was low and stable at anoxic conditions, even during low tide (Fig. 5.5), thereby indicating that pore-water seepage might be too small. Therefore, CH_4 transport through lenticels on the surface of mangrove stems could primary contribute to changes in the depth profile of pore-water CH_4**.**

Unclear patterns in the depth profiles of pore-water CH_4 further indicated the possibility of tree-mediated CH_4 fluxes. Basically, pore-water CH_4 concentrations in wetland soils exponentially increase with depth, but the depth profile may change significantly when vegetation grows on that soil. Bazhin (2004) pointed out that the depth profiles would have maxima and minima at a certain depth, depending on the distributions of roots, as also found in my depth profile of pore-water CH_4. In fact, CH_4 supersaturation of pore-water within a 50 cm depth reflected potential sources of CH_4 emissions ranging from 20 to 30,000 times saturation). This result indicates that vertical transport via plant stems might be contributing to remove CH_4 from the pore-water. Therefore, vertical transports of CH_4 through mangrove trees should be elucidated in further studies, as it is an emerging topic in CH_4 studies in freshwater forested wetlands as well as mangrove forests.

The importance of woody plants as a pathway for CH_4 transport in vegetated wetlands has very recently attracted much attention in CH_4 flux studies. The idea of CH_4 transport through the woody plant was first proposed by Zeikus and Ward (1974), who found that new borer holes of a Cotton Wood tree stem released high-pressure flammable gas. However, there was a lack of interest in this idea until the 1990s, when Pulliam (1992) observed CH_4 fluxes from knee roots of Bald Cypress (*Taxodium distichum*), and Rusch and Rennenberg (1998) experimented with Black Alder seedlings (*Alnus glutinosa*). In fact, while the fieldwork for my study was being conducted, there were several additional reports of methane fluxes through the woody stems of trees (Pangala *et al*., 2015; Terazawa *et al*., 2015; Pangala *et al*., 2017; Maier *et al*., 2018; Pitz *et al*., 2018).

Table 5.3 presents a summary and comparison of CH_4 fluxes through sediment surface and woody stems. It is no surprise that CH_4 emissions are higher in flooded than non-flooded forests. This is because continuous soil flooding is known to cause anaerobic conditions and hence an increase in CH_4 production, as is well documented in studies of CH_4 and water management in rice paddies (Wassmann *et al*., 2000; Xu *et al*., 2015; Islam *et al*., 2018). Interestingly, in flooded forests, methane fluxes through woody stems appear to be much larger (by a factor of five to 20) than soil fluxes. In contrast, unflooded forests exhibit lower CH_4 fluxes through tree stems than the soil surface (Table 5.3, No. 6). In addition, some observations have indicated CH_4 absorption by soils, yet CH_4 emission by tree stems (Table 5.3, No. 4, 5 and 7). Nevertheless, the previous studies in this table highlight the possibility of a CH_4 flux pathway through tree stems, which can be higher than soil surface CH_4 flux in flooded soils.

Table 5.3. CH_4 fluxes from tree stem and soil surface in the literature, presented in the same unit (milligram CH_4 per metre square ground surface per hour).

No.	References	Locations	CH_4 flux mg m^{-2} (ground surface) h^{-1}	
			Stem	**Soil**
	Flooded			
1	Pangala *et al*. (2017)	Negro River, floodplain forest	3.9 ± 1.3	0.6 ± 0.5
		Amazon River, floodplain forest	6.9 ± 1.8	0.4 ± 1.5
		Solimões River, floodplain forest	15.6 ± 3.9	0.7 ± 0.9
		Madeira River, floodplain forest	6.9 ± 2.7	2.1 ± 2.4
		Tapajos River, floodplain forest	23.9 ± 6.3	3.8 ± 4.7
	Non-flooded			
2	Pangala *et al*. (2013)	Sebangau River catchment, tropical peatland	0.2 ± 0.02	0.03 ± 0.01
3	Terazawa *et al*. (2007)	Northern Japan, floodplain forest	0.003	-0.004
4	*Pitz *et al*. (2018)	Upland forest	0.01	-0.06 ± 0.01
		Transitional	0.03	0.01 ± 0.03
		Wetland forest	0.08	0.2 ± 0.1
5	*Terazawa *et al*. (2015)	Floodplain forest	0.01–0.18	
6	*Gauci *et al*. (2010)	Freshwater wetlands	0.004–0.01	0.3–0.8
7	*Maier *et al*. (2018)	Upland forest	0.01	-0.07

*In the original paper, fluxes were reported per unit stem surface area. This was converted to per unit ground surface area using an approximate relation (see Appendix 3).

5.5.4 A conceptual model

In summary, pore-water CH_4 variability in this study could be conceptualised as a simple relationship between the pore-water CH_4 and successional stages. This is in accordance with the successional pattern of NPP (see Fig. 5.8). In freshwater wetlands, based on the relationships between CH_4 emissions and NPP, 3% of fixed carbon (NPP) is released back into the atmosphere as CH_4 (Aselmann and Crutzen, 1989; Whiting and Chanton, 1993). Therefore, assuming that this fraction applies to mangrove wetlands, my findings might reconcile missing carbon in the carbon budget calculations in mangrove forests (Bouillon *et al*., 2008; Alongi, 2009; Twilley *et al*., 2017).

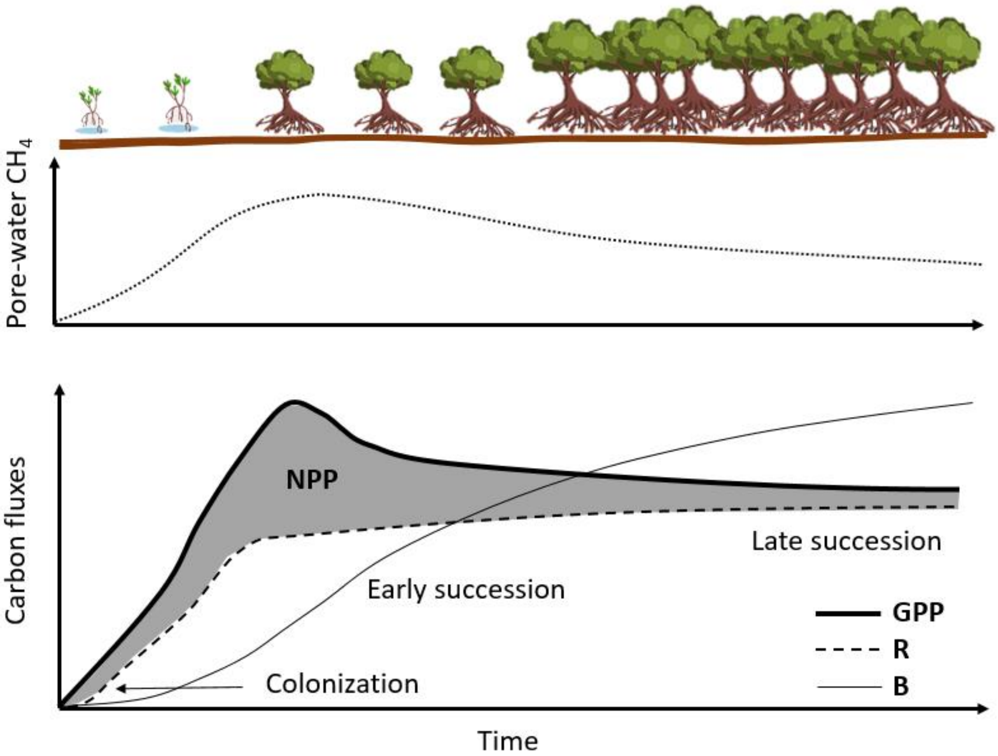

Figure 5.8. **(A) Conceptual model of pore-water dissolved CH_4 in mangrove rehabilitations. Vertical axis represents pore-water dissolved CH_4 and horizontal axis represents time (current study). (B) Forest successional development. NPP = net primary productivity, GPP = gross primary productivity, R = respiration, B = biomass (Odum, 1969; Alongi, 2011).**

5.6 Conclusion

I tracked for the first time the annual cycle of pore-water CH_4 concentrations at contrasting sites of mangrove rehabilitation. Such data are essential to refine greenhouse gas emissions from restored mangroves given the increase interest in blue carbon ecosystem restoration/rehabilitation as a mechanism of GHG abatement. The pore-water at all eight sites was supersaturated with CH_4, with a wide range of CH_4 fluxes from the soil surface, ranging between 0.02 and 17 mg m^2 h^{-1}. The variability of the pore-water CH_4 showed a seasonal pattern that correlated with the successional stages in the rehabilitation (Fig. 5.7 and 5.8). The implication is that the concentration of CH_4 in pore-water is likely to be largely controlled by the availability of carbon substrate, which varies with NPP and hence the stage of mangrove regrowth. Future research should consider: (i) CH_4 fluxes through woody stems in combination with pore-water CH_4 to confirm CH_4 pathways in a soil–plant–atmosphere system and mangrove contributions to CH_4 emissions, and (ii) root exudates and NPP in relation to pore-water CH_4. With that knowledge, we can better characterise the complete carbon budget on mangrove ecosystems.

Chapter 6: The pathway of methane production in overwash mangroves

6.1 Introduction

Methanogenesis or methane production in wetland ecosystems is an important process in the global carbon cycle. This is a final stage of organic matter decomposition in anaerobic conditions, generating methane gas (CH_4)—one of the strongest greenhouse gases. Along with methanotrophy or CH_4 oxidation in the aerobic zone of wetlands, methanogenesis controls CH_4 emissions from the sediment to the atmosphere. Currently, wetlands contribute 20 to 40% of global CH_4 emissions (Reeburgh, 2003; Kirschke *et al*., 2013; Saunois *et al*., 2016). These emissions may increase because of climate change, which is connected to warming temperatures, increasing inundation frequency and increasing organic carbon supply (Dean *et al*., 2018; Reay *et al*., 2018).

With climate change, the increase in the Earth's surface temperature and CO_2 could amplify the feedback of wetland sediment to climate change through controlling methanogenesis and methanotrophy. Warming temperatures trigger more methanogen microorganisms to accelerate methanogenesis (Zhang *et al*., 2018), which has an optimum temperature range of 35 to 42°C (Zeikus and Winfrey, 1976). This warming could also drive methanotroph bacteria to oxidise CH_4, such as in permafrost and alpine grass meadows (R. He *et al*., 2012; Kao-Kniffin *et al*., 2015). However, in rice wetlands, methanogenesis only occurs at the ripening stage (D. Liu *et al*., 2016). This is not only because of the warm temperature, but also because, at this stage, CH_4 concentrations are higher than in other stages (i.e., tillering and heading) when the paddy soil is drained. Elevated CO_2 concentration in the atmosphere generally increases plant productivity (Gamage *et al*., 2018; Lahijani *et al*., 2018), leading to increased root exudation, which enhances the supply of organic substrates for consumption by methanogens (Whiting and Chanton, 1993; Chanton *et al*., 1995; Kao-Kniffin and Zhu, 2013). In contrast, increases in the atmospheric CO_2 level reduces the abundance of methanotrophs (Kolb *et al*., 2005; Das and Adhya, 2012; Y. Liu *et al*., 2016).

As a result of climate change, increased rainfall frequency and sea level rise also have a critical role in the positive feedback of CH_4 production in wetland sediments. Increasing frequency of heavy rainfall results in an increase in the time that soils are saturated, and should enhance methanogenesis (Wei and Wang, 2017; Zhang *et al*., 2018), yet is also anticipated to reduce methanotrophy (Ni and Groffman, 2018). In coastal wetlands, sea level rise alters the extent and frequency of inundation (Grenfell *et al.*, 2016), thereby promoting new anoxic zones (Geselbracht *et al*., 2015), which are an ideal environment for methanogen growth (Lu *et al*., 2018). However, to date, the effects of sea level rise on methanotrophy in coastal areas have not been investigated (Dean *et al.*, 2018).

In coastal wetlands, sulfate reduction makes the CH_4 cycle more complicated. SRB, which are often found in marine environments, are believed to out-compete methanogens for the same substrates of H_2/CO_2 and acetate (Ferry, 1993). The methanogen groups that use these compounds are called hydrogenotrophic and acetotrophic methanogens. However, there is a methanogen group—methylotrophic methanogens—that can coexist with SRB. The methylotrophic methanogens use methylated compounds (e.g., methanol, trimethylamine and dimethylamine) as carbon sources, whereas SRB do not. Oremland and Polcin (1982) found this phenomenon in laboratory investigations, and defined the compounds as non-competitive substrates. Numerous *in-situ* studies have also provided evidence that methylotrophic methanogens always involve the coexistence of methanogens and SRB (Lyimo *et al*., 2002; Cadena *et al*., 2018; Maltby *et al*., 2018; Zalman *et al*., 2018; Zhuang *et al*., 2018). Nevertheless, under laboratory conditions, SRB can oxidise some methylated compounds (i.e., methanol, dimethyl sulfide and methanethiol) (King *et al*., 1983; Lyimo *et al*., 2009), producing other methyl compounds, and thus feeding methylotrophic methanogens (Moran *et al*., 2008; Mitterer, 2010). More intriguingly, SRB may also interact with methanotrophs to oxidise CH_4 in anaerobic conditions (Hinrichs *et al*., 1999; Orphan *et al*., 2001; Reeburgh, 2007).

Mangroves are one of the coastal wetlands that are thought to produce less CH_4 than freshwater wetlands because of the inhibiting influence of sulfate abundance in seawater (Alongi *et al*., 2004; Alongi *et al*., 2005; Welti *et al*., 2017; Cabezas *et al*., 2018). However, in my previous investigation (Chapter 5), pore-water in mangroves of Tanakeke Island was supersaturated with CH_4, compared with its equilibrium state with atmospheric CH_4. In addition, pore-water sulfate did not correlate with CH_4 concentrations. Therefore, this indicates that methylotrophic methanogens may play a critical role in methanogenesis in Tanakeke's mangroves.

Although the importance of methylotrophic methanogens in mangrove forests has been identified since the 1990s by Ramamurthy *et al*. (1990) and Mohanraju and Natarajan (1992), there appear to be a few studies that further investigate this topic. Mohanraju *et al*. (1997) and Lyimo *et al*. (2009) were successful in isolating a species of methylotrophic methanogens from mangrove sediments. Lymo *et al*. also tested metabolic responses of methylotrophic methanogens and SRB to various substrates (Lyimo *et al*., 2000; Lyimo *et al*., 2002; Lyimo *et al*., 2009). Later, Jing *et al*. (2016) investigated methanogenic communities using deoxyribonucleic acid (DNA) analysis, indicating methylotrophic methanogens are the most abundant. In contrast, Chuang *et al*. (2016) noted that there is concurrence between sulfate reduction and methanogenesis in some sites when observing CH_4 and SO_4^{2-} dynamics in the pore-water sediment of a mangrove lagoon.

In this study, I investigated methanogenic pathways in overwash mangrove forests by combining analysis of sediment geochemistry, microbial functional groups and potential CH_4

production. Depth profile analysis of CH_4, SO_4^{2-}, S^{2-}, Cl^- and Fe^{2+} was used as a proxy to elucidate which processes (methanogenesis, sulfate reduction or pyritisation) were occurring in the system. I used the spread plate count method, as well as an analysis of extractable functional genes, to gain insight into which group of methanogens was dominant. Finally, laboratory experiments with additional methanogenic substrates (methanol, acetate and hydrogen) added to sediment slurries were used to provide evidence of which substrates were more favourable to methane production.

6.2 Study location and sampling site

The study was conducted in Dusun Lantangpeo, Tanakeke Island, South Sulawesi, Indonesia, which was fully described in Chapter 3. According to Lugo and Snedaker (1974), this mangrove forest is categorised as an overwash forest because it is located very close to sea level and is completely overwashed during high tides. The sampling sites for sediment geochemistry were the same as those described in Chapter 5—Sites 1 to 9 (also see Fig. 6.1). The sediment sampling for microbial enumerations and sediment slurry experiments was undertaken in the three sites used for geochemical analysis of sediment—Sites 3, 5 and 8.

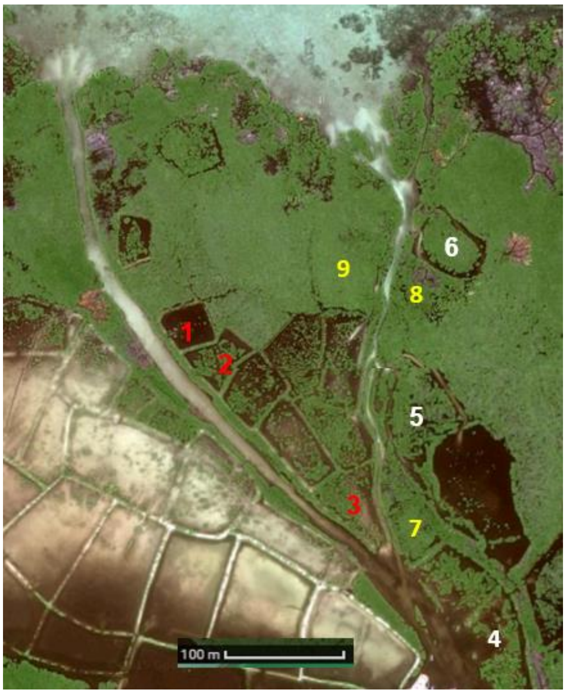

Figure 6.1. **Site locations in the study area. Distribution of sampling sites (1–9) plotted on Google Earth imagery, depicting the landscape of aquaculture ponds and mangroves with two creeks splitting the landscapes. White and brown colour spotted by green (lower section of figure) depicts recently abandoned ponds; patches of green colour surrounded by a brown line depict long abandoned ponds; green colour blocks show undisturbed mangrove vegetation.**

6.3 Sample collection and analytical methods

6.3.1 Sediment geochemistry

I used sediment geochemical data collected in February 2017 for the analysis (see Chapter 5 for details). These data were selected because the maximum concentration of pore-water CH_4 was found at the wet season. The data may depict a strong indication of CH_4 production, while I assumed that sulfate reduction always occur in the saline environment. Thus, depth profile analysis of CH_4 and SO_4^{2-} was conducted to provide a more detailed interpretation of anaerobic respiration, which had been indicated by the pore-water CH_4 and SO_4^{2-} relationship reported in Chapter 5. Besides CH_4 and SO_4^{2-}, the data for sulfide (S^{2-}) concentrations were also selected to assist in the analysis of sulfate reduction. In addition, the geochemical data for Site 7 were included in this chapter, yet excluded in Chapter 5. As explained in Chapter 5, some mangrove trees in Site 7 were chopped down during the fieldwork program, and this disturbance apparently affected the local sediment geochemistry and made the interpretation of pore-water CH_4 difficult with respect to mangrove successional status. However, the disturbance appeared to generate peculiar depth profiles of SO_4^{2-} and CH_4 that clearly showed the concurrence of CH_4 production and SO_4^{2-} reduction.

Chapter 4 described the method for collecting the data for the geochemistry of Tanakeke's mangrove sediment. Here, I also report measurements of pore-water salinity (‰), which have not previously been reported. Salinity was used to estimate chlorine concentrations (Cl^-). The Cl^- and SO_4^{2-} ion concentrations were used to calculate the ratio $[SO_4^{2-}]/[Cl^-]$ and used as an indicator of sulfate reduction (Howarth and Giblin, 1983; Graedel and Keene, 1996). Salinity was measured using a salinity refractometer (S-10E 2422 Atago), with a scale range of 0.0 to 10.0% sodium chloride and minimum scale of 0.1%. Cl^- was estimated using Eqn. 6.1 (Wright *et al*., 2011):

$$[Cl^-] = \frac{(Salinity.10^3)}{35.453},$$ **Equation 6.1**

where Cl^- is in mM and salinity is in ‰.

At Site 3, repeated sampling to assess the sediment geochemistry was performed at two-hour intervals from 8.00 am to 6.00 pm on 24 August 2016. This was to capture diurnal changes of CH_4 and SO_4^{2-} profiles to depict methane production and sulfate reduction in a short timescale.

6.3.2 Microbial enumeration

The microbial enumerations were undertaken using the spread plate count method and quantitative polymerase chain reaction (qPCR) method of extractable functional genes. These approaches were incorporated in this study because they provided complementary results showing all possible processes in sediment respiration. The spread plate count method required a 1 g sediment sample, while the qPCR method required around 0.25 g. The sediment sampling was undertaken only once in the dry season for the first method, while, for the second, it was completed during both the dry and wet seasons.

The sediment sampling for both the plate count and qPCR method was performed with the same technique. The sampling was undertaken in the dry and wet season for the qPCR method, yet only in the dry season for the other method. One sediment core was collected at each selected site (Sites 3, 5 and 8) using a 100 cm hand auger. The sediment core was sampled from the surface to 50 cm depth and then sliced into five separate 10 cm sections. Each 10 cm slice was sub-sampled by scooping the inner section of the slice with a spatula. The sub-samples were then placed into three sterile Eppendorf tubes until they were full. The tubes containing sediment samples were stored in a zip-lock plastic bag. Before zipping the bag, the air inside the bag was flushed with UHP nitrogen (N_2) for around one minute and then the air was squeezed out. The bag was wrapped with sticky tape to minimise air exchange, and stored in a cool box to be sent to a laboratory. In the laboratory, the sediment samples for the spread plate count method had to proceed as soon as possible, while the sediment samples for qPCR analysis were stored (at -4°C) until further processing.

For the spread plate counting, the sediment samples were inoculated into the selective agar media by pouring the slurry of sediments. The slurry was made from serial 10 × dilutions of the sediment samples. Initially, 1 g sediment was added by 0.85% NaCl to make a total solution volume of 5 mL. After vortexing this sediment suspension, 0.1 mL suspension was transferred to the clean tube and diluted with 0.85% NaCl to a total volume of 1 mL. This dilution was then repeated 10 times and the last three dilutions (10^{-8} to 10^{-10}) were selected to be poured into the agar medium for isolation of methylotrophic methanogens. To isolate acetotrophic methanogens, 10^{-4} to 10^{-6} dilutions were selected. Hydrogenotrophic methanogens were not involved in this microbial enumeration because I used agar medium for the isolation of methanogens, and I found it difficult to amend CO_2/H_2 into this medium for hydrogenotrophic substrates.

The agar medium for methanogen isolations in this study referred to the recipe for rumen methanogens, known as *artificial saliva* (McDougall, 1947). It was made from 250 mL Aqua Dest, 30 mL macro-mineral, 0.15 mL micro-mineral, 30 mL buffer solution, 1.6 mL Resazurin, 20 mL reduction solution and 10 g agarose. The macro-mineral consisted of 5.7 g L^{-1} Na_2HPO_4, 6.2 g L^{-1} KH_2PO_4 and 1 g L^{-1} $MgSO_4.7H_2O$, while the micro-mineral contained 132 g L^{-1} $CaCl_2.2H_2O$, 100 g L^{-1} $MnCl_2.4H_2O$, 10 g L^{-1} $CaCl_2.6H_2O$ and 10 g L^{-1} $FeCl_3$. The buffer solution was made from 35 g $NaHCO_3$ and 4 g NH_4HCO_3 diluted in 1 L Aqua Dest. The Resazurin solution was made from 1 g Resazurin in 1 L Aqua Dest, while the reduction solution was made from 373 mg $Na_2S.H_2O$ and 2.6 mL of 1 mol L^{-1} NaOH diluted in 62 mL Aqua Dest. The agar media for isolation of methylotrophic methanogens were enriched by 25 mL of 5% methanol, while the media for acetotrophs were enriched by 25 mL of 25% acetate. The methanogens colony count was conducted after a 72-hour incubation in an anaerobic jar, and expressed as colony forming unit per gram of wet sediment (CFU g^{-1}).

Prior to functional gene enumerations, bacterial or archaeal DNA was isolated using a MOBIO PowerSoil Kit (Zhuang *et al*., 2016). DNA was extracted following the kit's protocol. Initially, 0.25 g samples were vortexed in the Power Bead tubes and centrifuged at 10,000 g for 30 seconds. Then, serial centrifugations with the provided solutions were conducted to obtain 100 µL DNA solution per sample. The DNA extracts were stored at -20°C before being used to construct the targeted genes and enumerate their abundance.

The construction of targeted genes was done by qPCR on a PCR—the LightCycler Nano Instrument (Roche). I used methyl coenzyme M reductase or *mcrA* gene to detect methanogen populations. The particulate methane monooxygenase (*pmoA*) and dissimilatory sulfite reductase beta subunit (*dsrB*) genes were used to detect methanotrophs and SRB. DNA extract of 1 µL was used as a template for PCR with a reaction mixture containing SYBR green I dye (Toyobo, Osaka, Japan), and the primers of the targeted genes, provided in Table 6.1. The temperature of qPCR in pre-incubation was set at 95°C for 1 minute. The PCR amplification was 45 cycles (denaturation at 95°C for 5 s, annealing at 60°C for 15 s and elongation at 72°C for 30 s).

Table 6.1. Primers used for qPCR.

Oligo name	Sequence	References
mcrA	Forward: M13F (5'-TGTAAAACGACGGCCAGTGGTGGTGTMGGATTCACACARTAYGCWACAGC-3') Reverse: M13R (5'-CA-GGAAACAGCTATGACCTTCATTGCRTAGTTWGGR-TAGTT-3')	Luton *et al*. (2002)
dsrB	Forward: DSRp2060F (5'-CAACATCGTYCAYACCCAGGG- 3') Reverse: DSR4R (5'- GTGTAGCAGTTACCGCA-3')	Geets *et al*. (2006)
pmoA	Forward: A189 (5'-GGNGACTGGGACTTCTGG-3') Reverse: A682 (5'-GAASGCNGAGAAGAASGC-3')	Holmes *et al*. (1995)

The enumeration of target genes was conducted based on cycle quantification value (C_q), which was generated by qPCR. The number of target gene copies was calculated using a standard curve of C_q and gene copies. Ideally, a standard curve is generated using a serial dilution of the solution of the pure target genes. Here, I made the standard curve by using gene copies of a pure culture of *Escherichia coli* strain InaCC B5. Ten standard suspensions of *E. coli* DNA with different concentrations were prepared from the *E. coli* suspension of 4.6×10^{10} CFU mL^{-1} ($\approx 4.6 \times 10^{10}$ CFU g^{-1}), diluted 10 times. According to Oliver *et al*. (2016), CFU g^{-1} correlates with gene copies g^{-1} samples and its linear regression has a slope of around one ($R = 0.82$). Therefore, I established the standard curve based on gene copies of *E. coli* and the values of Cq generated from qPCR. This standard curve, then, was used to estimate a relative abundance of *mcrA*, *pmoA* and *dsrB*, as the functional genes of methanogens, methanotrophs and SRB. However, it should be kept in mind that this estimation was not to indicate the absolute copy numbers of target genes, but to compare the relative abundance among different bacteria/archaea groups (in CFU g^{-1} sediments).

6.3.3 Sediment slurry experiments

Sediment slurry experiments were performed to identify the methanogenesis pathways through CH_4 production from sediment samples. Three kinds of substrates were tested, which represented the major methanogenic pathways (Table 6.2). The control treatments consisted of an untreated sediment and an autoclaved sediment in which all living organisms were killed at a temperature of 121°C for two hours. Two replicates were prepared for each combination (sampling sites/treatments). The sampling of gas headspace was conducted once per week, starting within seven days after preparation and continuing for around five weeks. An exception was the autoclaved treatments, where the sampling was performed only at Day 7, as well as the last day of the experiment. The microbial enumerations were also undertaken for all the sediment slurries at Days 0 and 28, using the spread plate count method in units of CFU mL^{-1} slurry.

Table 6.2. Treatment conditions for sediment slurry experiments.

	Treatments	Volume, duration and concentration	Experiment length (days)	Replicates	Sites	Depth levels
Controls	No additional substrates	N_2 headspace	37	2	3	5
	Autoclaved	N_2 headspace	37	2	3	5
Treatments (methanogenic substrates)	Methanol	30 µL, 10 mM	37	2	3	5
	Acetate	30 µL, 10 mM	37	2	3	5
	H_2 gas	100%, 1 min	37	2	3	5

The sediment samples were obtained from the same sites as the sampling for microbial enumerations (Sites 3, 5 and 8). In the laboratory, a 10 g sediment sample of each slice was weighed, stored in a 120 mL bottle, and then mixed with 10 mL seawater collected from the mangrove waters. During this preparation, UHP N_2 was flushed continuously inside the bottle to maintain a consistently low oxygen environment. For the addition of liquid methanogenic substrates (methanol and acetate), 30 µL, 10 mM of these solutions was poured into the sediment slurry, before the bottles were sealed with grey butyl rubber stoppers. H_2 amendment was made by flushing 100% H_2 into the sediment slurry for around one minute just before sealing. All bottles used were placed in the dark at room temperature.

Gas headspace samples were collected using plastic syringes. A 20 mL gas sample was withdrawn from each bottle. The same volume of UHP N_2 was injected into the experiment bottle to compensate the gas pressure change. The gas samples were transferred into gas-tight aluminium bags to be sent to another laboratory that was equipped with GC-FID. Details of the GC setting can be found in Chapter 4.

6.4 Results

6.4.1 Sediment geochemistry

The geochemical data, selected from the full-year measurement, showed a full range of pore-water CH_4 concentrations, ranging between 0.06 and 63 µmol L^{-1} (Fig. 6.2A). This range was similar to the pore-water CH_4 data in the full-year measurement (0.04 to 59.87 µmol L^{-1}—see Chapter 5). Pore-water SO_4^{2-} concentrations had a narrow range of 30.2 to 59.3 mM. The selected CH_4 data were then plotted alongside pore-water SO_4^{2-} against depth. SO_4^{2-} depth profiles showed similar figures (except for Site 7), while CH_4 profiles showed variability among sites. However, site comparison of these profiles is not of concern in the current chapter because it has been discussed in Chapter 5. In addition, incorporating this aspect is not necessary for the analysis of geochemical data regarding the concurrence of methane production and sulfate reduction in the current chapter. Nevertheless, this phenomenon was more obvious at Site 7 than the other sites. SO_4^{2-} concentrations at this site were uniform (10 mmol L^{-1}) at all depths, while CH_4 concentrations varied between 0.09 and 63 µmol L^{-1}. In addition, the occurrence of sulfate reduction was evidenced by the presence of pore-water sulfide (Fig. 6.2B) and $[SO_4^{2-}]:[Cl^-]$ ratio (Fig. 6.2C). Fig. 6.2C shows that the ratio was always lower in the pore-water than in the seawater (solid line at 0.0518), except for Site 5 at a depth of 30 cm.

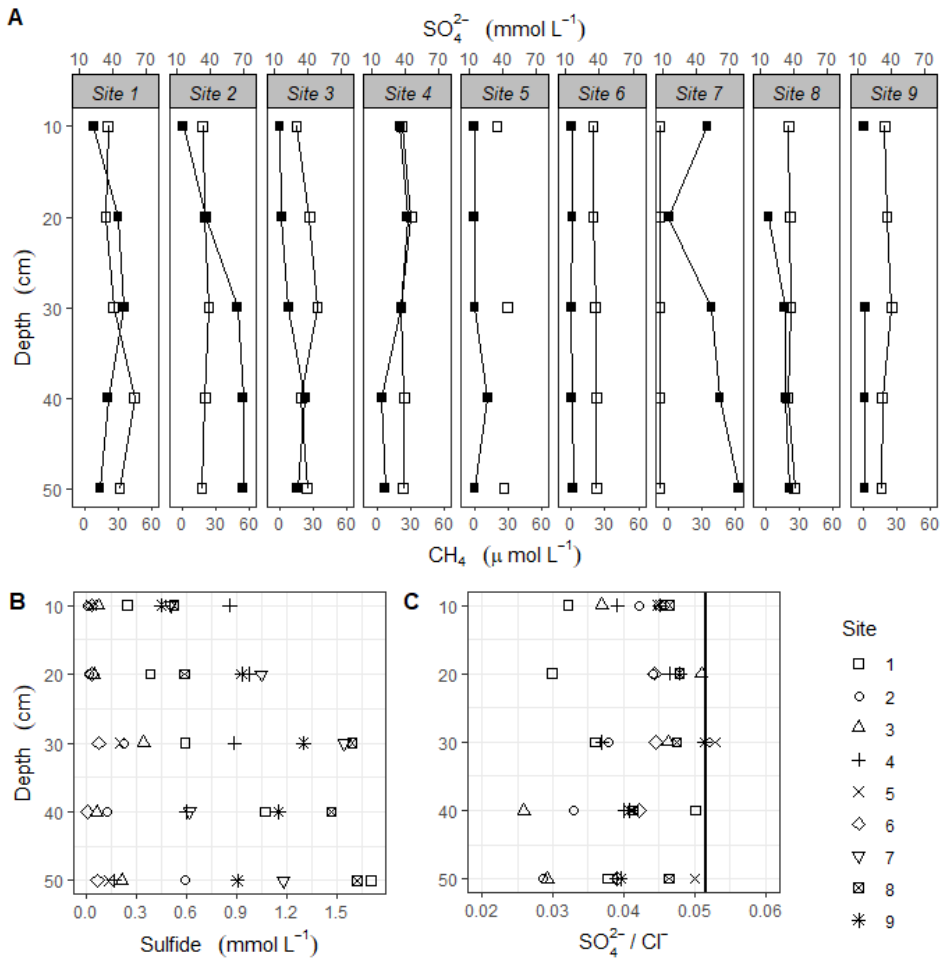

Figure 6.2. Sulfate-methane systems in pore-water mangroves. (A) Depth profiles of dissolved methane (closed squares) and sulfate (open squares) in pore-water. Panels represent study sites (note missing data at 20 and 40 cm for Site 5). (B) Pore-water sulfide concentrations. (C) Sulfate and chloride ratio—a proxy for sulfate reduction compared with this ratio in seawater (vertical heavy solid line at 0.0518 represents reference seawater).

The diurnal evolution of SO_4^{2-} and CH_4 concentrations provided much clearer results in the analysis of geochemical data regarding the co-occurrence of methane production and sulfate reduction (Fig. 6.3). At Site 3, CH_4 concentrations were near-minimum at 08.00 hrs and generally increased until sunset, with the largest increases at depths of 20 and 40 cm (Fig. 6.3B). For example, CH_4 concentrations at 20 cm depth increased rapidly from 2.3 to 17.8 µmol L^{-1} within 10 hours (8.00 am to 6.00 pm). The ratio of $[SO_4^{2-}]:[Cl^-]$ further supported the concurrence of methane production and sulfate reduction with the lower value in the pore-water compared with those in the seawater (Fig. 6.3B). Sulfide was detected in the pore-water samples, yet its values were very low (0 to 0.13 mmol L^{-1}) (Fig. 6.3C).

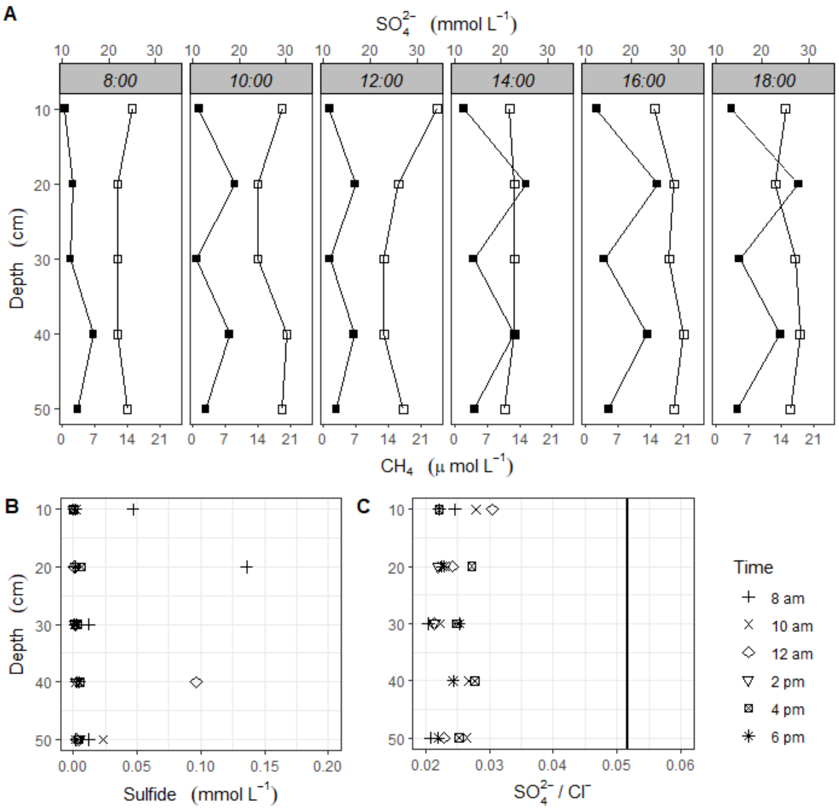

Figure 6.3. Diurnal dynamics of the sulfate-methane system at Site 3. (A) Measurements of pore-water sulfate (open squares) and methane (closed squares) over daylight hours. First measurement was at 8.00 am and last was at 6.00 pm (depicted in the panels). (B) Pore-water sulfide concentrations. (C) Sulfate and chloride ratio—a proxy for sulfate reduction compared with this ratio in seawater (vertical heavy solid line at 0.0518).

6.4.2 Abundances of methanogens, methanotrophs and SRBs

According to qPCR analysis, the abundance of methanogens in the sediment samples ranged between 72 and 6×10^5 CFU g^{-1} sediment, while the abundance of SRB ranged from 2×10^2 to 2×10^5 CFU g^{-1} sediment (Fig. 6.4). At the three sampling sites (Sites 3, 5 and 8), the abundance of methanogens was generally higher than those of SRB. However, in the wet season, the abundance of SRB was greater than the methanogens that were observed at the surface sediments, around 10 to 20 cm. The range of methanotroph abundance accounted for between 7 and 8×10^4 CFU g^{-1} wet sediment. The maximum abundance of methanotrophs was observed to be one order of magnitude lower than methanogens and SRB.

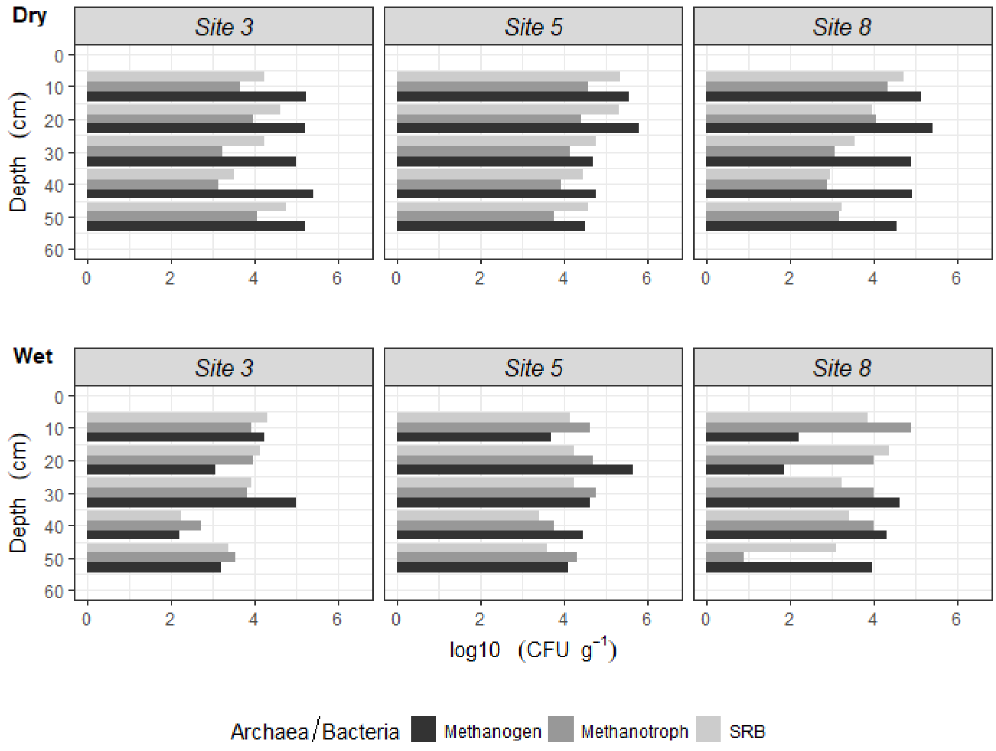

Figure 6.4.The abundances of archaea/bacteria groups (methanogens, methanotrophs and SRBs). Panels represent the three selected sites. Sediment samples were collected in the dry and wet seasons.

Fig. 6.5 indicates the abundance of methylotrophic and acetotrophic methanogens (CFU g^{-1}), revealed from the plate count method. The abundances of methylotrophic methanogens ranged between 8.3 × 10^2 and 5.1 × 10^4 CFU g^{-1}, while those of acetotrophs ranged from 0 to 7.7 × 10^2 CFU g^{-1}. In other words, the abundance of methylotrophic methanogens was two orders of magnitude greater than that of acetotrophs. This domination was observed in all 50 cm sediment depths at the three selected sites (Sites 3, 5 and 8) only in the dry season. Here, I assumed that hydrogenotrophic methanogens were considerably low compared with methylotrophic methanogens. This is due to the sediment geochemistry and qPCR results consistently shows an indication that hydrogenotrophic methanogens may be out-competed by SRBs (Fig. 6.2, 6.3 and 6.4). Therefore, domination of methylotrophic pathways at the current study sites was evident.

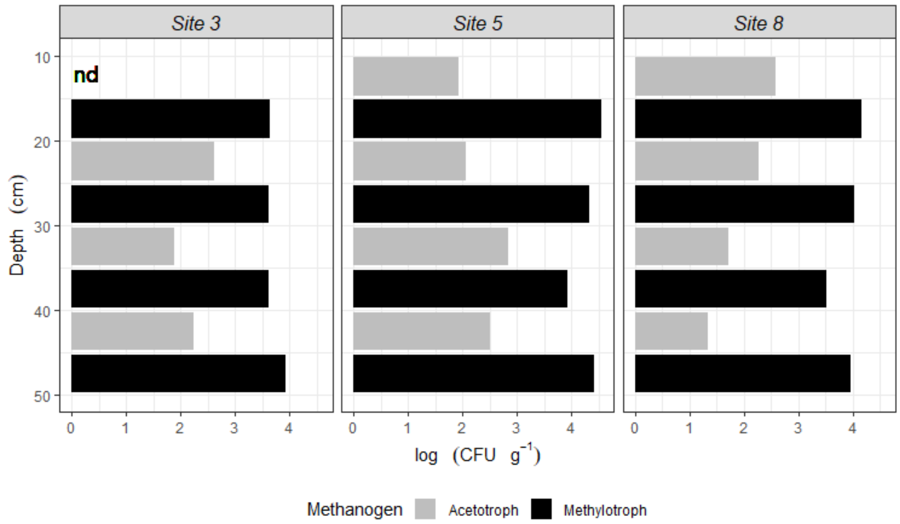

Figure 6.5. The abundance of methylotrophic and acetotrophic methanogens. The number of panels represents the three sampling sites. Data were collected only in the dry season. The values are the average of two replicates. 'nd' means 'not detected'.

6.4.3 Potential CH_4 production

Methanol amendment into the sediment slurries yielded a massive amount of CH_4, as much as 9×10^4 ppm (Fig. 6.6). At this figure, the headspace CH_4 was presented as an average of two replicates and five depths because there was no clear pattern with depth. The surge of CH_4 in the methanol amendment occurred similarly in the three selected sites and was observed from the first measurement at Day 7 to the end at Day 37. The headspace CH_4 at Site 3 accounted for 1.9 (±1.8) × 10^4 ppm at Day 7 and continued to increase afterwards. It reached the maximum value of 5.8 (±2.1) × 10^4 ppm at Day 28 and then decreased slightly by Day 37. Similarly, Sites 5 and 8 exhibited peaks at Day 28 with the values of 7.3 (±1.2) × 10^4 and 6.8 (±2.5) × 10^4 ppm, respectively. They also showed a slight decrease by Day 37. The minimum value of CH_4 at Site 5 was 4.4 (±3.2) × 10^4 ppm (Day 21), while at Site 8 was 2 (±3.4) × 10^4 ppm (Day 14). The headspace CH_4 observed in the treatment of methanol amendment was one to two orders of magnitude higher than that in the control experiments. For the autoclaved sediments, the magnitudes ranged from 3.3 (±8.3) × 10^2 to 1.9 (±2.1) × 10^3 ppm, while, for the no substrate amendments, values ranged from 4 (±9) × 10^2 to 3.7 (±3.6) × 10^3 ppm. Meanwhile, the other two treatments had the same order of magnitude of headspace CH_4 as the controls.

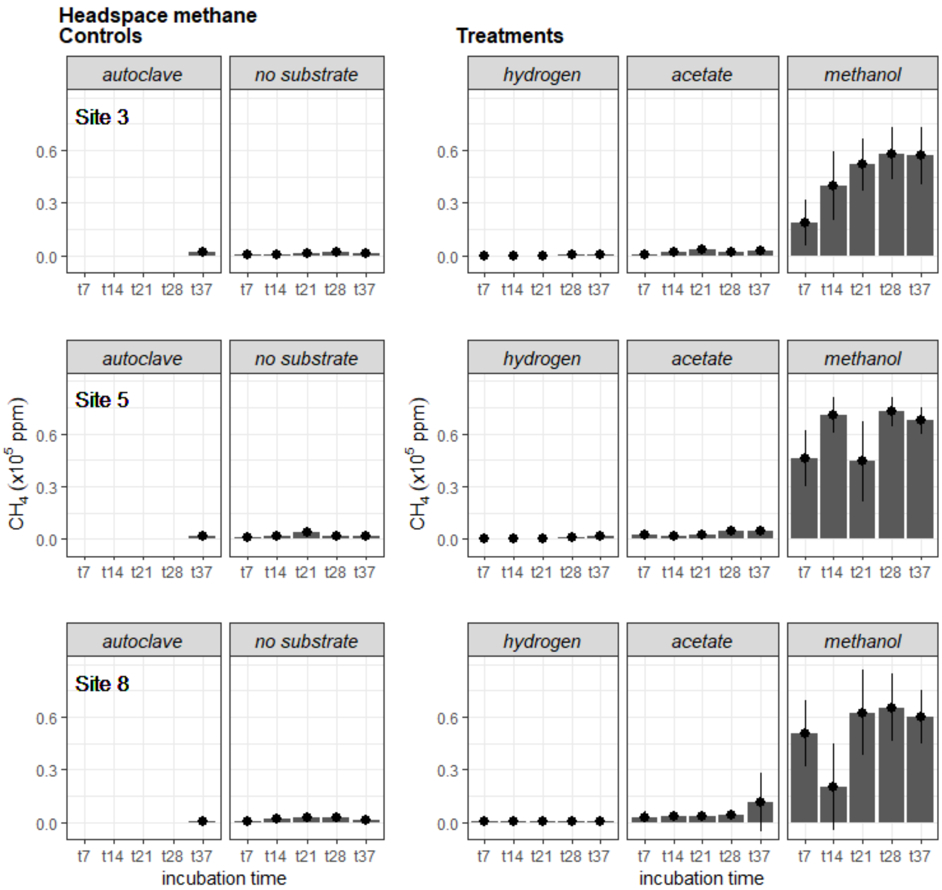

Figure 6.6. **CH_4 concentrations in the headspace following the sampling times. Incubation times (t7 to t37) denote sampling times from Day 7 to 37. Controls and treatments are indicated at the top of each panel. The values are the average of the two replicates and five depths, and error bars represent 1 standard deviation.**

The enumerations of the methanogen colony at Days 0 and 28 of the incubation times confirmed that methylotrophic methanogens played a critical role in methane production in the sediment samples (Fig. 6.7). The treatment of methanol amendments clearly depicted that the abundance of methylotrophs at Day 28 was around eight orders of magnitude greater than those at Day 0. Further, similar figures were observed in the other treatments, as well as in the controls, which indicated that SRB did not inhibit methylotrophic methanogens. These figures were observed at all three selected sites (Sites 3, 5 and 8). More interestingly, methylotrophic methanogens survived and were able to grow normally, although the sediment samples had been autoclaved.

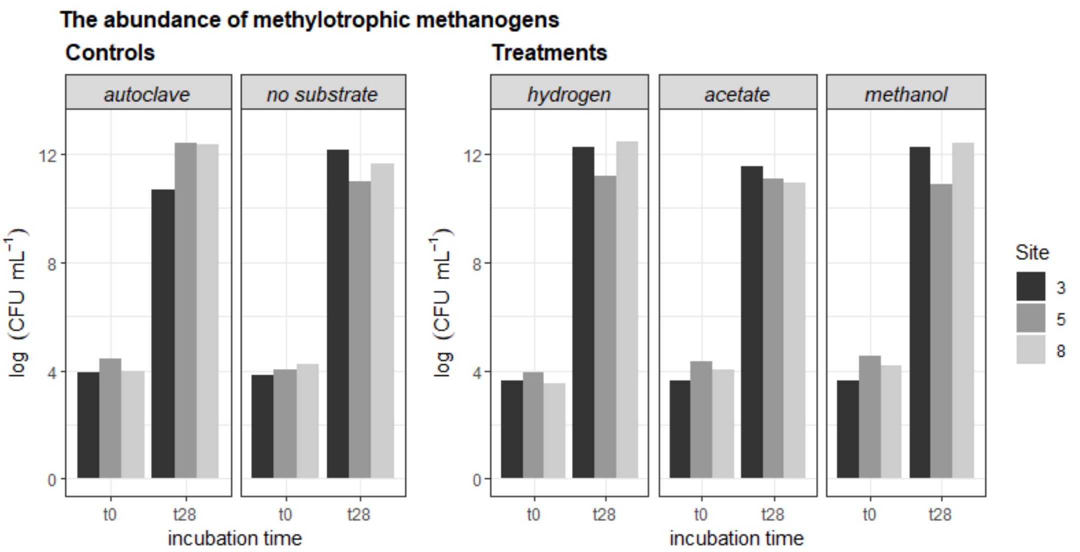

Figure 6.7. **The abundance of methylotrophic methanogens in the sediment slurries at Day 0 and 28. Treatment indicated at the top of each panel. The values are the average of two replicates and five depths.**

In contrast, acetotrophic methanogens apparently were out-competed by SRB in the slurry sediment experiments. First, it was indicated by the five experiments that acetotrophs were not detected at Day 28, although at Day 0 they were abundant (Fig. 6.8). This occurred in all the treatments, as well as the control (no substrate amendments). Second, the experiment of autoclaved sediments showed that acetotrophic methanogens survived and were able to grow. Thus, at Day 28, the abundance of acetotrophs was 10 orders of magnitude greater than at Day 0. This indicated that SRB might be killed after the sediments were autoclaved, and hence did not inhibit the acetotrophic methanogens.

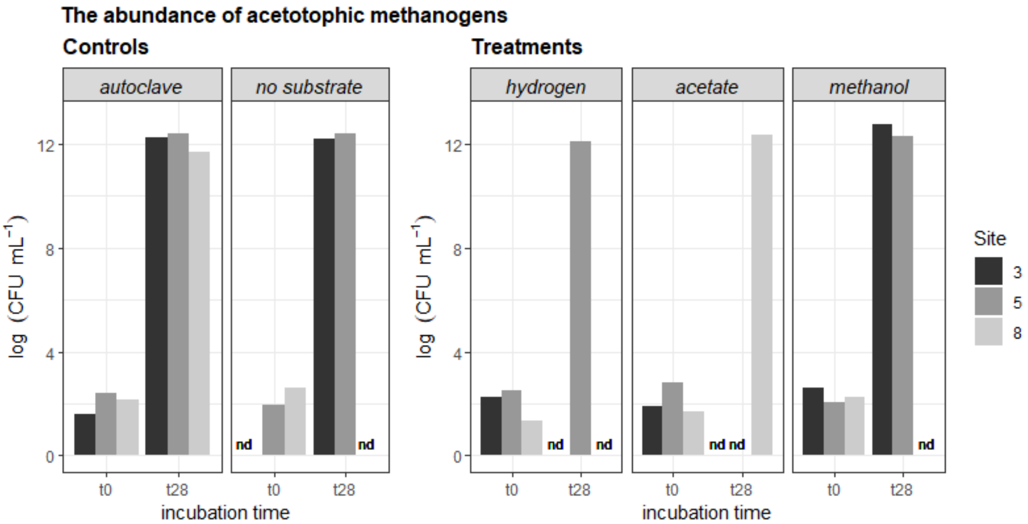

Figure 6.8. **The abundance of acetotrophic methanogens in the sediment slurries at Day 0 (t0) and 28 (t28). Treatment indicated at the top of each panel. The values are the average of two replicates and five depths. 'nd' means 'not detected'.**

6.5 Discussion

Here, I have investigated sediment geochemistry, microbial enumerations and potential methane production to identify the dominant pathway of methanogenesis at the study sites. Sediment geochemistry reported in Fig. 6.2 indicated that methane production and sulfate reduction co-occurred at all the sites. In addition, Fig. 6.3 displayed this concurrence within a short timeframe (one day). The functional gene quantification further confirmed that SRB and methanogens coexisted in the sediment samples. Indeed, the plate count method provided an insight that the abundance of methylotrophic methanogens was two orders of magnitude greater than that of acetotrophs. Further, when methanol was added to the sediment samples in the sediment slurry experiments, CH_4 production increased substantially (Fig. 6.6). In total, these results indicate that methylotrophic methanogens were the dominant pathway for methane production at the study sites.

6.5.1 Sediment geochemistry

In general, the concentration of pore-water SO_4^{2-} remained high (25 to 30 mM) (see Fig. 6.2A and 6.3A). However, Site 7 in Fig. 6.2A showed low concentrations of SO_4^{2-} at all depths (~7 mM), which means that sulfate reduction occurred at this site. For the other sites, sulfate reduction could be detected by the $[SO_4^{2-}]/[Cl^-]$ ratio presented in Fig. 6.2C and 6.3C, where the ratio was always lower in the pore-water than in the reference seawater (0.0518). In sulfate reduction, SO_4^{2-} is reduced, while Cl^- in seawater is assumed to be conservative, allowing the $[SO_4^{2-}]/[Cl^-]$ ratio to decrease (Howarth and Giblin, 1983; Graedel and Keene, 1996).

The ratio of $[SO_4^{2-}]/[Cl^-]$ has been widely used to detect sulfate reduction. It should be kept in mind that this ratio basically represents sulfate depletion because it is not only sulfate reduction, but also sulfide re-oxidation and pore-water exchange with seawater. At my sites, sulfide oxidation in aerobic conditions was unlikely because the mangrove sediments were always anaerobic at depths > 10 cm. Sulfate oxidation may occur at the top 10 cm, but I did not measure it (see Chapter 5). In anaerobic conditions, sulfide could be converted to sulfate by the presence of MnO_2 (King, 1990; Schippers and Jorgensen, 2002; Machado *et al.*, 2008). Although MnO_2 was not measured here, it can be inferred from the positive relationships between reactive manganese and silt percentage (Roy *et al.*, 2013). Given that the sediments at my sites were typically sandy (see Chapter 4) or had a low percentage of silt, MnO_2 contents could be low. Thus, I could postulate that sulfide oxidation by this compound was unlikely to occur.

One may argue that periodic inundation may dilute pore-water with seawater, adding more SO_4^{2-}, thereby leading to bias in the interpretation of the $[SO_4^{2-}]/[Cl^-]$ ratio as an indicator of sulfate reduction. This typical dilution is particularly true in mangrove ecosystems situated in a steep landscape, with high inundation amplitudes (Susilo *et al.*, 2005; Xia and Li, 2012).

However, my study sites had a relatively flat terrain, where sediment surfaces were near MSL. In addition, the pore-water did not totally drain out during the low tide (see Chapter 5). Hence, seawater dilution into pore-water occurred, but may only have added a small amount of seawater to the pore-water. Another argument posits that Cl^- in mangrove pore-water may decrease as *Rhizophora* spp. trees (also found as a dominant species in my study location) uptake saline water and release Cl^- through salt glands in the leaves (Carlson *et al*., 1983). However, this should make the $[SO_4^{2-}]/[Cl^-]$ ratio higher in the pore-water than in the seawater (Carlson *et al*., 1983), while my results showed a lower ratio. Therefore, I suggest that the $[SO_4^{2-}]/[Cl^-]$ ratio reported here may represent sulfate reduction.

The presence of pore-water sulfide (S^{2-}) may also suggest that sulfate reduction occurred. However, the concentrations of sulfide were low at all sites, ranging from 3×10^{-3} to 1.6 mmol L^{-1} (Fig. 6.2B), while in previous studies it was substantially higher, ranging from 1 to 6 mmol L^{-1} (Nickerson and Thibedou, 1985; Lyimo and Mushi, 2005). The range of sulfide in the diurnal measurement at Site 3 was even lower (0 to 0.13 mmol L^{-1}) (Fig. 6.3B). According to these figures, I speculate that S^{2-} reacted with Fe^{2+}, forming metastable compounds of FeS or FeS_2 (pyrite), as previously reported (Araújo *et al*., 2012; Nóbrega *et al*., 2013). This mechanism could occur because pore-water Fe^{2+} was also in low concentrations (see Chapter 5). Alternatively, Fe^{2+} concentration in my study sites was inherently low because of the sediments being sandy, while Fe^{2+} is commonly associated with silty sediments (Roy *et al*., 2013). In contrast, a low concentration of S^{2-} was probably due to SO_4^{2-} not being totally depleted, which was depicted from SO_4^{2-} concentrations that remained high (30.2 to 60 mmol L^{-1}). Nevertheless, the presence of sulfide likely indicated sulfate reduction at my study sites.

The occurrence of sulfate reduction, however, did not seem to inhibit methane production. Sulfate reductions did occur at the sampling sites, at depths>10 cm and so did methane productions. Further, if sulfate reduction inhibits methane production, the depth profiles of SO_4^{2-} and CH_4 should mirror each other (Martens and Berner, 1974), yet this was not observed in my study. The concurrence of sulfate reduction and methane production was more clearly depicted at Site 7, where the pore-water SO_4^{2-} ranged between 7 and 7.3 mmol L^{-1}, while pore-water dissolved CH_4 ranged between 0.09 and 62.8 mmol L^{-1}. At this site, trees were chopped down during the sampling, possibly leading to a greater supply of labile organic matter from the decomposition of the dead roots, which could supply non-methylotrophic substrates. Thus, the abundance of these substrates in the sediments could provide enough supplies for both SRBs and methanogens (Holmer and Kristensen, 1994). In this condition, SRB initially dominate the substrate use, incorporating SO_4^{2-} as the energy source. Once SO_4^{2-} depletes, methanogens use the remaining substrates. In the limited substrates—which could be the case at most study sites—SRBs could coexist with methanogens because they are unable to inhibit the metabolism of methylotrophic methanogens, given that the SRB and methylotrophic methanogens use different kinds of substrates, with methylotrophs using more specific substrates—that is, methylated compounds (Oremland and Polcin, 1982; Kiene *et al*., 1986). Alternatively, SRB may use substrates (e.g., methylated amines and methanethiol) that can produce methylated compounds, and thus feed methylotrophic methanogens.

As explained in Chapter 5, the sediments in the study sites contained organic matter that was mainly supplied by mangrove vegetation. The import of terrestrial organic matter into this mangrove forest was negligible because of it being located on a small coralline island situated 10 km from the mainland. In contrast, marine organic matter, including from mangrove trees, is rich in methylated compounds (e.g., methanol, trimethylamine and dimethyl sulfide), which are derived from cell fluids or cytoplasm. The cytoplasm of marine organisms contains taurine, betaine, glycine, choline and alanine as osmolytes, which allow cells to maintain an osmotic balance with saline water (Yancey *et al*., 1982; Slama *et al*., 2015; Downing *et al*., 2018). Further, some methanogens can use choline directly—a precursor of methylated compounds (Watkins *et al*., 2012). Therefore, there is a high possibility that methane production co-occurred with sulfate reduction at my study sites, as has been suggested in previous studies (Mitterer, 2010; Ramírez-Pérez *et al*., 2015; Sela-Adler *et al*., 2017; Cadena *et al*., 2018).

6.5.2 Microbial enumerations

The abundance of methanogens ranged from 7.2×10^1 to 6×10^5 CFU g^{-1}, or it can be said that the abundance of the functional gene of methanogens (*mcrA*) ranged from 72 to 6×10^5 gene copies g^{-1} (see the method section and Fig. 6.4). This range was comparatively lower than those reported previously—for example, 10^8 gene copies g^{-1} in river sediments (Chaudhary *et al*., 2017; Tong *et al*., 2017), 2.5×10^6 to 3.7×10^9 gene copies g^{-1} in paddy soils (Bao *et al*., 2014) and 10^6 gene copies g^{-1} in saltmarshes (Zeleke *et al*., 2013; Gao *et al*., 2018). However, it is comparable with those found in the subsurface of a tidal flat (0 to 4×10^5 gene copies g^{-1} sediments) and in lake sediment (5×10^6 gene copies g^{-1}) (Wilms *et al*., 2007; Yang *et al*., 2017). The low population of methanogens in my study may be due to the low supply of methanogenic substrates, given that the geochemical evidence suggested that the sediments were conducive for methanogen growth (see Chapter 5), whereas sulfate reduction is unlikely to inhibit methane production.

The abundance of SRB seemed to reflect some signs that sulfate reduction has less influence on methane production. The abundance of SRB was generally lower than methanogens (Fig. 6.4). However, the abundance of SRB can be greater than methanogens—for example, at the top layer of sediments (10 to 20 cm)—during the wet season. In such a case, I could interpret that methanogens can be inhibited by SRB because there is a shift of methanogenic communities driven by environmental changes. For example, Reshmi *et al*. (2015) found that, during the wet season, more organic matter was supplied from terrestrial ecosystems, and enhanced the metabolism of acetotrophic methanogens in estuarine sediments. Thus, this methanogen group was more abundant during the wet than dry season, while the abundance of methylotrophic methanogens did not differ significantly between the seasons. Meanwhile, Jing *et al*. (2016) reported that heavy metals caused a shift of methanogenic pathways in polluted mangrove sediments. Further, this kind of shift may occur because of vegetation changes in the wetland, which lead to changes in methanogenic substrates (Yuan *et al*., 2016). In my case, SRBs were likely to coexist with methanogens, but seasonal variations in pore-water and sediment geochemistry could alter the methanogenic communities at the top layer of sediments, thereby leading SRB at this layer to be more abundant in the wet than dry season.

The coexistence between SRB and methanogens was supported by the fact that methylotrophic methanogens were more abundant than acetotrophic methanogens in all the samples. Methylotrophic methanogens made up a huge colony in my mangrove sediments, with the abundance range of 8.3×10^2 to 5.1×10^4 CFU g^{-1}, while the abundance of acetotrophs ranged from 0 to 7.7×10^2 CFU g^{-1}. For comparison, Reshmi *et al*. (2015) reported that the abundance of methylotrophs in estuarine sediments ranged from 1.9×10^2 to 10^3 CFU g^{-1}, while the abundance of acetotrophs ranged between 2×10^2 and 8.1×10^2 CFU g^{-1}. Torres-Alvarado *et al*. (2013) also observed that methylotrophs were the most abundant in estuarine sediments during the dry season (10^6 to 2×10^7 cells g^{-1}), while acetotrophs accounted for between 3×10^4 and 10^5 cells g^{-1}. In the wet season, they found that the abundance of acetotrophs (10^6 to 2×10^7 cells g^{-1}) and methylotrophic methanogens (10^7 to 2×10^7 cells g^{-1}) could be within a similar range.

To my knowledge, there are few studies in mangrove sediments addressing the enumeration of methanogens. This renders it difficult to compare my work with previous studies. An early attempt by Mohanraju and Natarajan (1992) noted that the total abundance of methanogens ranged from 3.6×10^2 to 1.1×10^5 cells g^{-1}. However, they did not mention the abundance of each group of methanogens. In contrast, Jing *et al*. (2016) presented a detailed study in methanogenic communities up to class-level taxonomic groups. They found that methylotrophic methanogens were predominant in almost all their samples. This is in accordance with my findings and thus might add evidence to support the premise that methylotrophic methanogenesis could be the dominant pathway of methane production in the current study.

6.5.3 Potential CH_4 production

The control experiment using autoclaved sediments demonstrated a surprising result that the sediments still produced CH_4 at around the same rate as the other control treatment (no additional substrates) (Fig. 6.6). Further, bacterial enumerations at Day 0 and 28 demonstrated that methanogens survived and grew well (Fig. 6.7 and 6.8). These are intriguing results. To my knowledge, methanogen archaea has no spores, which allows survival in extreme heat (Peter and Conrad, 1995). In addition, to date, only methanogen archaea living in thermal vents are known to survive in the autoclave temperature of 110°C (Miller *et al*., 1988; Takai *et al*., 2008). Therefore, further investigation should be undertaken to characterise the methanogens in my study sites.

Meanwhile, the addition of methanol into the sediment slurry resulted in the rapid and high production of CH_4 (Fig. 6.6), which occurred similarly in the sediments from all three selected sites (Sites 3, 5 and 8). For example, on Day 7 of Site 3, CH_4 concentrations in the bottle headspace with methanol amendment were two orders of magnitude higher {1.9 (±1.8) × 10^4 ppm} than the control (no additional substrates) {4 (±9.2) × 10^2 ppm}. Afterwards, this headspace CH_4 increased gradually to reach a peak at Day 28. This is in agreement with Chuang *et al*. (2016), Xiao *et al*. (2017) and Lyimo *et al*. (2002). According to them, methylated compounds are more favourable for methanogens than competitive substrates (hydrogen and acetate), even though the *in-situ* concentrations are extremely low. In contrast, the experiments with hydrogen and acetate amendments yielded CH_4 of the same order of magnitude as in the controls. Therefore, only the experiments with methanol amendment demonstrated significantly increased CH_4 production.

When the number of methanogens in the sediment slurry of experiments was enumerated, methylotrophic methanogens were detected in all the treatments and controls (Fig. 6.7). In addition, methylotrophic methanogens proliferated successfully, even in the autoclaved sediments. The abundance of methanogens at Day 28 was eight orders of magnitude higher than those at Day 0. In contrast, not all the treatment conditions showed that acetotrophic methanogens survived until Day 28, particularly in the treatments with acetate and H_2 amendments (Fig. 6.8). This indicated that SRB inhibited acetotrophs through competition for the same substrates (acetate or H_2) (Oremland and Polcin, 1982). Therefore, the slurry sediment experiments provided further evidence that methylotrophic methanogenesis was the dominant pathway at my study sites.

6.6 Synthesis

Despite SO_4^{2-} being abundant in the pore-water at the mangrove sites, apparently it did not reduce methane production. The presence of SO_4^{2-} controls methane production through two mechanisms. First, SRB out-compete acetotrophic and hydrogenotrophic methanogens for common substrates (Oremland and Polcin, 1982). Second, SRB interact with anaerobic methanotrophs to oxidise methane (Bebout *et al*., 2004; Avrahamov *et al*., 2014). My study provides evidence for these two mechanisms.

I found that SRB out-competed acetotrophic and hydrogenotrophic methanogens, while methylotrophic methanogens played a major role in methane production. I found that the abundance of methanogens was generally higher than SRB. Further, methanogens comprised more methylotrophic methanogens than acetotrophs. The *in-situ* measurements revealed that the depth profiles of pore-water CH_4 were not mirroring SO_4^{2-} profiles, indicating that CH_4 productions did not depend on sulfate reduction. Moreover, the ratio of $[SO_4^{2-}]/[Cl^-]$ provided evidence that sulfate reduction really occurred, while pore-water CH_4 was abundant. The sediment slurry experiments further indicated that stimulation by methanol amendments into sediment samples resulted in the highest yield of headspace CH_4. Investigations into the methanogens in the sediment samples revealed that methylotrophic methanogens grew well, while acetotrophic methanogens were undetected on Day 28 of incubation. In contrast, hydrogen and acetate stimulation produced CH_4 at the same order of magnitudes as those without stimulation.

SRB may cooperate with anaerobic methanotrophs, yet their low abundance and the high abundance of SO_4^{2-} indicated that this pathway may be less important in controlling pore-water CH_4. I detected the presence of methanotrophs in my sediment samples. These methanotrophs were likely anaerobic methanotrophs because mangrove sediments are always anaerobic (see Chapter 5). The abundance of methanotrophs (7 to 8×10^4 CFU g^{-1}) was one order of magnitude lower than methanogens (72 and 6×10^5 CFU g^{-1}). Thus, I could interpret that the rate of CH_4 production was higher than the rate of CH_4 oxidation. However, this interpretation should be used with caution, as suggested by Tong *et al*. (2015b), since they found a weak correlation between methane production and methanogen abundance.

6.7 Conclusion

This study confirms the importance of the methylotrophic pathway for methane production in overwash mangrove environments. The results from sediment geochemistry analysis, microbial enumerations and potential CH_4 production provide evidence for this pathway. In fact, the rate of *in-situ* methane production would mainly rely on the concentrations of methylated compounds supplied into the sediment. Therefore, future studies should consider this supply and the mass balance of methanogenesis to quantify the relative importance of methylotrophic methanogenesis with the other pathways in mangrove forests, and determine how it controls methane emissions.

Chapter 7: Conclusion and recommendations

7.1 Background

In designing climate policy mechanisms based around the blue carbon concept, a key consideration has been carbon sequestration potential (McLeod *et al*., 2011; Ullman *et al*., 2013). Likewise, CO_2 emissions—particularly due to coastal ecosystem degradation or land use changes—have also been a fundamental concern (Ahmed and Glaser, 2016; Atwood *et al*., 2017; Lovelock *et al*., 2017) because these activities offset the gains made by sequestration. However, CH_4 emissions have been overlooked because of the comparatively smaller fluxes involved (Twilley *et al*., 2017; Cabezas *et al*., 2018). For example, a typical CO_2 flux is three to four orders of magnitude higher than a typical CH_4 flux (Song and Liu, 2016; Gao *et al*., 2018). On a mass basis, it is easy to see why attention has focused on CO_2 fluxes. However, CH_4 has 25 times more GWP than CO_2 (Forster *et al*., 2007) and, from the perspective of reducing global warming, CH_4 is of interest.

In early attempts, CH_4 emissions from mangrove ecosystems were mostly investigated by taking measurements at the sediment–atmosphere interface. However, recent studies have reported that CH_4 produced in mangrove sediments could be transported to surrounding waters (Call *et al*., 2015) and released through the water surface (Jacotot *et al*., 2018). Rosentreter *et al*. (2018) posited that this could partially offset the rates of carbon burial. Further, a number of very recent papers reported that a substantial fraction of the total methane flux to the atmosphere is via plant stems (Pangala *et al*., 2015; Pangala *et al*., 2017; Maier *et al*., 2018; Pitz *et al*., 2018). Therefore, CH_4 emissions from mangrove ecosystems are likely to be under-reported in the existing literature.

7.2 Research findings and contributions

This study described CH_4 in the pore-water of mangrove rehabilitation sites on a tropical island in Indonesia. The study included the development of a measurement system of pore-water CH_4, application of the system and analysis of the mechanisms underpinning the observed space–time variability of pore-water CH_4. The main findings of the thesis are summarised in Fig. 7.1.

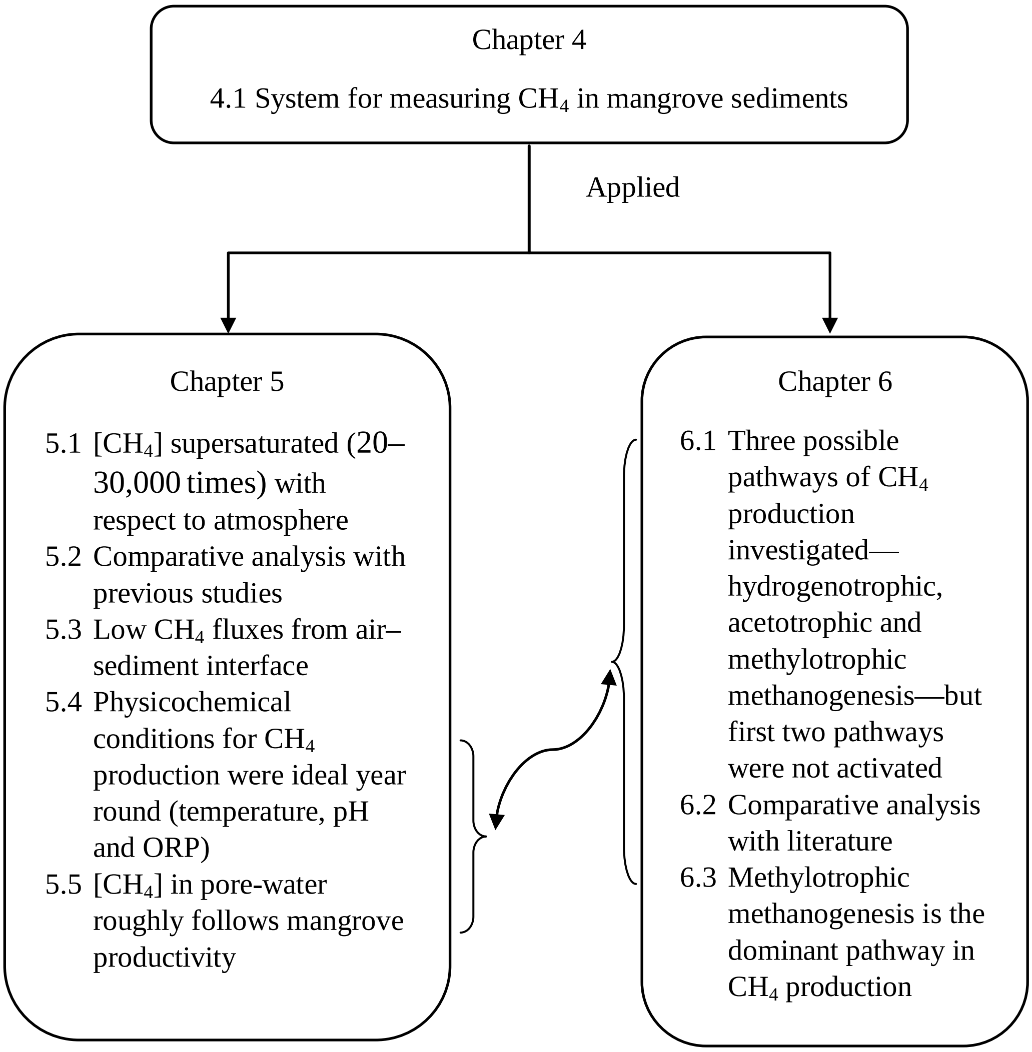

Figure 7.1. Summary of findings.

Finding 1: A system for measuring CH_4 in mangrove sediments was developed by using readily available materials (Point 4.1, Fig. 7.1 and Fig. 4.2). This system is capable of extracting pore-water from various depths simultaneously and repeatedly at a typical rate of ~4,000 mL hour^{-1} in sandy sediments. In this study, the CH_4 contents in the gas samples that were evacuated from pore-water samples were measured using GC. Besides CH_4 measurements, various physicochemical parameters of pore-water can also be measured simultaneously. Therefore, this measurement system can provide depth profiles of multi-parameters, allowing for the analysis of geochemical or biological mechanisms underpinning space–time variability in the amount of CH_4 dissolved in pore-water.

Finding 2: Applications of the measurement system revealed that pore-water in mangrove sediments was supersaturated (20 to 30,000 times) with CH_4 with respect to the atmospheric equilibrium (1.75 µmol L^{-1}) (Point 5.1, Fig. 7.1 and Fig. 5.3). The pore-water CH_4 varied seasonally, but the pattern was different from site to site. Moreover, the depth profiles of pore-water CH_4 did not show any distinct pattern.

Finding 3: Pore-water CH_4 concentrations in my study (0.04 to 59.9 µmol L^{-1}) were within the range of those found in previous studies in mangrove sediments (0 to 875 µmol L^{-1}) (Point 5.3, Fig. 7.1 and Table 5.1). However, the concentrations were generally one order of magnitude lower than those reported from freshwater wetlands (Table 5.1).

Finding 4: In this study, CH_4 emissions were estimated from pore-water CH_4 concentrations that were measured in the top sediment layer (0 to 10 cm) (Point 5.3, Fig. 7.1). The results showed that the study sites were relatively low emitters of CH_4, with average and median estimated fluxes of 2.1 and 0.6 mg m^{-2} h^{-1}, respectively (Table 5.2). This aligns with many previous studies. However, this fact has raised the question of how pore-water CH_4 can be oxidised. Anoxic conditions in mangrove sediments suggested that CH_4 oxidation was unlikely, while the flat terrain and tidal cycle in the study sites indicated that tidal pumping was also unlikely to drain out the pore-water. Consequently, I deduced that mangrove pore-water CH_4 was most likely transported to the atmosphere via plant stems.

Finding 5: In the study area, the prevailing physicochemical conditions (temperature, pH and ORP) were ideal year round for the production of CH_4 (Point 5.4, Fig. 7.1). For example, pore-water was always in the anaerobic condition needed by microorganisms to produce CH_4. Interestingly, pore-water CH_4 was not correlated with SO_4^{2-}, indicating that SO_4^{2-} reduction did not inhibit CH_4 production. Consequently, to identify the underpinning mechanisms that control pore-water, I further investigated the regrowth effects of mangrove forests on pore-water CH_4 and the concurrence of CH_4 production and SO_4^{2-} reduction. The results are explained below in Finding 6 (Point 5.5, Fig. 7.1) and Finding 7 (Point 6.1–3, Fig. 7.1), respectively.

Finding 6: Pore-water CH_4 correlated with mangrove stand BA, which is in turn a surrogate of stand age (Point 5.5, Fig. 7.1). Given that mangrove productivity is expected to scale with stand age, an association between CH_4 concentration in pore-water and mangrove productivity is reasonable. The general pattern of forest productivity has long been known to follow stand age, while pore-water CH_4 roughly follows a similar pattern. This association might occur because of changes over time (with stand age) in the carbon allocation pattern of mangrove vegetation. For example, a high allocation of photosynthate to root exudates and fine roots would lead to the use of that carbon by methanogen microorganisms. Hence, at the study site, CH_4 production was apparently controlled by mangrove productivity, rather than the prevailing physicochemical conditions.

Therefore, **Finding 6** has a crucial implication for blue carbon management. It has long been known that above-ground carbon increases exponentially in the initial stages of growth, yet levels off as mangrove forests mature (> 25 years old) (Fig. 7.2A) (Alongi, 2011). In contrast, below-ground carbon may continue to increase, like in Sasmito *et al.* (2019) (Fig. 7.2B). Hence, carbon sequestration in the soil has made mangrove ecosystems attractive for climate change mitigation. However, CH_4 production in mangrove sediment should be considered in mangrove rehabilitation for mitigation projects, particularly in the intermediate stage (~5 to 10 years old), when CH_4 production reaches its peak (Fig. 7.2C).

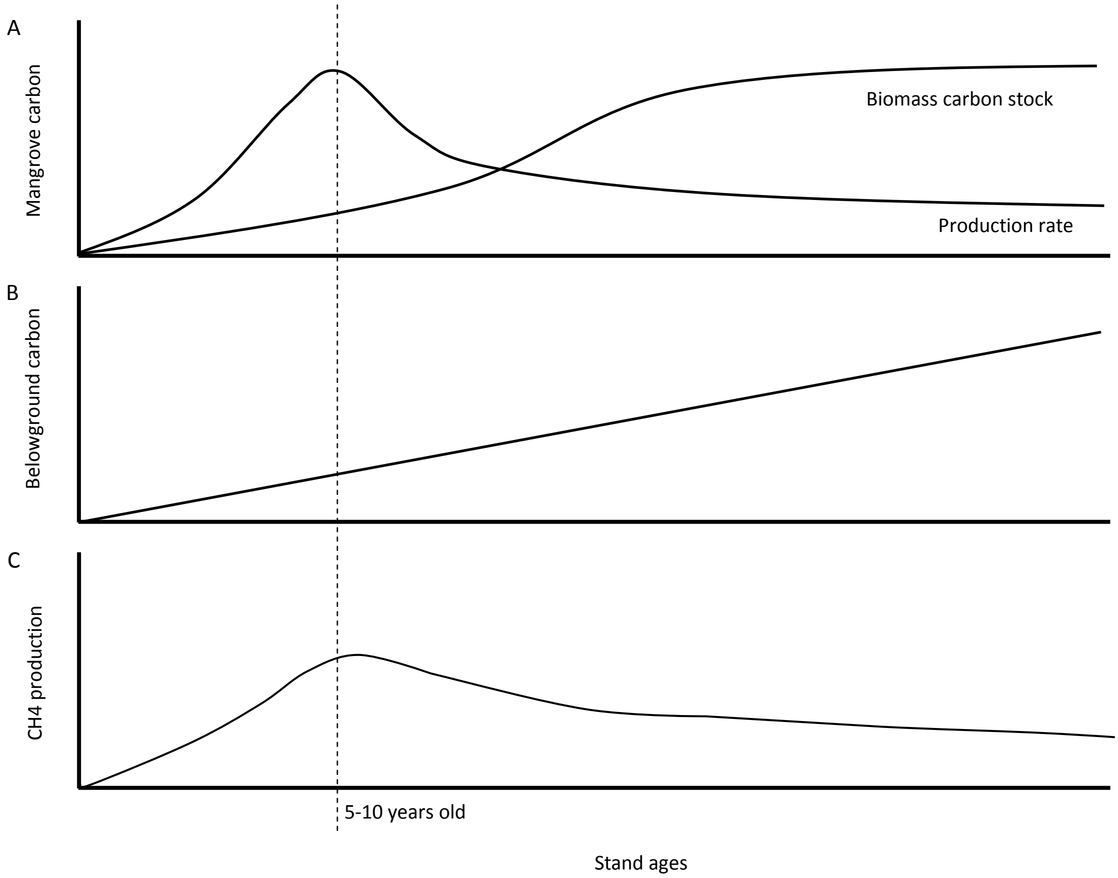

Figure 7.2. Conceptual model of carbon accumulation in mangrove forests.

Finding 7: Among three pathways for CH_4 production (hydrogenotrophic, acetotrophic and methylotrophic), the first two pathways were not activated (Point 6.1, Fig. 7.1 and Fig 6.6). This means that CH_4 production was mainly through the methylotrophic pathway, which does not depend on SO_4^{-2} reduction. This result aligns with **Finding 5** (Point 5.4, Fig. 7.1) that SO_4^{2-} did not correlate with pore-water CH_4.

Finding 8: Although **Finding 7** is uncommon in most previous studies, especially those from freshwater wetlands, my results on CH_4 production pathways (dominated by the methylotrophic pathway) align with other studies in mangrove environments (Point 6.2, Fig. 7.1). Further, recent studies in deep-sea sediments also reported the relative importance of the methylotrophic pathway in the sea sediment.

Finding 9: With multiple approaches, the methylotrophic pathway was consistently detected as the dominant process (Point 6.3, Fig. 7.1 and Fig. 6.3 to 6.6). This detection was achieved through analysis of sediment geochemistry, microbial functional groups and potential CH_4 production.

7.3 Recommendations for future research

This study has found that physicochemical conditions are optimum for methane production, and this result is likely to hold in tropical environments worldwide. The findings demonstrate that vegetation plays a central role in the supply of substrates for methane production, and very recent literature indicates that at least some of this methane is transported to the atmosphere via the woody stems of mangroves. Based on this, I recommend future research investigate the following.

The role of vegetation productivity in CH_4 production (Chapter 5). This can be studied at macro levels to include the following questions: (i) What is the allocation of carbon production to fine roots and exudates? (ii) How does the seasonal variability of productivity shape CH_4 production and/or emission? (iii) How does the productivity of different mangrove species determine CH_4 production and/or emission? (iv) If there are non-mangrove sources of methanogenic substrates (Chapter 6), how does the relative importance of mangrove productivity control CH_4 production? With that knowledge, we could better understand the total carbon budget on mangrove ecosystems. The line of questions can also be approached from micro-levels to examine: (i) fine root production and decomposition (e.g., seasonal pattern and contribution to methanogenic substrates), (ii) exudates (e.g., chemical compositions, quantity and variability) and (iii) the microbial community in the rhizosphere and its interaction with mangrove roots (Chapter 6).

Measurement of CH_4 emissions through woody plant tissues of mangrove species (Chapter 5). This investigation could include the following questions: (i) What is the magnitude of CH_4 fluxes through woody plant stems or specialised root structures (i.e., prop and stilt roots)? (ii) Do the fluxes come from pore-water CH_4, CH_4 produced in the stems/roots or both? (iii) What are the mechanisms of CH_4 transport from sediment to the atmosphere through the woody plant stems/roots? (iv) What is the proportion of CH_4 emissions that occur through the woody plant stems/roots?

The extension of CH_4 observations in various geomorphological and hydrological settings. The oceanic mangroves in the study region represented a very simple system because the mangrove vegetation was the sole source of carbon (see Chapters 5 and 6). This result needs to be extended to the more general case, where carbon can be supplied from upstream flows. This leads to a final recommendation regarding how different geomorphological and hydrological settings determine CH_4 production and emissions. This includes: (i) lateral carbon inputs from terrestrial ecosystems, (ii) freshwater inputs, (iii) seasonal patterns of carbon and freshwater inputs, (iv) tidal cycles and anaerobic conditions and (v) shifts in methanogen or microbial communities.

References

Ahmed, N. and Glaser, M., 2016. Coastal aquaculture, mangrove deforestation and blue carbon emissions: is REDD+ a solution? *Marine Policy*, 66: 58–66.

Aksornkoae, S., 1993. *Ecology and Management of Mangroves*, IUCN, Bangkok, Thailand.

Allen, D.E., Dalal, R.C., Rennenberg, H., Meyer, R.L., Reeves, S., and Schmidt, S., 2007. Spatial and temporal variation of nitrous oxide and methane flux between subtropical mangrove sediments and the atmosphere, *Soil Biology and Biochemistry*, 39(2): 622–631.

Allen, D.E., Pringle, M.J., Page, K.L., and Dalal, R.C., 2010. A review of sampling designs for the measurement of soil organic carbon in Australian grazing lands, *Rangeland Journal*, 32(2): 227–246.

Allen, D.E., Dalal, R.C., Rennenberg, H., and Schmidt, S., 2011. Seasonal variation in nitrous oxide and methane emissions from subtropical estuary and coastal mangrove sediments, Australia, *Plant Biology*, 13(1): 126–133.

Alongi, D.M., 2009. *The Energetics of Mangrove Forests*. Dodrecht, Springer Netherlands.

Alongi, D.M., 2011. Carbon payments for mangrove conservation: ecosystem constraints and uncertainties of sequestration potential, *Environmental Science and Policy*, 14(4): 462–470.

Alongi, D.M., 2014. Carbon cycling and storage in mangrove forests, *Annual Review of Marine Science*, 6(1): 195–219.

Alongi, D.M., Sasekumar, A., Chong, V.C., Pfitzner, J., Trott, L.A., Tirendi, F., Dixon, P., and Brunskill, G.J., 2004. Sediment accumulation and organic material flux in a managed mangrove ecosystem: Estimates of land-ocean-atmosphere exchange in peninsular Malaysia, *Marine Geology*, 208(2–4): 383–402.

Alongi, D.M., Pfitzner, J., Trott, L.A., Tirendi, F., Dixon, P., and Klumpp, D.W., 2005. Rapid sediment accumulation and microbial mineralization in forests of the mangrove *Kandelia candel* in the Jiulongjiang Estuary, China, *Estuarine, Coastal and Shelf Science*, 63(4): 605–618.

Alongi, D.M., Murdiyarso, D., Fourqurean, J.W., Kauffman, J.B., Hutahaean, A., Crooks, S., Lovelock, C.E., Howard, J., Herr, D., Fortes, M., Pidgeon, E., and Wagey, T., 2015. Indonesia’s blue carbon: a globally significant and vulnerable sink for seagrass and mangrove carbon, *Wetlands Ecology and Management*, 24: 3–13.

Alongi, D.M., Tirendi, F., and Trott, L.A., 1999. Rates and pathways of benthic mineralization in extensive shrimp ponds of the Mekong delta, Vietnam, *Aquaculture*, 175(3–4): 269–292.

Arai, H., Yoshioka, R., Hanazawa, S., Minh, V.Q., Tuan, V.Q., Tinh, T.K., Phu, T.Q., Jha, C.S., Rodda, S.R., Dadhwal, V.K., Mano, M., and Inubushi, K., 2016. Function of the methanogenic community in mangrove soils as influenced by the chemical properties of the hydrosphere, *Soil Science and Plant Nutrition*, 62(2): 150–163.

Araújo, J.M.C., Otero, X.L., Marques, A.G.B., Nóbrega, G.N., Silva, J.R.F., and Ferreira, T.O., 2012. Selective geochemistry of iron in mangrove soils in a semiarid tropical climate: effects of the burrowing activity of the crabs *Ucides cordatus* and *Uca maracoani*, *Geo-Marine Letters*, 32(4): 289–300.

Aselmann, I. and Crutzen, P.J., 1989. Global distribution of natural freshwater wetlands and rice paddies, their net primary productivity, seasonality and possible methane emissions, *Journal of Atmospheric Chemistry*, 8(4): 307–358.

Atwood, T.B., Connolly, R.M., Almahasheer, H., Carnell, P.E., Duarte, C.M., Lewis, C.J.E., Irigoien, X., Kelleway, J.J., Lavery, P.S., Macreadie, P.I., Serrano, O., Sanders, C.J., Santos, I., Steven, A.D.L., and Lovelock, C.E., 2017. Global patterns in mangrove soil carbon stocks and losses, *Nature Climate Change*, 7(7): 523–528.

Aulakh, M.S., Wassmann, R. and Rennenberg, H., 2001. Methane emissions from rice fields—quantification, mechanisms, role of management, and mitigation options, *Advances in Agronomy*, 70(C): 193–260.

Avrahamov, N., Antler, G., Yechieli, Y., Gavrieli, I., Joye, S.B., Saxton, M., Turchyn, A.V., and Sivan, O., 2014. Anaerobic oxidation of methane by sulfate in hypersaline groundwater of the Dead Sea aquifer, *Geobiology*, 12(6): 511–528.

Bao, Q.L., Xiao, K.Q., Chen, Z., Yao, H.Y., and Zhu, Y.G., 2014. Methane production and methanogenic archaeal communities in two types of paddy soil amended with different amounts of rice straw, *FEMS Microbiology Ecology*, 88(2): 372–385.

Bartlett, K.B., Bartlett, D.S., Harriss, R.C., Sebacher, D. I., 1987. Methane emissions along a salt marsh salinity gradient, *Biogeochemistry*, 4(3): 183–202.

Bazhin, N.M., 2003. Theoretical consideration of methane emission from sediments, *Chemosphere*, 50(2): 191–200.

Bazhin, N.M., 2004. Influence of plants on the methane emission from sediments, *Chemosphere*, 54(2): 209–215.

Bebout, B.M., Hoehler, T.M., Thamdrup, B., Albert, D., Carpenter, S.P., Hogan, M., Turk, K., and Des Marais, D.J., 2004. Methane production by microbial mats under low sulphate concentrations, *Geobiology*, 2(2): 87–96.

Beck, M., Dellwig, O., Kolditz, K., Freund, H., Liebezeit, G., Schnetger, B., and Brumsack, H.-J., 2007. In situ pore water sampling in deep intertidal flat sediments, *Limnology and Oceanography-Methods*, 5: 136–144.

Belger, L., Forsberg, B.R. and Melack, J.M., 2011. Carbon dioxide and methane emissions from interfluvial wetlands in the upper Negro River basin, Brazil, *Biogeochemistry*, 105(1): 171–183.

Bertolin, A., Rudello, D. and Ugo, P., 1995. A new device for in-situ pore-water sampling, *Marine Chemistry*, 49(2–3): 233–239.

Biswas, H., Mukhopadhyay, S.K., Sen, S., and Jana, T.K., 2007. Spatial and temporal patterns of methane dynamics in the tropical mangrove dominated estuary, NE coast of Bay of Bengal, India, *Journal of Marine Systems*, 68(1–2): 55–64.

Bodelier, P.L., Roslev, P., Henckel, T., and Frenzel, P., 2000. Stimulation by ammonium-based fertilizers of methane oxidation in soil around rice roots, *Nature*, 403: 421–424.

Boon, P.I. and Lee, K., 1997. Methane oxidation in sediments of a floodplain wetland in south-eastern Australia, *Letters in Applied Microbiology*, 25(2): 138–142.

Boon, P.I. and Mitchell, A., 1995. Methanogenesis in the sediments of an Australian freshwater wetland: comparison with aerobic decay, and factors controlling methanogenesis, *FEMS Microbiology Ecology*, 18(3): 175–190.

Borges, A.V., Delille, B., Schiettecatte, L., Gazeau, F., Abril, G., Frankignoulle, M., and Gazeau, F. 2004. Gas transfer velocities of CO_2 in three European estuaries, *Limnology and Oceanography*, 49(5): 1630–1641.

Borges, A.V. and Abril, G., 2011. Carbon dioxide and methane dynamics in estuaries, in *Treatise on Estuarine and Coastal Science, Volume 5: Biogeochemistry*, eds E. Wolanski and D. McLusky, Academic Press, Waltham.

Bosire, J.O., Dahdouh-guebas, F., Walton, M., Crona, B.I., Lewis, R.R., Field, C., Kairo, J.G., and Koedam, N., 2008. Functionality of restored mangroves : A review. *Aquatic. Botany*. 89: 251–259.

Bourgeois, C., Alfaro, A.C., Dencer-Brown, A., Duprey, J.L., Desnues, A. and Marchand, C. 2019. Stocks and soil-plant transfer of macro-nutrients and trace metals in temperate New Zealand estuarine mangroves. *Plant Soil*, 436:565-586

Bouillon, S., Middelburg, J.J., Dehairs, F., Borges, A.V., Abril, G., Flindt, M.R., Ulomi, S., and Kristensen, E., 2007. Importance of intertidal intertidal sediment processes and porewater exchange on the water column biogeochemistry in a pristine mangrove creek (Ras Dege, Tanzania), *Biogeosciences*, 4(3): 311–322.

Bouillon, S., Borges, A.V., Castañeda-Moya, E., Diele, K., Dittmar, T., Duke, N.C., Kristensen, E., Lee, S.Y., Marchand, C., Middelburg, J.J., Rivera-Monroy, V.H., Smith, T.J., and Twilley, R.R., 2008. Mangrove production and carbon sinks: A revision of global budget estimates, *Global Biogeochemical Cycles*, 22(2): 1–12.

Breithaupt, J.L., Smoak, J.M., Smith, T.J., Sanders, C.J., and Hoare, A., 2012. Organic carbon burial rates in mangrove sediments: Strengthening the global budget, *Global Biogeochemical Cycles*, 26(3): 1–12.

Brown, B., Fadillah, R., Nurdin, Y., Soulsby, I., and Ahmad, R., 2014. Community Based Ecological Mangrove Rehabilitation (CBEMR) in Indonesia, *S.a.p.i.en.s*, 7(2): 1–13.

Bufflap, S. and Allen, H., 1995. Sediment pore water collection methods for trace metal analysis: a review, *Water Research*, 29(1): 165–177.

Cabezas, A., Mitsch, W.J., MacDonnell, C., Zhang, L., Bydałek, F., and Lasso, A., 2018. Methane emissions from mangrove soils in hydrologically disturbed and reference mangrove tidal creeks in southwest Florida, *Ecological Engineering*, 114: 57–65.

Cadena, S., García-Maldonado, J.Q., López-Lozano, N.E., and Cervantes, F.J., 2018. Methanogenic and Sulfate-Reducing Activities in a Hypersaline Microbial Mat and Associated Microbial Diversity, *Microbial Ecology*, 75(4): 930–940.

Call, M., Maher, D.T., Santos, I.R., Ruiz-Halpern, S., Mangion, P., Sanders, C.J., Erler, D.V., Oakes, J.M., Rosentreter, J., Murray, R., and Eyre, B.D., 2015. Spatial and temporal variability of carbon dioxide and methane fluxes over semi-diurnal and spring-neap-spring timescales in a mangrove creek, *Geochimica et Cosmochimica Acta*, 150: 211–225.

Cameron, C., Hutley, L.B., Friess, D.A., and Munksgaard, N.C., 2019a. Hydroperiod, soil moisture and bioturbation are critical drivers of greenhouse gas fluxes and vary as a function of landuse change in mangroves of Sulawesi, Indonesia, *Science of the Total Environment*, 654: 365–377.

Cameron, C., Hutley, L.B., Friess, D.A., and Brown, B., 2019b. Community structure dynamics and carbon stock change of rehabilitated mangrove forests in Sulawesi, Indonesia, *Ecological Applications*, 29(1): 1-20.

Cao, W., Hong, H. and Yue, S., 2005. Modelling agricultural nitrogen contributions to the Jiulong River estuary and coastal water, *Global and Planetary Change*, 47: 111–121.

Carlson, P.R., Yarbro, L.A., Zimmermann, C.F., and Montgomery, J.R., 1983. Pore water chemsitry of an overwash mangrove island, *Florida Scientist*, 46(3–4): 239–242.

Chambers, L.G., Davis, S.E., Troxler, T., Boyer, J.N., Downey-Wall, A., and Scinto, L.J., 2014. Biogeochemical effects of simulated sea level rise on carbon loss in an Everglades mangrove peat soil, *Hydrobiologia*, 726(1): 195–211.

Chang, T.C. and Yang, S.S., 2003. Methane emission from wetlands in Taiwan, *Atmospheric Environment*, 37(32): 4551–4558.

Chanton, J.P., Bauer, J.E., Glaser, P.A., Siegel, D.I., Kelley, C.A., Tyler, S.C., Romanowicz, E.H., and Lazrus, A., 1995. Radiocarbon evidence for the substrates supporting methane formation within northern Minnesota peatlands, *Geochimica et Cosmochimica Acta*, 59(17): 3663–3668.

Chaudhary, P.P., Rulík, M. and Blaser, M., 2017. Is the methanogenic community reflecting the methane emissions of river sediments? Comparison of two study sites, *MicrobiologyOpen*, 6(4): 1–9.

Chauhan, R., Datta, A., Ramanathan, A.L., and Adhya, T.K., 2015. Factors influencing spatio-temporal variation of methane and nitrous oxide emission from a tropical mangrove of eastern coast of India, *Atmospheric Environment*. 107: 95–106.

Chauhan, R., Ramanathan, A.L. and Adhya, T.K., 2008. Assessment of methane and nitrous oxide flux from mangroves along Eastern coast of India, *Geofluids*, 8(4): 321–332.

Chen, G.C., Chen, B., Yu, D., Tam, N. F. Y., Ye, Y., and Chen, S. 2016. Soil greenhouse gas emissions reduce the contribution of mangrove plants to the atmospheric cooling effect, *Environmental Research Letters*, 11:1-10.

Chen, G.C., Ulumuddin, Y.I., Pramudji, S., Chen, S.Y., Chen, B., Ye, Y., Ou, D.Y., Ma, Z.Y., Huang, H., and Wang, J.K., 2014. Rich soil carbon and nitrogen but low atmospheric greenhouse gas fluxes from North Sulawesi mangrove swamps in Indonesia, *Science of the Total Environment*, 487(1): 91–96.

Chen, G.C., Tam, N.F.Y. and Ye, Y., 2010. Summer fluxes of atmospheric greenhouse gases N_2O, CH_4 and CO_2 from mangrove soil in South China, *Science of the Total Environment*, 408(13): 2761–2767.

Chen, H., Wu, N., Gao, Y., Wang, Y., Luo, P., and Tian, J., 2009. Spatial variations on methane emissions from Zoige alpine wetlands of Southwest China, *Science of the Total Environment*, 407(3): 1097–1104.

Chen, W., Chen, J.M., Price, D.T., and Cihlar, J., 2002. Effects of stand age on net primary productivity of boreal black spruce forests in Ontario, Canada, *Canadian Journal of Forest Research*, 32(5): 833–842.

Cheng, C.H., Hung, C.Y., Chen, C.P., and Pei, C.W., 2013. Biomass carbon accumulation in aging Japanese cedar plantations in Xitou, central Taiwan, *Botanical Studies*, 54(1): 1–9.

Cheng, X., Peng, R., Chen, J., Luo, Y., Zhang, Q., An, S., Chen, J., and Li, B., 2007. CH_4 and N_2O emissions from *Spartina alterniflora* and *Phragmites australis* in experimental mesocosms, *Chemosphere*, 68(3): 420–427.

Chowdhury, T.R. and Dick, R.P., 2013. Ecology of aerobic methanotrophs in controlling methane fluxes from wetlands, *Applied Soil Ecology*, 65: 8–22.

Chuang, P.C., Young, M.B., Dale, A.W., Miller, L.G., Herrera-Silveira, J.A., and Paytan, A., 2016. Methane and sulfate dynamics in sediments from mangrove-dominated tropical coastal lagoons, Yucatan, Mexico, *Biogeosciences*, 13(10): 2981–3001.

Chuang, P.C., Young, M.B., Dale, A.W., Miller, L.G., Herrera-Silveira, J.A., and Paytan, A., 2017. Methane fluxes from tropical coastal lagoons surrounded by mangroves, Yucatán, Mexico, *Journal of Geophysical Research: Biogeosciences*, 122(5): 1156–1174.

Conrad, R., 1999. Contribution of hydrogen to methane production and control of hydrogen concentrations in methanogenic soils and sediments, *FEMS Microbiology Ecology*, 28: 39–58.

Conrad, R., 2007. Microbial ecology of methanogens and methanotrophs, *Advances in Agronomy*, 96(07): 1–63.

Cui, J., Li, C. and Trettin, C., 2005. Analyzing the ecosystem carbon and hydrologic characteristics of forested wetland using a biogeochemical process model, *Global Change Biology*, 11(2): 278–289.

Darrouzet-Nardi, A. and Weintraub, M.N., 2014. Evidence for spatially inaccessible labile N from a comparison of soil core extractions and soil pore water lysimetry, *Soil Biology and Biochemistry*, 73(3): 22–32.

Das, S. and Adhya, T.K., 2012. Dynamics of methanogenesis and methanotrophy in tropical paddy soils as influenced by elevated CO_2 and temperature interaction, *Soil Biology and Biochemistry*, 47: 36–45.

Datta, A., Yeluripati, J.B., Nayak, D.R., Mahata, K.R., Santra, S.C., and Adhya, T.K., 2013. Seasonal variation of methane flux from coastal saline rice field with the application of different organic manures, *Atmospheric Environment*, 66: 114–122.

Day Jr., J.W., Coronado-Molina, C., Vera-Herrera, F.R., Twilley, R.R., Rivera-Monroy, V.H., Alvarez-Guillen, H., Day, R., and Conner, W., 1996. A 7 year record of above-ground net primary production in a southeastern Mexican mangrove forest', *Aquatic Botany*, 55: 39–60.

Dean, J.F., Middelburg, J.J., Röckmann, T., Aerts, R., Blauw, L.G., Egger, M., Jetten, M.S.M., de Jong, A.E.E., Meisel, O.H., Rasigraf, O., Slomp, C.P., in't Zandt, M.H., and Dolman, A.J., 2018. Methane Feedbacks to the Global Climate System in a Warmer World, *Reviews of Geophysics*, 56(1): 207–250.

de Lange, G.J., Cranston, R.E., Hydes, D.H., and Boust, D., 1992. Extraction of pore water from marine sediments: A review of possible artifacts with pertinent examples from the North Atlantic, *Marine Geology*, 109(1–2): 53–76.

DelSontro, T., Beaulieu, J.J., and Downing, J.A., 2018. Greenhouse gas emissions from lakes and impoundments: Upscaling in the face of global change, *Limnology and Oceanography Letters*, 3:64–75.

Ding, W., Cai, Z. and Tsuruta, H., 2004. Methane concentration and emission as affected by methane transport capacity of plants in freshwater marsh, *Water, Air, and Soil Pollution*, 158(1): 99–111.

Donato, D.C., Kauffman, J.B., Murdiyarso, D., Kurnianto, S., Stidham, M., and Kanninen, M., 2011. Mangroves among the most carbon-rich forests in the tropics, *Nature Geoscience*, 4(5): 293–297.

Dorodnikov, M., Knorr, K. H., Kuzyakov, Y., and Wilmking, M., 2011. Plant-mediated CH_4 transport and contribution of photosynthates to methanogenesis at a boreal mire: a ^{14}C pulse-labeling study, *Biogeosciences*, 8(8): 2365–2375.

Downing, A.B., Wallace, G.T. and Yancey, P.H., 2018. Organic osmolytes of amphipods from littoral to hadal zones: increases with depth in trimethylamine N-oxide, scyllo-inositol and other potential pressure counteractants, *Deep-Sea Research Part I: Oceanographic Research Papers*, 138: 1–10.

Dutta, M.K., Bianchi, T.S. and Mukhopadhyay, S.K., 2017. Mangrove methane biogeochemistry in the Indian Sundarbans: a proposed budget, *Frontiers in Marine Science*, 4: 1–15.

Dutta, M.K., Chowdhury, C., Jana, T.K., and Mukhopadhyay, S.K., 2013. Dynamics and exchange fluxes of methane in the estuarine mangrove environment of the Sundarbans, NE coast of India, *Atmospheric Environment*, 77: 631–639.

Dutta, M.K., Mukherjee, R., Jana, T.K., and Mukhopadhyay, S.K., 2015. Biogeochemical dynamics of exogenous methane in an estuary associated to a mangrove biosphere; The Sundarbans, NE coast of India', *Marine Chemistry*, 170: 1–10.

Fechner, E.J. and Hemond, H.F., 1992. Methane transport and oxidation in the unsaturated zone of a Sphagnum peatland, *Global Biogeochemical Cycles*, 6(1): 33–44.

Fernández, A.M., Sánchez-Ledesma, D.M., Tournassat, C., Melón, A., Gaucher, E.C., Astudillo, J., and Vinsot, A., 2014. Applying the squeezing technique to highly consolidated clayrocks for pore water characterisation: Lessons learned from experiments at the Mont Terri Rock Laboratory, *Applied Geochemistry*, 49: 2–21.

Ferry, J.G. eds., 1993. *Methanogenesis: Ecology, Physiology, Biochemistry & Genetics*, Chapman & Hall, New York.

Fisher, M.M. and Reddy, K.R., 2013. Soil pore water sampling methods, in *Methods in Biogeochemistry of Wetlands*, eds R.D. DeLaune, K.R. Reddy, C.J. Richardson; J.P. Megonigal, Soil Science of America, Madison, pp. 55–70.

Forster, P., Ramaswamy, V., Artaxo, P., Berntsen, T., Betts, R., Fahey, D.W., Haywood, J., Lean, J., Lowe, D. C., Myhre, G., Nganga, J., Prinn, R., Raga, G., Schulz, M., and Dorland, R. Van., 2007. Changes in Atmospheric Constituents and in Radiative Forcing, in

Climate Change 2007: The Physical Science Basis. Contribution of Working Group I to the Fourth Assessment Report of the Intergovernmental Panel on Climate Change, eds S. Solomon, D. Qin, M. Manning, Z. Chen, M. Marquis, K.B. Averyt, M.Tignor and H.L. Miller, 30(22): 129–234.

Fritz, C., Pancotto, V.A., Elzenga, J.T.M., Visser, E.J W., Grootjans, A.P., Pol, A., Iturraspe, R., Roelofs, J.G.M., and Smolders, A.J.P., 2011. Zero methane emission bogs: Extreme rhizosphere oxygenation by cushion plants in Patagonia, *New Phytologist*, 190(2): 398–408.

Gamage, D., Thompson, M., Sutherland, M., Hirotsu, N., Makino, A., and Seneweera, S., 2018. New insights into the cellular mechanisms of plant growth at elevated atmospheric carbon dioxide, *Plant, Cell & Environment*, 41: 1233–1246.

Gao, F., Deng, J., Li, Q., Hu, L., Zhu, J., Hang, H., and Hu, W., 2012. A new collector for in situ pore water sampling in wetland sediment, *Environmental Technology*, 33(3): 257–264.

Gao, G.F., Li, P.F., Shen, Z.J., Qin, Y.Y., Zhang, X.M., Ghoto, K., Zhu, X.Y., and Zheng, H.L., 2018. 'Exotic *Spartina alterniflora* invasion increases CH_4 while reduces CO_2 emissions from mangrove wetland soils in southeastern China, *Scientific Reports*, 8(1): 9233-9243.

Garcia, J.L., Patel, B.K. and Ollivier, B., 2000. Taxonomic, phylogenetic, and ecological diversity of methanogenic archaea, *Anaerobe*, 6(4): 205–226.

Gauci, V., Gowing, D.J.G., Hornibrook, E.R.C., Davis, J.M., and Dise, N.B., 2010. Woody stem methane emission in mature wetland alder trees, *Atmospheric Environment*, 44(17): 2157–2160.

Gedney, N., Cox, P.M. and Huntingford, C., 2004. Climate feedback from wetland methane emissions, *Geophysical Research Letters*, 31(20): 1–4.

Geets, J., Borremans, B., Diels, L., Springael, D., Vangronsveld, J., van der Lelie, D., and Vanbroekhoven, K., 2006. DsrB gene-based DGGE for community and diversity surveys of sulfate-reducing bacteria, *Journal of Microbiological Methods*, 66(2): 194–205.

Geselbracht, L.L., Freeman, K., Birch, A.P., Brenner, J., and Gordon, D.R., 2015. Modelled sea level rise impacts on coastal ecosystems at six major estuaries on Florida's gulf coast: Implications for adaptation planning, *PLoS ONE*, 10(7):1-28

Giani, L., Bashan, Y., Holguin, G., and Strangmann, A., 1996. Characteristics and methanogenesis of the Balandra lagoon mangrove soils, Baja California Sur, Mexico', *Geoderma*, 72(1–2): 149–160.

Girkin, N.T., Turner, B.L., Ostle, N., Craigon, J., and Sjögersten, S., 2018. Root exudate analogues accelerate CO_2 and CH_4 production in tropical peat, *Soil Biology and Biochemistry*, 117: 48–55.

Gonsalves, M.J., Fernandes, C.E.G., Fernandes, S.O., Kirchman, D.L., and Bharathi, P.A.L., 2011. Effects of composition of labile organic matter on biogenic production of methane in the coastal sediments of the Arabian Sea, *Environmental Monitoring and Assessment*, 182(1–4): 385–395.

Gontharet, S., Cremiere, A., Blanc-valleron, M., Sebilo, M., Gros, O., Laverman, A.M., and Dessailly, D., 2017. Sediment characteristics and microbial mats in a marine mangrove, Manche-a-eau lagoon (Guadeloupe), *Journal of Soils and Sediments*, 17(1): 1999-2010.

Gosper, C.R., Prober, S.M. and Yates, C.J., 2013. Multi-century changes in vegetation structure and fuel availability in fire-sensitive eucalypt woodlands, *Forest Ecology and Management*, 310: 102–109.

Graedel, T.E. and Keene, W.C., 1996. The budget and cycle of Earth's natural chlorine, *Pure and Apply Chemistry*, 68(9): 1689–1697.

Grenfell, S.E., Callaway, R.M., Grenfell, M.C., Bertelli, C.M., Mendzil, A.F., and Tew, I., 2016. Will a rising sea sink some estuarine wetland ecosystems?, *Science of the Total Environment*, 554–555: 276–292.

Gross, M.F., Hardisky, M.A., Wolf, P.L., and Klemas, V., 1993. Relationships among Typha Biomass, Pore Water Methane, and Reflectance in a Delaware (U.S.A.) Brackish Marsh, *Journal of Coastal Research*, 9(2): 339–355.

Ha, T.H., Marchand, C., Aimé, J., Dang, H.N., Phan, N.H., Nguyen, X.T., and Nguyen, T.K.C., 2018. Belowground carbon sequestration in a mature planted mangrove (Northern Viet Nam), *Forest Ecology and Management*, 407: 191–199.

Hanson, R.S. and Hanson, T.E., 1996. Methanotrophic bacteria, *Microbiology and Molecular Biology Reviews*, 60(2): 439–471.

He, L., Chen, J. M., Pan, Y., Birdsey, R., and Kattge, J., 2012. Relationships between net primary productivity and forest stand age in U.S. forests, *Global Biogeochemical Cycles*, 26(3): 1–19.

He, R., Wooller, M.J., Pohlman, J.W., Quensen, J., Tiedje, J.M., and Leigh, M.B., 2012. Shifts in identity and activity of methanotrophs in Arctic Lake sediments in response to temperature changes, *Applied and Environmental Microbiology*, 78(13): 4715–4723.

Hinrichs, K.U., Hayes, J.M., Sylva, S.P., Brewer, P.G., and DeLong, E.F., 1999. Methane - consuming archaebacteria in marine sediments, *Nature (Letters to nature)*, 398: 802-805.

Holmer, M. and Kristensen, E., 1994. Coexistence of sulfate reduction and methane production in an organic-rich sediment, *Marine Ecology Progress Series*, 107(1–2): 177–184.

Holmes, A.J., Costello, A., Lidstrom, M.E., and Murrell, J.C., 1995. Evidence that particulate methane monooxygenase and ammonia monooxygenase may be evolutionary related, *FEMS Microbiology Letters.*, 132: 203–208.

Howarth, R., Chan, F., Conley, D.J., Garnier, J., Doney, S.C., Marino, R., and Billen, G., 2011. Coupled biogeochemical cycles: Eutrophication and hypoxia in temperate estuaries and coastal marine ecosystems, *Frontiers in Ecology and the Environment*, 9(1): 18–26.

Howarth, R.W. and Giblin, A., 1983. Sulfate reduction in the salt marshes at Sapelo Island, Georgia, *Limnology and Oceanography*, 28(1): 70–82.

Huerta-Diaz, M.A., Rivera-Duarte, I., Sañudo-Wilhelmy, S.A., and Flegal, A.R., 2007. Comparative distributions of size fractionated metals in pore waters sampled by in situ dialysis and whole-core sediment squeezing: Implications for diffusive flux calculations, *Applied Geochemistry*, 22(11): 2509–2525.

Inamori, R., Gui, P., Dass, P., Matsumura, M., Xu, K.Q., Kondo, T., Ebie, Y., and Inamori, Y., 2007. Investigating CH_4 and N_2O emissions from eco-engineering wastewater treatment processes using constructed wetland microcosms, *Process Biochemistry*, 42(3): 363–373.

Inglett, P.W., Reddy, K.R., and Costanje, R., 2004. Anaerobic Soil, in *Encyclopedia of Soils in the Environment,* eds. D. Hillel, J.L. Hatfield, D.S. Powlson, C. Rosenweig, K.M. Scow, M.J. Singer, and D.L. Sparks, , Elsevier Ltd., Oxford UK.

Inubushi, K., Sugii, H., Nishino, S., and Nishino, E., 2001. Effect of Aquatic Weeds on Methane Emission from submerged Paddy Soil, *American Journal of Botany*, 88(6):975-979.

IPCC, 2013. *Climate change 2013: the physical science basis*. T.F. Stocker, D. Qin, G.K. Plattner, M.M.B. Tignor, S.K. Allen, J. Boschung, A. Nauels, Y. Xia, V. Bex, and P.M. Midgley, eds., Cambridge University Press, New York.

Islam, S.F.U., van Groenigen, J.W., Jensen, L.S., Sander, B.O., and de Neergaard, A., 2018. The effective mitigation of greenhouse gas emissions from rice paddies without compromising yield by early-season drainage, *Science of the Total Environment*. 612: 1329–1339.

Jacotot, A., Marchand, C. and Allenbach, M., 2018. Tidal variability of CO_2 and CH_4 emissions from the water column within a Rhizophora mangrove forest (New Caledonia), *Science of the Total Environment*, 631–632: 334–340.

Jardim, W.F. 2014. Medição e interpretação de valores do potencial redox (*Eh*) em matrizes ambientais. *Quim. Nova*, 37(7):1233-1235.

Jayakumar, D.A., Naqvi, S.W.A., Narvekar, P.V., and George, M.D., 2001. Methane in coastal and offshore waters of the Arabian Sea, *Marine Chemistry*, 74(1): 1–13.

Jeffrey, L.C., Reithmaier, G., Sippo, J.Z., Johnston, S.G., Tait, D.R., Maher, D.T., Harada, Y., 2019. Are methane emissions from mangrove stems a cryptic carbon loss pathway? Insights from a catastrophic forest mortality, *New Phytologist*, 1–9.

Jenny, J.P., Normandeau, A., Francus, P., Taranu, Z.E., Gregory-Eaves, I., Lapointe, F., Jautzy, J., Ojala, A.E.K., Dorioz, J.M., Schimmelmann, A., and Zolitschka, B., 2016. Urban point sources of nutrients were the leading cause for the historical spread of hypoxia across European lakes, *Proceedings of the National Academy of Sciences*, 113(45): 12655–12660.

Jing, H., Cheung, S., Zhou, Z., Wu, C., Nagarajan, S., and Liu, H., 2016. Spatial variations of the methanogenic communities in the sediments of tropical mangroves, *PLoS ONE*, 11(9): 1–19.

Joabsson, A., Christensen, T.R. and Wallén, B., 1999. Vascular plant controls on methane emissions from northern peatforming wetlands, *Trends in Ecology and Evolution*, 14(10): 385–388.

Kao-Kniffin, J., Woodcroft, B.J., Carver, S.M., Bockheim, J.G., Handelsman, J., Tyson, G.W., Hinkel, K.M., and Mueller, C.W., 2015. Archaeal and bacterial communities across a chronosequence of drained lake basins in arctic Alaska, *Scientific Reports*, 5: 1–13.

Kao-Kniffin, J. and Zhu, B., 2013. A microbial link between elevated CO_2 and methane emissions that is plant species-specific, *Microbial Ecology*, 66(3): 621–629.

Kauffman, J. and Donato, D., 2012. *Protocols for the measurement, monitoring and reporting of structure, biomass and carbon stocks in mangrove forests*, *Working Paper 86*, CIFOR, Bogor. Indonesia.

Keys, M., Tilstone, G., Findlay, H.S., Widdicombe, C.E., and Lawson, T., 2018. Effects of elevated CO_2 on phytoplankton community biomass, species composition and photosynthesis during an experimentally induced autumn bloom in the western English Channel, *Biogeosciences*, 15(10): 3203–3222.

Kiene, R.P., Oremland, R.S., Catena, A., Miller, L.G., and Capone, D.G., 1986. Metabolism of Reduced Methylated Sulfur Compounds in Anaerobic Sediments and by a Pure Culture of an Estuarine Methanogen, *Applied and Environmental Microbiology*, 52(5): 1037–1045.

King, G.M., 1990. Effects of added manganic and ferric oxides on sulfate reduction and sulfide oxidation in intertidal sediments, *FEMS Microbiology Letters*, 73(2): 131–138.

King, G.M., Klug, M.J. and Lovley, D.R., 1983. Metabolism of acetate, methanol, and methylated amines in intertidal sediments of Lowes Cove, Maine, *Applied and Environmental Microbiology*, 45(6): 1848–1853.

King, J.Y., Reeburgh, W.S., Thieler, K.K., Kling, G.W., Loya, W.M., Johnson, L.C., and Nadelhoffer, K.J., 2002. Pulse-labelling studies of carbon cycling in Arctic tundra ecosystems: The contribution of photosynthates to methane emission, *Global Biogeochemical Cycles*, 16(4): 48-1–48-8.

Kirschke, S., Bousquet, P., Ciais, P., Saunois, M., Canadell, J.G., Dlugokencky, E.J., Bergamaschi, P., Bergmann, D., Blake, D.R., Bruhwiler, L., Cameron-Smith, P., Castaldi, S., Chevallier, F., Feng, L., Fraser, A., Heimann, M., Hodson, E. L., Houweling, S., Josse, B., Fraser, P.J., Krummel, P.B., Lamarque, J.F., Langenfelds, R.L., Le Quéré, C., Naik, V., O'doherty, S., Palmer, P. I., Pison, I., Plummer, D., Poulter, B., Prinn, R. G., Rigby, M., Ringeval, B., Santini, M., Schmidt, M., Shindell, D.T., Simpson, I.J., Spahni, R., Steele, L. P., Strode, S.A., Sudo, K., Szopa, S., Van Der Werf, G.R., Voulgarakis, A., Van Weele, M., Weiss, R.F., Williams, J.E., and Zeng, G., 2013. Three decades of global methane sources and sinks, *Nature Geoscience*, 6(10): 813–823.

Koebsch, F., Glatzel, S. and Jurasinski, G., 2013. Vegetation controls methane emissions in a coastal brackish fen, *Wetlands Ecology and Management*, 21(5): 323–337.

Kolb, S., Carbrera, A., Kammann, C., Kämpfer, P., Conrad, R., and Jäckel, U., 2005. Quantitative impact of CO_2 enriched atmosphere on abundances of methanotrophic bacteria in a meadow soil, *Biology and Fertility of Soils*, 41(5): 337–342.

Konnerup, D., Betancourt-Portela, J.M., Villamil, C., and Parra, J.P., 2014. Nitrous oxide and methane emissions from the restored mangrove ecosystem of the Ciénaga Grande de Santa Marta, Colombia, *Estuarine, Coastal and Shelf Science*, 140: 43–51.

Kreuzwieser, J., Buchholz, J. and Rennenberg, H., 2003. Emissions of methane and nitrous oxide by Australian mangrove ecosystem, *Plant Biology*, 5: 9.

Krithika, K., Purvaja, R. and Ramesh, R., 2008. Fluxes of methane and nitrous oxide from an Indian mangrove, *Current Science*, 94(2): 218–224.

Krupadam, R.J., Ahuja, R., Wate, S.R., and Anjaneyulu, Y., 2007. Forest bound estuaries are higher methane emitters than paddy fields: A case of Godavari estuary, East Coast of India, *Atmospheric Environment*, 41(23): 4819–4827.

Kuzyakov, Y., 2010. Priming effects: interactions between living and dead organic matter, *Soil Biology and Biochemistry*, 42(9): 1363–1371.

Lahijani, M.J.A., Kafi, M., Nezami, A., Nabati, J., Mehrjerdi, M.Z., Shahkoomahally, S., and Erwin, J., 2018. Variations in assimilation rate, photoassimilate translocation, and cellular fine structure of potato cultivars (*Solanum tuberosum* L.) exposed to elevated CO_2, *Plant Physiology and Biochemistry*, 130: 303–313.

Lallier-Vergès, E., Marchand, C., Disnar, J.R., and Lottier, N., 2008. Origin and diagenesis of lignin and carbohydrates in mangrove sediments of Guadeloupe (French West Indies): Evidence for a two-step evolution of organic deposits, *Chemical Geology*, 255(3–4): 388–398.

Lashof, D. and Ahuja, D., 1990. Relative contributions of greenhouse gas emissions to global warming, *Nature*, 344: 529–531.

Le Mer, J. and Roger, P., 2001. Production, oxidation, emission and consumption of methane by soils: a review, *European Journal of Soil Biology*, 37(1): 25–50.

Lee, R.Y., Porubsky, W.P., Feller, I.C., McKee, K.L., and Joye, S.B., 2008. Porewater biogeochemistry and soil metabolism in dwarf red mangrove habitats (Twin Cays, Belize), *Biogeochemistry*, 87(2): 181–198.

Lekphet, S., Nitisoravut, S. and Adsavakulchai, S., 2005. Estimating methane emissions from mangrove area in Ranong Province, Thailand, *Songklanakarin Journal of Science and Technology*, 27(1): 153–163.

Lewis, R.R., 2005. Ecological engineering for successful management and restoration of mangrove forests, *Ecological Engineering*, 24(4): 403–418.

Lewis, R.R. and Brown, B., 2014. Ecological Mangrove Rehabilitation: A Field Manual for Practitioners. Version 3. Mangrove Action Project Indonesia, Blue Forests, Canadian International Development Agency, and OXFAM.

Lin, Y., Liu, D., Ding, W., Kang, H., Freeman, C., Yuan, J., and Xiang, J., 2015. Substrate sources regulate spatial variation of metabolically active methanogens from two contrasting freshwater wetlands, *Applied Microbiology and Biotechnology*, 99(24): 10779–10791.

Linto, N., Barnes, J., Ramachandran, R., Divia, J., Ramachandran, P., and Upstill-Goddard, R.C., 2014. Carbon Dioxide and Methane Emissions from Mangrove-Associated Waters of the Andaman Islands, Bay of Bengal, *Estuaries and Coasts*, 37(2): 381–398.

Liu, D., Tago, K., Hayatsu, M., Tokida, T., Sakai, H., Nakamura, H., Usui, Y., Hasegawa, T., and Asakawa, S., 2016. Effect of Elevated CO_2 Concentration, Elevated Temperature and No Nitrogen Fertilization on Methanogenic Archaeal and Methane-Oxidizing Bacterial Community Structures in Paddy Soil, *Microbes and environments*, 31(3): 349–356.

Liu, G., Lu, C., Zhao, H., Liu, J., Liu, Z., He, Z., Bai, M., Wu, X., and Xu, Z., 2018. Design Improvement and Sea Test about In Situ Pore Water Sampler System for Deep-Sea Sediments, *Advances in Geosciences*, 08(01): 141–151.

Liu, X. and Xiong, Y., 2017. Relative contributions of leaf litter and fine roots to soil organic matter accumulation in mangrove forests, *Plant Soil*, 421: 493–503.

Liu, Y., Liu, X., Cheng, K., Li, L., Zhang, X., Zheng, J., Zheng, J., and Pan, G., 2016. Responses of methanogenic and methanotrophic communities to elevated atmospheric CO_2 and temperature in a paddy field, *Frontiers in Microbiology*, 7: 1–14.

Liu, Y. and Whitman, W.B., 2008. Metabolic, phylogenetic, and ecological diversity of the methanogenic archaea, *Annals of the New York Academy of Sciences*, 1125: 171–189.

Lofton, D.D., Whalen, S.C. and Hershey, A.E., 2014. Effect of temperature on methane dynamics and evaluation of methane oxidation kinetics in shallow Arctic Alaskan lakes, *Hydrobiologia*, 721(1): 209–222.

Lohbeck, M., Poorter, L., Paz, H., Pla, L., van Breugel, M., Martínez-Ramos, M., and Bongers, F., 2012. Functional diversity changes during tropical forest succession, *Perspectives in Plant Ecology, Evolution and Systematics*, 14(2): 89–96.

Lopes, I. and Ribeiro, R., 2005. Optimization of a pressurization methodology for extracting pore-water, *Chemosphere*, 61(10): 1505–1511.

Lovelock, C.E., Atwood, T., Baldock, J., Duarte, C.M., Hickey, S., Lavery, P.S., Masque, P., Macreadie, P.I., Ricart, A.M., Serrano, O., and Steven, A., 2017. Assessing the risk of carbon dioxide emissions from blue carbon ecosystems, *Frontiers in Ecology and the Environment*, 15(5):257–265.

Lu, C.Y., Wong, Y.S., Tam, N.F.Y., Ye, Y., and Lin, P., 1999. Methane flux and production from sediments of a mangrove wetland on Hainan Island, China, *Mangroves and Salt Marshes*, 3(1): 41–49.

Lu, X., Zhou, Y., Zhuang, Q., Prigent, C., Liu, Y., and Teuling, A., 2018. Increasing Methane Emissions From Natural Land Ecosystems due to Sea-Level Rise, *Journal of Geophysical Research: Biogeosciences*, 123(5): 1756–1768

Lu, Y., Wassmann, R., Neue, H.U., Huang, C., and Bueno, C.S., 2000. Methanogenic responses to exogenous substrates in anaerobic rice soils, *Soil Biology and Biochemistry*, 32(11–12): 1683–1690.

Lugo, A.E. and Snedaker, S.C., 1974. The ecology of mangroves, *Annual Review of Ecology and Systematics*, 5(1): 39–64.

Luton, P.E., Wayne, J.M., Sharp, R.J., and Riley, P.W., 2002. The mcrA gene as an alternative to 16S rRNA in the phylogenetic analysis of methanogen populations in landfill, *Microbiology*, 148(11): 3521–3530.

Lyimo, T.J. and Mushi, D., 2005. Sulfide Concentration and Redox Potential Patterns in Mangrove Forests of Dar es Salaam: Effects on Avicennia Marina and Rhizophora Mucronata Seedling Establishment, *Western Indian Ocean Journal of Marine Science,* 4(2): 163-173.

Lyimo, T.J., Pol, A., Op Den Camp, H.J.M., Harhangi, H.R., and Vogels, G.D., 2000. *Methanosarcina semesiae* sp. nov., a dimethylsulfide-utilizing methanogen from mangrove sediment, *International Journal of Systematic and Evolutionary Microbiology*, 50(1): 171–178.

Lyimo, T.J., Pol, A., and Op den Camp, H.J.M., 2002. Sulfate Reduction and Methanogenesis in Sediments of Mtoni Mangrove Forest, *Ambio*, 31(7): 614–616.

Lyimo, T.J., Pol, A., Harhangi, H.R., Jetten, M.S.M., and Op den Camp, H.J.M., 2009. Anaerobic oxidation of dimethylsulfide and methanethiol in mangrove sediments is dominated by sulfate-reducing bacteria, *FEMS Microbiology Ecology*, 70(3): 483–492.

Lyimo, T.J., Pol, A., Jetten, M.S.M., and Op den Camp, H.J.M., 2009. Diversity of methanogenic archaea in a mangrove sediment and isolation of a new Methanococcoides strain, *FEMS Microbiology Letters*, 291(2): 247–253.

Machado, W., Santelli, R.E., Carvalho, M.F., Molisani, M.M., Barreto, R.C., and Lacerda, L.D., 2008. Relation of Reactive Sulfides with Organic Carbon, Iron, and Manganese in Anaerobic Mangrove Sediments: Implications for Sediment Suitability to Trap Trace Metals, *Journal of Coastal Research*, 4: 25–32.

Magen, C., Lapham, L.L., Pohlman, J.W., Marshall, K., Bosman, S., Casso, M., and Chanton, J.P., 2014. A simple headspace equilibration method for measuring dissolved methane, *Limnology and Oceanography: Methods*, 12: 637–650.

Maier, M., Machacova, K., Lang, F., Svobodova, K., and Urban, O., 2018. Combining soil and tree-stem flux measurements and soil gas profiles to understand CH_4 pathways in *Fagus sylvatica* forests, *Journal of Plant Nutrition and Soil Science*, 181(1): 31–35.

Malik, A., Mertz, O. and Fensholt, R., 2017. Mangrove forest decline: consequences for livelihoods and environment in South Sulawesi, *Regional Environmental Change*, 17(1): 157–169.

Maltby, J., Steinle, L., Löscher, C.R., Bange, H.W., Fischer, M.A., Schmidt, M., and Treude, T., 2018. Microbial methanogenesis in the sulfate-reducing zone of sediments in the Eckernförde Bay, SW Baltic Sea, *Biogeosciences*, 15(1): 137–157.

Man, K.W., Zheng, J., Leung, A.P.K., Lam, P.K.S., Lam, M.H.W., and Yen, Y.F., 2004. Distribution and behavior of trace metals in the sediment and porewater of a tropical coastal wetland, *Science of the Total Environment*, 327(1–3): 295–314.

Marchand, C., 2017. Soil carbon stocks and burial rates along a mangrove forest chronosequence (French Guiana), *Forest Ecology and Management*, 384: 92–99.

Marchand, C., Lallier-Vergès, E., Disnar, J.R., and Kéravis, D., 2008. Organic carbon sources and transformations in mangrove sediments: A Rock-Eval pyrolysis approach, *Organic Geochemistry*, 39(4): 408–421.

Marinho, C., Campos, E., Guimarães, J., and Esteves, F., 2012. Effect of sediment composition on methane concentration and production in the transition zone of a mangrove (Sepetiba Bay, Rio de Janeiro, Brazil), *Brazilian Journal of Biology*, 72(3): 429–436.

Marín-Muñiz, J.L., Hernández, M.E. and Moreno-Casasola, P., 2015. Greenhouse gas emissions from coastal freshwater wetlands in Veracruz Mexico: effect of plant community and seasonal dynamics, *Atmospheric Environment*, 107(26): 107–117.

Martens, C.S. and Berner, R.A., 1974. Methane Production in the Interstitial Waters of Sulfate-Depleted Marine Sediments, *Science*, 185(4157): 1167-1169.

Martin, J.B., Hartl, K.M., Corbett, D.R., Swarzenski, P.W., and Cable, J.E., 2003. A multilevel pore-water sampler for permeable sediments, *Journal of Sedimentary Research*, 73(1): 128–132.

Martins, C.S.C., Macdonald, C.A., Anderson, I.C., and Singh, B.K., 2016. Feedback responses of soil greenhouse gas emissions to climate change are modulated by soil characteristics in dryland ecosystems, *Soil Biology and Biochemistry*. 100: 21–32.

Masch, F.D. and Denny, K.J., 1966. Grain size distribution and its effect on the permeability of unconsolidated sands, *Water Resources Research*, 2(4): 665–677.

Mason-Jones, K. and Kuzyakov, Y., 2017. 'Non-metabolizable' glucose analogue shines new light on priming mechanisms: triggering of microbial metabolism, *Soil Biology and Biochemistry*, 107: 68–76.

Mazurek, M., Oyama, T., Wersin, P., and Alt-Epping, P., 2015. Pore-water squeezing from indurated shales, *Chemical Geology*, 400: 106–121.

McDougall, E.I., 1947. Studies on ruminant saliva. I. The composition and output of sheep's saliva, *Biochemical Journal*, 43(1):99-109.

McLeod, E., Chmura, G.L., Bouillon, S., Salm, R., Björk, M., Duarte, C.M., Lovelock, C.E., Schlesinger, W.H., and Silliman, B.R., 2011. A blueprint for blue carbon: Toward an improved understanding of the role of vegetated coastal habitats in sequestering CO_2, *Frontiers in Ecology and the Environment*, 9(10): 552–560.

Megonigal, J.P., 2002. Methane-limited methanotrophy in tidal freshwater swamps, *Global Biogeochemical Cycles*, 16(4): 1–10.

Megonigal, J.P. and Schlesinger, W.H., 1997. Enhanced CH_4 emissions from a wetland soil exposed to elevated CO_2, *North*, 37(1): 77–88.

Megonigal, J.P., Hines, M.E. and Visscher, P.T., 2013. *Anaerobic Metabolism: Linkages to Trace Gases and Aerobic Processes*, 10th edn, Elsevier Ltd.

Milich, L., 1999. The role of methane in global warming: where might mitigation strategies be focused? *Global Environmental Change*, 9(3): 179–201.

Miller, J.F., Shah, N.N., Nelson, C.M., Ludlow, J.M., and Clark, D.S., 1988. Pressure and Temperature Effects on Growth and Methane Production of the Extreme Thermophile *Methanococcus jannaschii*, *Applied and Environmental Microbiology*, 54(12): 3039-3042.

Mitterer, R.M., 2010. Methanogenesis and sulfate reduction in marine sediments: a new model, *Earth and Planetary Science Letters*, 295(3–4): 358–366.

Mohanraju, R., Rajagopal, B.S., Daniels, L., and Natarajan, R., 1997. Isolation and characterization of a methanogenic bacterium from mangrove sediments, *Journal of Marine Biotechnology*, 5: 147–152.

Mohanraju, R. and Natarajan, R., 1992. Methanogenic bacteria in mangrove sediments, *Hydrobiologia*, 247(1–3): 187–193.

Moran, J.J., Beal, E.J., Vrentas, J.M., Orphan, V.J., Freeman, K.H., and House, C.H., 2008. Methyl sulfides as intermediates in the anaerobic oxidation of methane, *Environmental Microbiology,* 10(1): 162–173.

Murdiyarso, D., Purbopuspito, J., Kauffman, J.B., Warren, M.W., Sasmito, S.D., Donato, D.C., Manuri, S., Krisnawati, H., Taberima, S., and Kurnianto, S., 2015. The potential of Indonesian mangrove forests for global climate change mitigation, *Nature Climate Change*, 5(12): 1089–1092.

Nayar, S., Miller, D., Bryars, S., and Cheshire, A.C., 2006. A simple, inexpensive and large volume pore water sampler for sandy and muddy substrates, *Estuarine, Coastal and Shelf Science*, 66(1–2): 298–302.

Nellemann, C., Corcoran, E., Duarte, C.M., Valdes, L., De Young, C., Fonseca, L., Grimsditch, G. eds. 2009. *Blue Carbon: The Role of Healthy Oceans in Binding Carbon*, United Nations Environment Programme, GRID-Arendal, Norway.

Ni, X. and Groffman, P.M., 2018. Declines in methane uptake in forest soils, *Proceedings of the National Academy of Sciences*, 115(34): 201807377.

Nickerson, N.H. and Thibodeau, F.R., 1985. Association between pore water sulphide concentrations and the distribution of mangroves, *Biogeochemistry,* 1(2): 183-192.

Nóbrega, G.N., Ferreira, T.O., Romero, R.E., Marques, A.G.B., and Otero, X.L., 2013. Iron and sulfur geochemistry in semi-arid mangrove soils (Ceará, Brazil) in relation to seasonal changes and shrimp farming effluents, *Environmental Monitoring and Assessment*, 185(9): 7393–7407.

Noronha-D'Mello, C.A. and Nayak, G.N., 2015. Geochemical characterization of mangrove sediments of the Zuari estuarine system, West coast of India, *Estuarine, coastal and shelf science*, 167: 313-325

Obermeier, W.A., Lehnert, L.W., Ivanov, M.A., Luterbacher, J., and Bendix, J., 2018. Reduced Summer Aboveground Productivity in Temperate C3 Grasslands Under Future Climate Regimes, *Earth's Future*, 6(5): 716–729.

Odum, E.P., 1969. The strategy of ecosystem development, *Science*, 164(3877): 262–270.

Okimoto, Y., Nose, A., Ikeda, K., Agarie, S., Oshima, K., Tateda, Y., Ishii, T., and Nhan, D.D., 2008. An estimation of CO_2 fixation capacity in mangrove forest using two methods of CO_2 gas exchange and growth curve analysis, *Wetlands Ecology and Management,* 16(2): 155–171.

Olafsson, E., 1995. Meiobenthos in mangrove areas in eastern Africa with emphasis on assemblage structure of free-living marine nematodes, *Hydrobiologia*, 312:47-57.

Oliver, D.M., Bird, C., Burd, E., and Wyman, M., 2016. Quantitative PCR profiling of *Escherichia coli* in livestock feces reveals increased population resilience relative to culturable counts under temperature extremes, *Environmental Science and Technology*, 50(17): 9497–9505.

Ong, J.E., Gong, W.K. and Wong, C.H., 1985. Seven years of productivity studies in a Malaysian managed mangrove forest then what?, in *Coasts and Tidal Wetlands of the Australian Monsoon Region—NARU Mangrove Monographs* 1, eds K.N. Beardsley, J.D.S. Davie and C.D. Woodroffe, Australian National University Press, Canberra, pp. 213–223.

Oremland, R.S., Marsh, L.M. and Polcin, S., 1982. Methane production and simultaneous sulphate reduction in anoxic, salt marsh sediments, *Nature*, 296(5853): 143–145.

Oremland, R.S. and Polcin, S., 1982. Methanogenesis and sulfate reduction: competitive and noncompetitive substrates in estuarine sediments, *Applied and Environmental Microbiology*, 44(6): 1270–1276.

Orphan, V.J., Hinrichs, K., Iii, W.U., Paull, C.K., Taylor, L.T., Sylva, S.P., Hayes, J.M., and Delong, E.F., 2001. Comparative Analysis of Methane-Oxidizing Archaea and Sulfate-Reducing Bacteria in Anoxic Marine Sediments, *Applied and Environmental Microbiology*, 67(4): 1922–1934.

Pacheco, F.S., Roland, F. and Downing, J.A., 2014. Eutrophication reverses whole-lake carbon budgets, *Inland Waters*, 4(1): 41–48.

Pangala, S.R., Moore, S., Hornibrook, E.R.C., and Gauci, V., 2013. Trees are major conduits for methane egress from tropical forested wetlands, *New Phytologist*, 197(2): 524–531.

Pangala, S.R., Hornibrook, E.R.C., Gowing, D.J., and Gauci, V., 2015. The contribution of trees to ecosystem methane emissions in a temperate forested wetland, *Global Change Biology*, 21(7): 2642–2654.

Pangala, S.R., Enrich-Prast, A., Basso, L.S., Peixoto, R.B., Bastviken, D., Hornibrook, E.R.C., Gatti, L.V., Marotta, H., Calazans, L.S.B., Sakuragui, C.M., Bastos, W.R., Malm, O., Gloor, E., Miller, J.B., and Gauci, V., 2017. Large emissions from floodplain trees close the Amazon methane budget, *Nature*, 552(7684): 230–234.

Patterson, J.A. and Hespell, R.B., 1979. Trimethylamine and methylamine as growth substrates for rumen bacteria and *Methanosarcina barkeri*, *Current Microbiology*, 3(2): 79–83.

Peters, V. and Conrad, R., 1995. Methanogenic and Other Strictly Anaerobic Bacteria in Desert Soil and Other Oxic Soils, *Applied and Environmental Microbiology*, 61(4): 1673-1676.

Pitz, S.L., Megonigal, J.P., Chang, C.H., and Szlavecz, K., 2018. Methane fluxes from tree stems and soils along a habitat gradient, *Biogeochemistry*, 137(3): 307–320.

Poffenbarger, H.J., Needelman, B.A. and Megonigal, J.P., 2011. Salinity influence on methane emissions from tidal marshes, *Wetlands*, 31: 831–842.

Poungparn, S., Charoenphonphakdi, T., Sangtiean, T., and Patanaponpaiboon, P., 2016. Fine root production in three zones of secondary mangrove forest in eastern Thailand, *Trees - Structure and Function*, 30(2): 467–474.

Prayitno, H.B., 2016. *Suction Multi-Level Pore Water Sampler: Optimising Its Use for Methane Dynamic Studies in Mangrove Ecosystems*, The Australian National University, Canberra, Australia.

Primavera, J.H. and Esteban, J.M.A., 2008. A review of mangrove rehabilitation in the Philippines: successes, failures and future prospects. *Wetland Ecology Management*, 16: 345–358.

Pszwaro, J.L., D'Amato, A.W., Burk, T.E., Russell, M.B., Palik, B.J., and Strong, T.F., 2016. Analysis of stand basal area development of thinned and unthinned *Acer rubrum* forests in the upper Great Lakes region, USA, *Canadian Journal of Forest Research*, 46(5): 645–655.

Pulliam, W.M., 1992. Methane emissions from cypress knees in a southeastern floodplain swamp, *Oecologia*, 91(1): 126–128.

Purvaja, R. and Ramesh, R., 2000. Human impacts on methane emission from mangrove ecosystems in India, *Regional Environmental Change*, 1(2): 86–97.

Purvaja, R. and Ramesh, R., 2001. Natural and anthropogenic methane emission from coastal wetlands of South India, *Environmental Management*, 27(4): 547–557.

Purvaja, R., Ramesh, R. and Frenzel, P., 2004. Plant-mediated methane emission from an Indian mangrove, *Global Change Biology*, 10(11): 1825–1834.

Rajkumar, A.N., Barnes, J., Ramesh, R., Purvaja, R., and Upstill-Goddard, R.C., 2008. Methane and nitrous oxide fluxes in the polluted Adyar River and estuary, SE India, *Marine Pollution Bulletin*, 56(12): 2043–2051.

Ramamurthy, T., Raju, R.M. and Natarajan, R., 1990. Distribution and ecology of methanogenic bacteria in mangrove sediments of Pitchavaram, east coast of India, *Indian Journal of Marine Sciences*, 19: 269–273.

Ramesh, R., Purvaja, G.R., Parashar, D.C., Gupta, P.K., and Mitra, A.P., 1997. Anthropogenic forcing on methane flux from polluted wetlands (Adyar River) of Madras City, India, *Ambio*, 26(6): 369–376.

Ramírez-Pérez, A.M., de Blas, E. and García-Gil, S., 2015. Redox processes in pore water of anoxic sediments with shallow gas, *Science of the Total Environment*, 538: 317–326.

Reay, D.S., Smith, P., Christensen, T.R., James, R.H., and Clark, H., 2018. *Methane and Global Environmental Change, Annual Review of Environment and Resources*, 43:165-192.

Reeburgh, W.S., 2003. Global methane biogeochemistry, in *The Atmosphere*, eds R. F. Keeling, vol.4: *Treatise on Geochemistry*, eds H. D. Holland and K. K. Turekian, Elsivier-Pergamon, Oxford, pp. 65-89.

Reeburgh, W.S., 2007. Oceanic methane biogeochemistry, *Chemical Reviews*, 107(2): 486–513.

Reeburgh, W.S., 2013. Global methane biogeochemistry, in *Treatise on Geochemistry: Second Edition*, eds H. D. Holland and K. K. Turekian, Elsevier, Oxford, pp 71–94.

Reshmi, R.R., Deepa Nair, K., Zachariah, E.J., and Vincent, S.G.T., 2015. Methanogenesis: Seasonal changes in human impacted regions of Ashtamudi estuary (Kerala, South India), *Estuarine, Coastal and Shelf Science*, 156(1): 144–154.

Robbins, J.A. and Gustinis, J., 1976. A squeezer for efficient extraction of pore water from small volumes of anoxic sediment, *Limnology and Oceanography*, 21(6): 905–909.

Robertson, A.I. and Alongi, D.M., 2016. Massive turnover rates of fine root detrital carbon in tropical Australian mangroves, *Oecologia*, 180(3): 841–851.

Rocha, A.C.S., Almeida, C.M.R., Basto, M.C.P., and Vasconcelos, M.T.S.D., 2015. Influence of season and salinity on the exudation of aliphatic low molecular weight organic acids (ALMWOAs) by *Phragmites australis* and *Halimione portulacoides* roots, *Journal of Sea Research*, 95: 180–187.

Ronday, R., 1997. Centrifugation method for soil pore water assessment of the bioavailability of organic chemicals in soil, *Communications in Soil Science and Plant Analysis*, 28(9–10): 777–785.

Rosentreter, J.A., Maher, D.T., Ho, D.T., Call, M., Barr, J.G., and Eyre, B.D., 2017. Spatial and temporal variability of CO_2 and CH_4 gas transfer velocities and quantification of the CH_4 microbubble flux in mangrove dominated estuaries, *Limnology and Oceanography*, 62(2): 561–578.

Rosentreter, J.A., Maher, D.T., Erler, D.V, Murray, R.H., and Eyre, B.D., 2018. Methane emissions partially offset ‘blue carbon’ burial in mangroves, *Science Advances*, 4: 1–11.

Roslev, P. and King, G.M., 1996. Regulation of methane oxidation in a freshwater wetland by water table changes and anoxia, *FEMS Microbiology Ecology*, 19(2): 105–115.

Ross, M.S., Ruiz, P.L., Telesnicki, G.J., and Meeder, J.F., 2001. Estimating above-ground biomass and production in mangrove communities of Biscayne National Park, Florida (USA), *Wetlands Ecology and Management*, 9(1): 27–37.

Roy, M., McManus, J., Goñi, M.A., Chase, Z., Borgeld, J.C., Wheatcroft, R.A., Muratli, J.M., Megowan, M.R., and Mix, A., 2013. Reactive iron and manganese distributions in seabed sediments near small mountainous rivers off Oregon and California (USA), *Continental Shelf Research*, 54: 67–79.

Rusch, H. and Rennenberg, H., 1998. Black alder (*Alnus glutinosa* (L.) Gaertn.) trees mediate methane and nitrous oxide emission from the soil to the atmosphere, *Plant and Soil*, 201(1): 1–7.

Saarnio, S., Winiwarter, W. and Leitão, J., 2009. Methane release from wetlands and watercourses in Europe, *Atmospheric Environment*, 43(7): 1421–1429.

Sarmiento, J.L. and Gruber, N., 2006. *Ocean Biogeochemical Dynamics*, Princeton University Press, Princeton, Woodstock.

Sasseville, D.R., Takacs, A.P., Norton, S.A., and Davis, R.B., 1974. A large-volume interstitial water sediment squeezer for lake sediments, *Limnology and Oceanography*, 19(6): 1001–1004.

Saunois, M., Bousquet, P., Poulter, B., Peregon, A., Ciais, P., Canadell, J.G., Dlugokencky, E.J., Etiope, G., Bastviken, D., Houweling, S., Janssens-Maenhout, G., Tubiello, F.N., Castaldi, S., Jackson, R.B., Alexe, M., Arora, V.K., Beerling, D.J., Bergamaschi, P., Blake, D.R., Brailsford, G., Brovkin, V., Bruhwiler, L., Crevoisier, C., Crill, P., Covey, K., Curry, C., Frankenberg, C., Gedney, N., Höglund-Isaksson, L., Ishizawa, M., Ito, A., Joos, F., Kim, H.S., Kleinen, T., Krummel, P., Lamarque, J.F., Langenfelds, R., Locatelli, R., Machida, T., Maksyutov, S., McDonald, K.C., Marshall, J., Melton, J.R., Morino, I., Naik, V., O'Doherty, S., Parmentier, F.J.W., Patra, P.K., Peng, C., Peng, S., Peters, G.P., Pison, I., Prigent, C., Prinn, R., Ramonet, M., Riley, W.J., Saito, M., Santini, M., Schroeder, R., Simpson, I.J., Spahni, R., Steele, P., Takizawa, A., Thornton, B.F., Tian, H., Tohjima, Y., Viovy, N., Voulgarakis, A., Van Weele, M., Van Der Werf, G.R., Weiss, R., Wiedinmyer, C., Wilton, D.J., Wiltshire, A., Worthy, D., Wunch, D., Xu, X., Yoshida, Y., Zhang, B., Zhang, Z., and Zhu, Q., 2016. The global methane budget 2000-2012, *Earth System Science Data*, 8(2): 697–751.

Schaefer, H., Fletcher, S.E.M., Veidt, C., Lassey, K.R., Brailsford, G.W., Bromley, T.M., Dlugokencky, E.J., Michel, S.E., Miller, J.B., Levin, I., Lowe, D.C., Martin, R.J., Vaughn, B.H., and White, J.W.C., 2016. A 21st-century shift from fossil-fuel to biogenic methane emissions indicated by $^{13}CH_4$, *Science*, 352(6281): 80–84.

Schile, L.M., Kauffman, J.B., Crooks, S., Fourqurean, J.W., Glavan, J., and Megonigal, J.P., 2017. Limits on carbon sequestration in arid blue carbon ecosystems, *Ecological Applications*, 27(3): 859–874.

Schippers, A. and Jorgensen, B.B., 2002. Biogeochemistry of pyrite and iron sulfide oxidation in marine sediments, *Geochimica et Cosmochimica Acta*, 66(1): 85–92.

Schulze, E.D., Wirth, C., Mollicone, D., and Ziegler, W., 2005. Succession after stand replacing disturbances by fire, wind throw, and insects in the dark Taiga of Central Siberia, *Oecologia*, 146(1): 77–88.

Scranton, M. and McShane, K., 1991. Methane fluxes in the southern North Sea: the role of European rivers, *Continental Shelf Research*, 11(1): 37–52.

Sela-Adler, M., Ronen, Z., Herut, B., Antler, G., Vigderovich, H., Eckert, W., and Sivan, O., 2017. Co-existence of Methanogenesis and Sulfate Reduction with Common Substrates in Sulfate-Rich Estuarine Sediments, *Frontiers in Energy*, 8: 1–11.

Setiawan, H. and Mursidin, 2018. Ecological Characteristic and Health of Mangrove Forest at Tanakeke Island, South Sulawesi, *Jurnal Penelitian Kehutanan Wallacea*, 7(1): 47–58.

Shalini, A., Ramesh, R., Purvaja, R., and Barnes, J., 2006. Spatial and temporal distribution of methaen in an extensive shallow estuary, south India, *Journal of Earth System Science*, 115(4): 451–460.

Shannon, R.D. and White, J.R., 1994. A three-year study of controls on methane emissions from two Michigan peatlands, *Biogeochemistry*, 27(1): 35-60

Shotbolt, L., 2010. Pore water sampling from lake and estuary sediments using Rhizon samplers, *Journal of Paleolimnology*, 44(2): 695–700.

Sasmito, S.D., Taillardat, P., Clendenning, J.N., Cameron, C., Friess, D.A., Murdiyarso, D., and Hutley, L.B., 2019. Effect of land- use and land- cover change on mangrove blue carbon: A systematic review, *Global Change Biology*, 00:1–12.

Siljanen, H.M.P., Saari, A., Krause, S., Lensu, A., Abell, G.C.J., Bodrossy, L., Bodelier, P.L.E., and Martikainen, P.J., 2011. Hydrology is reflected in the functioning and community composition of methanotrophs in the littoral wetland of a boreal lake, *FEMS Microbiology Ecology*, 75(3): 430–445.

Slama, I., Abdelly, C., Bouchereau, A., Flowers, T., and Savouré, A., 2015. Diversity, distribution and roles of osmoprotective compounds accumulated in halophytes under abiotic stress, *Annals of Botany*, 115(3): 433–447.

Smith, L.K., Lewis, W.M., Chanton, J.P., Cronin, G., and Hamilton, S.K., 2000. Methane emissions from the Orinoco River floodplain, Venezuela, *Biogeochemistry*, 51(2): 113–140.

Song, H. and Liu, X., 2016. Anthropogenic Effects on Fluxes of Ecosystem Respiration and Methane in the Yellow River Estuary, China, *Wetlands*, 36: 113–123.

Sotomayor, D., Corredor, J.E. and Morell, J.M., 1994. Methane flux from mangrove sediments along the southwestern coast of Puerto Rico, *Estuaries*, 17(1): 140.

Steinmann, P. and Shotyk, W., 1996. Sampling anoxic pore waters in peatlands using ‘peepers’ for in situ-filtration, *Analytical and Bioanalytical Chemistry*, 354: 709–713.

Strangmann, A., Bashan, Y. and Giani, L., 2008. Methane in pristine and impaired mangrove soils and its possible effect on establishment of mangrove seedlings, *Biology and Fertility of Soils*, 44(3): 511–519.

Sturm, K., Keller-Lehmann, B., Werner, U., Raj Sharma, K., Grinham, A. R., and Yuan, Z., 2015. Sampling considerations and assessment of Exetainer usage for measuring dissolved and gaseous methane and nitrous oxide in aquatic systems, *Limnology and Oceanography: Methods*, 13(7): 375–390.

Sun, Z., Wang, L., Tian, H., Jiang, H., Mou, X., and Sun, W., 2013. Fluxes of nitrous oxide and methane in different coastal Suaeda salsa marshes of the Yellow River estuary, China, *Chemosphere*, 90(2): 856–865.

Sundh, I., Mikkela, C., Nilsson, M., and Svensson, B.H., 1995. Potential aerobic methane oxidation in a sphagnum-dominated peatland - controlling factors and relation to methane emission, *Soil Biology and Biochemistry*, 27(6): 829–837.

Susilo, A., Ridd, P.V. and Thomas, S., 2005. Comparison between tidally driven groundwater flow and flushing of animal burrows in tropical mangrove swamps, *Wetlands Ecology and Management*, 13(4): 377–388.

Sutton-Grier, A.E. and Megonigal, J.P., 2011. Plant species traits regulate methane production in freshwater wetland soils, *Soil Biology and Biochemistry*, 43(2): 413–420.

Tabak, N.M., Laba, M. and Spector, S., 2016. Simulating the effects of sea level rise on the resilience and migration of tidal wetlands along the Hudson River, *PLoS ONE*, 11(4): 1–25.

Takai, K., Nakamura, K., Toki, T., Tsunogai, U., Miyazaki, M., Miyazaki, J., Hirayama, H., Nakagawa, S., Nunoura, T., and Horikoshi, K., 2008. Cell proliferation at 122°C and isotopically heavy CH_4 production by a hyperthermophilic methanogen under high-pressure cultivation, *PNAS*, 105(31): 10949-10954.

Tangko, A.M. and Pantjara, B., 2007. Dinamika Pertambakan Perikanan di Sulawesi Selatan Kurun Waktu 1990–2005, *Media Akuakultur*, 2(2): 118–123.

Terazawa, K., Ishizuka, S., Sakata, T., Yamada, K., and Takahashi, M., 2007. Methane emissions from stems of *Fraximum mandshurica* var. *japonica* trees in a floodplain forest, *Soil Biology and Biochemistry*, 39: 2689–2692.

Terazawa, K., Yamada, K., Ohno, Y., Sakata, T., and Ishizuka, S., 2015. Spatial and temporal variability in methane emissions from tree stems of *Fraxinus mandshurica* in a cool-temperate floodplain forest, *Biogeochemistry*, 123(3): 349–362.

Thomas, B. and Arthur, M.A., 2010. Correcting porewater concentration measurements from peepers: application of a reverse tracer, *Limnology and Oceanography: Methods*, 8: 403–413.

Tokida, T., Adachi, M., Cheng, W., Nakajima, Y., Fumoto, T., Matsushima, M., Nakamura, H., Okada, M., Sameshima, R., and Hasegawa, T., 2011. Methane and soil CO_2 production from current-season photosynthates in a rice paddy exposed to elevated CO_2 concentration and soil temperature, *Global Change Biology*, 17(11): 3327–3337.

Tong, C., Huang, J., and Jia, Y., 2015a. Small-Scale Spatial Variability of Soil Methane Production Potential and Porewater Characteristics in an Estuarine *Phragmites australis* Marsh, *Journal of Coastal Research*, 314(4): 994–1004.

Tong, C., She, C.X., Yang, P., Jin, Y.F., and Huang, J.F., 2015b. Weak Correlation Between Methane Production and Abundance of Methanogens Across Three Brackish Marsh Zones in the Min River Estuary, China, *Estuaries and Coasts*, 38(6): 1872–1884.

Tong, C., Cadillo-Quiroz, H., Zeng, Z.H., She, C.X., Yang, P., and Huang, J.F., 2017. Changes of community structure and abundance of methanogens in soils along a freshwater–brackish water gradient in subtropical estuarine marshes, *Geoderma*, 299: 101–110.

Torres, N.T., Hauser, P.C., Furrer, G., Brandl, H., and Müller, B., 2013. Sediment porewater extraction and analysis combining filter tube samplers and capillary electrophoresis, *Environmental Sciences: Processes and Impacts*, 15(4): 715–720.

Torres-Alvarado, M.D.R., Fernández, F.J., Ramírez Vives, F., and Varona-Cordero, F., 2013. Dynamics of the methanogenic archaea in tropical estuarine sediments, *Archaea*, 2013: 1–13.

Twilley, R.R., Castañeda-Moya, E., Rivera-Monroy, V.H., and Rovai, A., 2017. Productivity and Carbon Dynamics in Mangrove Wetlands, in *Mangrove Ecosystems: A Global Biogeographic Perspective*, eds V. H. Rivera-Monroy, S. Yip Lee, E. Kristensen, and R.R. Twilley, Springer International Publishing, Cham, Switzerland, pp. 113-162.

Ugo, P., Bertolin, A. and Moretto, L.M., 1999. Monitoring sulphur species and metal ions in salt-marsh pore-waters by using an in-situ sampler, *International Journal of Environmental Analytical Chemistry*, 73(2): 129–143.

Ullman, R., Bilbao-Bastida, V. and Grimsditch, G., 2013. Including blue carbon in climate market mechanisms, *Ocean and Coastal Management*, 83: 15–18.

Van Bodegom, P., Stams, F., Mollema, L., Boeke, S., and Leffelaar, P., 2001. Methane Oxidation and the Competition for Oxygen in the Rice Rhizosphere, *Applied and Environmental Microbiology*, 67(8): 3586–3597.

Van Der Nat, F., Middelburg, J.J., Meteren, D. Van, and Wielemakers, A., 1998. Diel Methane Emission Patterns from *Scirpus lacustris* and *Phragmites australis*, *Biogeochemistry*, 41(1): 1–22.

Van Der Nat, F. and Middelburg, J.J., 2000. Methane Emission from Tidal Freshwater Marshes, *Biogeochemistry*, 49(2): 103–121.

van Nugteren, P., Moodley, L., Brummer, G.J., Heip, C.H.R., Herman, P.M.J., and Middelburg, J.J., 2009. Seafloor ecosystem functioning: The importance of organic matter priming, *Marine Biology*, 156(11): 2277–2287.

Vann, C.D. and Megonigal, J.P., 2003. Elevated CO_2 and water depth regulation of methane emissions: Comparison of woody and non-woody wetland plant species, *Biogeochemistry*, 63(2): 117–134.

Verma, A., Subramanian, V. and Ramesh, R., 2002. Methane emissions from a coastal lagoon: Vembanad Lake, West Coast, India, *Chemosphere*, 47(8): 883–889.

Wang, H., Liao, G., D'Souza, M., Yu, X., Yang, J., Yang, X., and Zheng, T., 2016. Temporal and spatial variations of greenhouse gas fluxes from a tidal mangrove wetland in Southeast China, *Environmental Science and Pollution Research*, 23(2): 1873–1885.

Wang, S., Zhou, L., Chen, J., Ju, W., Feng, X., and Wu, W., 2011. Relationships between net primary productivity and stand age for several forest types and their influence on China's carbon balance, *Journal of Environmental Management*, 92(6): 1651–1662.

Wang, Z.P., DeLaune, R.D., Patrick, W.H., and Masscheleyn, P.H., 1993. Soil Redox and pH Effects on Methane Production in a Flooded Rice Soil, *Soil Science Society of America Journal*, 57(2): 382.

Wania, R., Ross, I. and Prentice, I.C., 2010. Implementation and evaluation of a new methane model within a dynamic global vegetation model: LPJ-WHyMe v1.3.1, *Geoscientific Model Development*, 3(2): 565–584.

Wanninkhof, R., Asher, W.E., Ho, D.T., Sweeney, C., and McGillis, W.R., 2009. Advances in Quantifying Air-Sea Gas Exchange and Environmental Forcing, *Annual Review of Marine Science*, 1(1): 213–244.

Wanninkhof, R., 1992. Relationship between wind speed and gas exchange, *Journal of Geophysical Research*, 97(92): 7373–7382.

Wassmann, R., Buendia, L.V., Lantin, R.S., Bueno, C.S., Lubigan, L.A, Umali, A., Nocon, N.N., Javellana, A.M., and Neue, H.U., 2000. Mechanisms of crop management impact on methane emissions from rice fields in Los Banos, Philippines, *Nutrient Cycling in Agroecosystems*, 58: 107–119.

Watkins, A.J., Roussel, E.G., Webster, G., Parkes, R.J., and Sass, H., 2012. Choline and N,N-dimethylethanolamine as direct substrates for methanogens, *Applied and Environmental Microbiology*, 78(23): 8298–8303.

Wei, D. and Wang, X., 2017. Recent climatic changes and wetland expansion turned Tibet into a net CH4 source, *Climatic Change*, 144(4): 657–670.

Weimer, P. and Zeikus, J., 1978. One carbon metabolism in methanogenic bacteria. Cellular characterization and growth of *Methanosarcina barkeri*, *Archives of Microbiology*, 119(1): 49-57.

Welti, N., Hayes, M. and Lockington, D., 2017. Seasonal nitrous oxide and methane emissions across a subtropical estuarine salinity gradient, *Biogeochemistry*, 132(1–2): 55–69.

West, W.E., Coloso, J.J. and Jones, S.E., 2012. Effects of algal and terrestrial carbon on methane production rates and methanogen community structure in a temperate lake sediment, *Freshwater Biology*, 57(5): 949–955.

Weston, N.B., Neubauer, S.C., Velinsky, D.J., and Vile, M.A., 2014. Net ecosystem carbon exchange and the greenhouse gas balance of tidal marshes along an estuarine salinity gradient, *Biogeochemistry*, 120(1–3): 163–189.

Whalen, S.C., 2005. Natural wetlands and the atmosphere, *Environmental Engineering Science*, 22(1): 73–94.

Whiting, G.J. and Chanton, J.P., 1993. Primary production control of methane emission from wetlands, *Nature*, 367(6463): 794–795.

Wilms, R., Sass, H., Köpke, B., Cypionka, H., and Engelen, B., 2007. Methane and sulfate profiles within the subsurface of a tidal flat are reflected by the distribution of sulfate-reducing bacteria and methanogenic archaea, *FEMS Microbiology Ecology*, 59(3): 611–621.

Wrigth, D.G., Pawlowicz, R., McDougall, T.J., Feistel, R., and Marion, G.M., 2011. Absolute Salinity, "Density Salinity" and the Reference-Composition Salinity Scale: present and future use in the seawater standard TEOS-10, *Ocean Science*, 7:1-26.

Wu, Z., Ren, D., Zhou, H., Gao, H., and Li, J., 2017. Sulfate reduction and formation of iron sulfide minerals in nearshore sediments from Qi'ao Island, Pearl River Estuary, Southern China, *Quaternary International*. 452: 137–147.

Wuebbles, D.J. and Hayhoe, K., 2002. Atmospheric methane and global change, *Earth-Science Reviews*, 57(x): 177–210.

Xia, Y.Q. and Li, H.L., 2012. A combined field and modeling study of groundwater flow in a tidal marsh, *Hydrology and Earth System Sciences*, 16(3): 741–759.

Xiang, J., Liu, D., Ding, W., Yuan, J., and Lin, Y., 2015. Invasion chronosequence of Spartina alterniflora on methane emission and organic carbon sequestration in a coastal salt marsh, *Atmospheric Environment*, 112: 72–80.

Xiao, K.Q., Beulig, F., Kjeldsen, K.U., Jørgensen, B.B., and Risgaard-Petersen, N., 2017. Concurrent methane production and oxidation in surface sediment from Aarhus Bay, Denmark, *Frontiers in Microbiology*, 8: 1–12.

Xie, X., Li, R., Zhang, Y., Shen, S., and Bao, Y., 2018. Effect of Elevated [CO_2] on Assimilation, Allocation of Nitrogen and Phosphorus by Maize (*Zea mays* L.), *Communications in Soil Science and Plant Analysis*, 49(9): 1032–1044.

Xiong, Y., Liu, X., Guan, W., Liao, B., Chen, Y., Li, M., and Zhong, C., 2017. Fine root functional group based estimates of fine root production and turnover rate in natural mangrove forests, *Plant and Soil*, 413(1–2): 83–95.

Xu, D., Wu, W., Ding, S., Sun, Q., and Zhang, C., 2012. A high-resolution dialysis technique for rapid determination of dissolved reactive phosphate and ferrous iron in pore water of sediments, *Science of the Total Environment*, 421–422: 245–252.

Xu, Y., Ge, J., Tian, S., Li, S., Nguy-Robertson, A.L., Zhan, M., and Cao, C., 2015. Effects of water-saving irrigation practices and drought resistant rice variety on greenhouse gas emissions from a no-till paddy in the central lowlands of China, *Science of the Total Environment*, 505: 1043–1052.

Yamamoto, S., Alcauskas, J.B., and Crozier, T.E., 1976. Solubility of Methane in Distilled Water and Sea Water, *Journal of Chemical and Engineering Data*, 21(1): 78–80.

Yancey, P.H., Clark, M.E., Hand, S.C., Bowlus, R.D., and Somero, G.N., 1982. Living with Water Stress: Evolution of Osmolyte Systems, *Science*, 217(4566): 1214–1222.

Yang, J., Liu, J., Hu, X., Li, X., Wang, Y., and Li, H., 2013. Effect of water table level on CO_2, CH_4 and N_2O emissions in a freshwater marsh of Northeast China, *Soil Biology and Biochemistry*. 61: 52–60.

Yang, Y., Li, N., Wang, W., Li, B., Xie, S., and Liu, Y., 2017. Vertical profiles of sediment methanogenic potential and communities in two plateau freshwater lakes, *Biogeosciences*, 14(2): 341–351.

Yavitt, J.B., Williams, C.J., and Wieder, R.K., 1997. Production of methane and carbon dioxide in Peatland ecosystems across north America: Effects of temperature, aeration, and organic chemistry of peat, *Geomicrobiology Journal*, 14(4): 299–316.

Yoshikawa, C., Hayashi, E., Yamada, K., Yoshida, O., Toyoda, S., and Yoshida, N., 2014. Methane sources and sinks in the subtropical South Pacific along 17°S as traced by stable isotope ratios, *Chemical Geology*, 382: 24–31.

Young, M., 2005. *Methane Cycling and Ground Water Sources in Mangrove-dominated Coastal Lagoons, Yucatan Peninsula, Mexico*, Stanford University, Stanford, USA.

Yu, B., Stott, P., Yu, H., and Li, X., 2013. Methane emissions and production potentials of forest swamp wetlands in the eastern great Xing'an Mountains, Northeast China, *Environmental Management*, 52(5): 1149–1160.

Yuan, J., Ding, W., Liu, D., Kang, H., Xiang, J., and Lin, Y., 2016. Shifts in methanogen community structure and function across a coastal marsh transect: Effects of exotic Spartina alterniflora invasion, *Scientific Reports*. 6: 1–12.

Zalman, C.A., Meade, N., Chanton, J., Kostka, J.E., Bridgham, S.D., and Keller, J.K., 2018 Methylotrophic methanogenesis in Sphagnum-dominated peatland soils, *Soil Biology and Biochemistry*, 118: 156–160.

Zeikus, J.G. and Ward, J.C., 1974. Methane formation in living trees: a microbial origin, *Source: Science, New Series*, 184(4142): 1181–1183.

Zeikus, J.G. and Winfrey, M.R., 1976. Temperature limitation of methanogenesis in aquatic sediments, *Applied and Environmental Microbiology*, 31(1): 99–107.

Zeleke, J., Sheng, Q., Wang, J.G., Huang, M.Y., Xia, F., Wu, J.H., and Quan, Z.X., 2013. Effects of *Spartina alterniflora* invasion on the communities of methanogens and sulfate-reducing bacteria in estuarine marsh sediments, *Frontiers in Microbiology*, 4: 1–13.

Zhang, C.B., Sun, H.Y., Ge, Y., Gu, B.J., Wang, H., and Chang, J., 2012. Plant species richness enhanced the methane emission in experimental microcosms, *Atmospheric Environment*, 62: 180–183.

Zhang, K., Cheng, X., Dang, H., Ye, C., Zhang, Y., and Zhang, Q., 2013. Linking litter production, quality and decomposition to vegetation succession following agricultural abandonment, *Soil Biology and Biochemistry*, 57: 803–813.

Zhang, M., Luo, Y., Lin, L., Lin, X., Hetharua, B., Zhao, W., Zhou, M., Zhan, Q., Xu, H., Zheng, T., and Tian, Y., 2018. Molecular and stable isotopic evidence for the occurrence of nitrite-dependent anaerobic methane-oxidizing bacteria in the mangrove sediment of Zhangjiang Estuary, China, *Applied Microbiology and Biotechnology*, 102(5): 2441–2454.

Zhang, X., Kirkwood, W.J., Walz, P.M., Peltzer, E.T., and Brewer, P.G., 2012. A review of advances in deep-ocean Raman spectroscopy, *Applied Spectroscopy*, 66(3): 237–249.

Zhang, Y. and Ding, W., 2011. Diel methane emissions in stands of *Spartina alterniflora* and *Suaeda salsa* from a coastal salt marsh, *Aquatic Botany*, 95(4): 262–267.

Zhang, Z., Zimmermann, N.E., Calle, L., Hurtt, G., Chatterjee, A., and Poulter, B., 2018. Enhanced response of global wetland methane emissions to the 2015–2016 El Niño-Southern Oscillation event, *Environmental Research Letters*, 13(7): 1–13.

Zhuang, G.C., 2014. *Methylotrophic Methanogenesis and Potential Methylated Substrates in Marine Sediment*, Universitat Bremen, Bremen, Germany.

Zhuang, G.C., Elling, F.J., Nigro, L.M., Samarkin, V., Joye, S.B., Teske, A., and Hinrichs, K.U., 2016. Multiple evidence for methylotrophic methanogenesis as the dominant methanogenic pathway in hypersaline sediments from the Orca Basin, Gulf of Mexico, *Geochimica et Cosmochimica Acta*, 187: 1–20.

Zhuang, G.C., Heuer, V.B., Lazar, C.S., Goldhammer, T., Wendt, J., Samarkin, V.A., Elvert, M., Teske, A.P., Joye, S.B., and Hinrichs, K.U., 2018. Relative importance of methylotrophic methanogenesis in sediments of the Western Mediterranean Sea, *Geochimica et Cosmochimica Acta*, 224: 171–186.

Appendix 1: Calculation of CH_4 concentrations based on headspace equilibration method

CH_4 concentration of pore-water was calculated using a set of equations as described by Magen *et al*. (2014). The molar concentration of CH_4 (mol L^{-1}) in the pore-water samples at the time of collection was calculated by dividing the amount (mol) of methane ($\boldsymbol{n}_{CH4}$) by the volume of water in the bottle (V_w):

$$[\boldsymbol{CH_4}] = \frac{\boldsymbol{n_{CH4}}}{\boldsymbol{V_w}} \qquad \text{Equation 1}$$

Given that the bottle was completely full of pore-water sample, V_w at the time of collection was 120 mL. After replacing 25 mL of the pore-water sample with UHP N_2 gas, the 120 mL bottle consisted of a liquid and gas phase. Hence, the volumes of the pore-water (V_L, liquid) and UHP nitrogen (V_G, gas) were 95 and 25 mL, respectively, while the gas pressure (P_G) in the head space was 1.8 atm. Before equilibration (by shaking), CH_4 concentration in the pore-water remained the same as Eqn. 1.1. After equilibration between the adjacent liquid and gas phases, some of the CH_4 originally in the pore-water was now in the gas phase in the headspace. Therefore, the total amount of methane ($\boldsymbol{n}_{CH4}$) was the sum of the amount of methane dissolved in the pore-water as liquid phase ($\boldsymbol{n}_{CH4L}$) and methane in the headspace as gas phase ($\boldsymbol{n}_{CH4G}$):

$$\boldsymbol{n}_{CH4} = \boldsymbol{n}_{CH4L} + \boldsymbol{n}_{CH4G} \qquad \text{Equation 2}$$

To calculate $\boldsymbol{n}_{CH4}$, $\boldsymbol{n}_{CH4L}$ and $\boldsymbol{n}_{CH4G}$ should be calculated separately based on the partial pressure of methane in the headspace (p_{CH4G}) in L of CH_4/L, which was obtained by measuring headspace gas samples after equilibration by using GC. The amount of methane ($\boldsymbol{n}_{CH4G}$) in the gas phase was then calculated according to:

$$\boldsymbol{n_{CH4G}} = \frac{\boldsymbol{p_{CH4G}\ P_G\ V_G}}{\boldsymbol{R(273.15+T)}}\ , \qquad \text{Equation 3}$$

where R is the ideal gas constant (0.08206 L atm K^{-1} mol^{-1}), T (°C) is the temperature and P_G is the gas pressure.

The amount of methane in the liquid phase ($\boldsymbol{n}_{CH4L}$) was determined using the following equation (Magen *et al*., 2014):

$$\boldsymbol{n_{CH4L}} = \boldsymbol{\beta}\frac{\boldsymbol{p_{CH4G}\ P_G\ V_L}}{\boldsymbol{R(273.15+T)}} \qquad \text{Equation 4}$$

where β is the Bunsen coefficient of methane reflecting the solubility of this gas in water at atmospheric pressure, temperature (T, K) and salinity (S, parts per thousand) (Yamamoto *et al*., 1976):

$$\ln\beta = -67.1962 + 99.1624\left(\frac{100}{T}\right) + 27.9015\ln\left(\frac{T}{100}\right) + S[-0.072909 + 0.041674\left(\frac{T}{100}\right) - 0.0064603\left(\frac{T}{100}\right)^2]$$

Equation 5

Appendix 2: Example of calculation for pore-water CH_4 and soil surface CH_4

Pore-water CH_4 calculation

CH_4 concentration in the headspace gas sample for an example calculation was 1,824 ppm, which was collected from the pore-water sample at the depth of 10 cm at Site 8 on May 2016, when the pore-water temperature was 30°C. Note that gas pressure and the volume of the gas in the headspace were 1.8 atm and 25 mL, while the volume of pore-water sample was 95 mL; thus, the amount of CH_4 in the gas phase in the headspace was calculated according to Eqn. 3:

$$\boldsymbol{n}_{CH4G} = \frac{\left(\frac{1824}{10^6} L\, L^{-1}\right)(1.8\; atm)\left(\frac{25}{10^3} L\right)}{(0.08206\, L\; atm\; K^{-1} mol^{-1})(273.15+30\; K)} = 3.2\; x\; 10^{-6}\; mol$$

Further, the amount of CH_4 dissolved in the pore-water as liquid phase was calculated as follows (Eqn. 4):

$$\boldsymbol{n}_{CH4L} = 0.02424\, \frac{\left(\frac{1824}{10^6} L\, L^{-1}\right)(1.8\; atm)\left(\frac{95}{10^3} L\right)}{(0.08206\, L\; atm\; K^{-1} mol^{-1})(273.15+30\; K)} = 3.04\; x\; 10^{-7}\; mol$$

Therefore, the molar concentration of CH_4 in the 95 mL of pore-water sample collected from a depth of 10 cm at Site 8 on May 2016 (see Eqn. 1 and 2) was as follows:

$$[CH_4] = \frac{(3.2\; x\; 10^{-6}\; mol)+(3.04\; x\; 10^{-7}\; mol)}{(95\; x\; 10^{-3}\; L)} = 3.7\; x\; 10^{-5}\; mol\; L^{-1} = 3.7\; x\; 10^{-2} mol\; m^{-3}$$

Soil surface CH_4 flux

The majority of CH_4 studies have used a gas diffusion model according to Fick’s first law, which is widely implemented in the calculation of molecular diffusion of chemical species either in fluid or solid media. The law assumes that soil surface CH_4 flux occurs due to molecular diffusions within a few centimetres at the top layer of soils (Van Der Nat and Middelburg, 2000) or at soil–air or soil–water interfaces (Man *et al*., 2004; Dutta *et al*., 2015) (see Fig. 1). In my case, I assumed that dissolved CH_4 at the top layer of soil (at 10 cm) was well mixed and the soils were saturated with water, where the water level keeps at the soil surface. Therefore, the molecular diffusion through the soil compartment within a 10 cm depth was assumed to be zero because of no gradient concentration (Fig. 1, dashed line). Thus, the diffusion primarily occurs as a result of gradient CH_4 concentration in the boundary layer (Fig. 1).

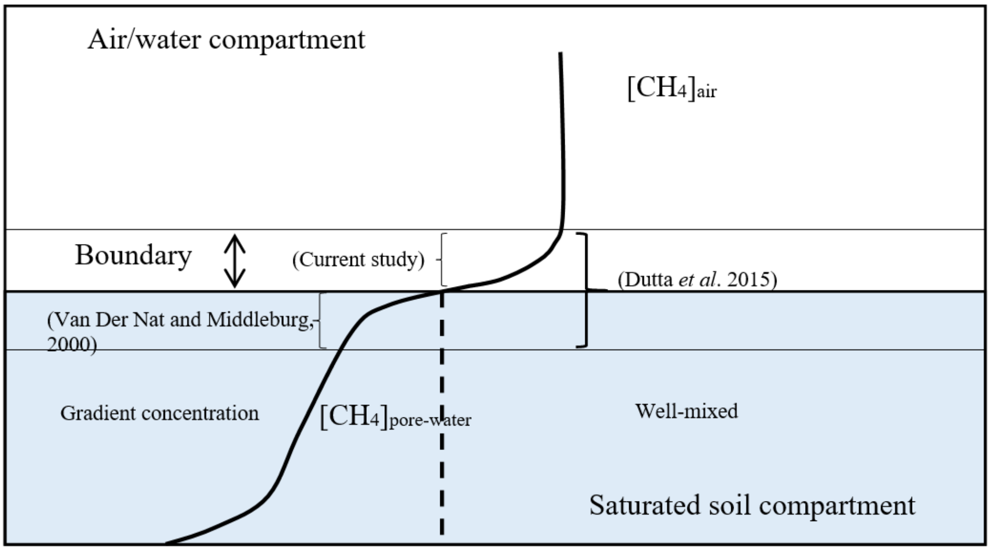

Figure 1. **Illustration of the conceptual model of gas transfer through an interface, and assumptions underlying the mathematical model used in the current study compared with previous studies.**

If one used Fick's first law for CH_4 diffusion across the boundary layer in Fig. 1, one would encounter difficulties determining the boundary conditions because gas diffusivities change by at least 10^4 times (Wania *et al.*, 2010). Thus, I used a more robust model flux in Eqn. 5.1, as Wania *et al.* (2010) suggested. In fact, Eqn. 5.1 is a modified equation of Fick's first law. Further explanations of this can be found in Sarmiento and Gruber (2006) and Wanninkhof *et al.* (2009).

Eqn. 5.1 contains a gas transfer coefficient (k, in cm h^{-1}), and the generic equation to estimate k is as follows:

$$k = k_{600}\left(\frac{Sc}{600}\right)^{n} \qquad \text{Equation 6}$$

where S_c is a Schmidt number that has been presented in Eqn. 5.3, and n is a Schmidt exponent. In the current study, the exponent of -0.5 was suitable for mangrove areas because of high turbulence, instead of -2/3, which is commonly used for open ocean waters at wind speeds below 3 m s^{-1} (Borges *et al.*, 2004). The gas transfer coefficient at a Schmidt number of 600 (k_{600}, cm h^{-1}) was used to normalise the gas transfer coefficient k. Many equations of k_{600} have been proposed, yet mostly for gas flux calculation in lakes or oceans (Wanninkhof *et al.*, 2009). Thus, I evaluated two equations that could be appropriate for the conditions of my study site. First, k_{600} is expressed as a function of wind speed at 10 m height (U_{10}, m s^{-1}) (Wania *et al.*, 2010):

$$k_{600} = 2.07 + 0.215\, U_{10}^{1.7} \qquad \text{Equation 7}$$

Second, k_{600} is a function of speed of the background water current (v, m s^{-1}):

$$k_{600} = 2.03 + 0.43\, v \qquad \text{Equation 8}$$

Eqn. 8 is an empirical model for CH_4 flux calculations from surface water in mangrove creeks (Rosentreter *et al*., 2017). Then, I assumed that U_{10} and v were 0 because the pore-water–atmosphere interface in mangrove soils is less influenced by wind, and the speed of the background water current was small. Hence, both Eqn. 7 and 8 were identical, and I then calculated the gas transfer coefficient (k) as Eqn. 5.2.

To apply Eqn. 5.1, I began with calculating the Schmidt number (Sc) by using Eqn. 5.3. The value of temperature to calculate Sc was set to 30°C and then:

$$S_c\,(CH_4) = 2101.2 - 131.54\,(30) + 4.4931\,(30^2) - 0.08676\,(30^3) + 0.000707\,(30^4) = 428.6$$

Thus, the gas transfer coefficient (k) calculation was as follows:

$$k = 2.03\left(\frac{Sc}{600}\right)^{-0.5} = 2.03\left(\frac{428.6}{600}\right)^{-0.5} = 2.4\ cm\ h^{-1} = 2.4 \times 10^{-2}\ m\ h^{-1}$$

Finally, by using this coefficient, I calculated soil surface CH_4 flux:

$$Flux_{CH4} = k\,([CH_4]_{pw} - \beta\,[CH_4]_a$$

$$= (2.4 \times 10^{-2}\ m\ h^{-1})\ [(3.7 \times 10^{-2}\ mol\ m^{-3}) - (0.02424)(7.2 \times 10^{-5}\ mol\ m^{-3})]$$

$$= (9 \times 10^{-4}\ mol\ m^{-2}\ h^{-1})(16\ g\ mol^{-1})(10^3\ mg\ g^{-1}) = 14\ mg\ m^{-2}\ h^{-1}$$

Appendix 3: CH_4 fluxes from tree stem and soil surface in the literature

Table 1. **CH_4 fluxes from tree stem and soil surface in the literature.**

No.	References	Locations	CH_4 fluxes		
			Stem	Stem*)	Soil
			mg m^{-2} (stem surface) h^{-1}	mg m^{-2} (ground surface) h^{-1}	
1	Pitz *et al*. (2018)	Upland forest	0.07 ± 0.01	0.01	-0.06 ± 0.01
		Transitional	0.2 ± 0.06	0.03	0.01 ± 0.03
		Wetland forest	0.6 ± 0.2	0.08	0.2 ± 0.1
2	Terazawa *et al*. (2015)	Floodplain forest	0.1–1.3	0.01–0.18	
3	Gauci *et al*. (2010)	Freshwater wetlands	0.03–0.1	0.004–0.01	0.3–0.8
4	Maier *et al*. (2018)	Upland forest	0.1	0.01	-0.07

Note the different area basis of expression.

*) Rough estimates according to the ratio between an average of stem surface area of mature trees in 13 plots (565 m^2) and the ground surface area of the plot (50 × 80 m^2) in a CH_4 study of the Amazon floodplain (Pangala *et al*., 2017).